UNIVERSIDADE FEDERAL DE SÃO CARLOS
CENTRO DE CIÊNCIAS EXATAS E DE TECNOLOGIA
DEPARTAMENTO DE QUÍMICA
PROGRAMA DE PÓS-GRADUAÇÃO EM QUÍMICA

"Investigating the Potential of Polysulfides Obtained via Inverse Vulcanization as Sustainable Fertilizers"

Stella Fortuna do Valle*

Thesis presented as part of the requirements to obtain the title of DOCTOR IN SCIENCES, concentration area: PHYSICAL-CHEMISTRY.

Advisor: Caue Ribeiro de Oliveira

*** Scholarship: CNPq**

São Carlos - SP
2022

UNIVERSIDADE FEDERAL DE SÃO CARLOS
CENTRO DE CIÊNCIAS EXATAS E DE TECNOLOGIA
DEPARTAMENTO DE QUÍMICA
PROGRAMA DE PÓS-GRADUAÇÃO EM QUÍMICA

“Investigando o Potencial de Polissulfetos Obtidos via Vulcanização Inversa como Fertilizantes Sustentáveis”

Stella Fortuna do Valle*

Tese apresentada como parte dos requisitos para obtenção do título de DOUTOR(A) EM CIÊNCIAS, área de concentração: FÍSICO-QUÍMICA.

Orientador(a): Caue Ribeiro de Oliveira

*** bolsista CNPq**

São Carlos - SP
2022

UNIVERSIDADE FEDERAL DE SÃO CARLOS

Centro de Ciências Exatas e de Tecnologia
Programa de Pós-Graduação em Química

Folha de Aprovação

Defesa de Tese de Doutorado da candidata Stella Fortuna do Valle, realizada em 07/11/2022.

Comissão Julgadora:

Prof. Dr. Cauê Ribeiro de Oliveira (EMBRAPA)

Prof. Dr. Hernane da Silva Barud (UNIARA)

Prof. Dr. Marcos Yassuo Kamogawa (ESALQ/USP)

Profa. Dra. Denise Bevilaqua (UNESP)

Prof. Dr. Alberto Carlos de Campos Bernardi (EMBRAPA)

gov.br
Documento assinado digitalmente
CAUE RIBEIRO DE OLIVEIRA
Data: 29/11/2022 17:22:15-0300
Verifique em https://verificador.iti.br

O Relatório de Defesa assinado pelos membros da Comissão Julgadora encontra-se arquivado junto ao Programa de Pós-Graduação em Química.

“Isso de querer
ser exatamente aquilo
que a gente é
ainda vai
nos levar além”
(Paulo Leminski)

Agradecimentos

Agradeço primeiramente ao Dr. Caue Ribeiro pela orientação e pela oportunidade de desenvolver este trabalho. Obrigada pela confiança, pelo apoio e por tudo o que me ensinou ao longo desta jornada.

Ao Dr. Nicolai D. Jablonowski por ter me recebido e acolhido com tanto carinho durante meu doutorado sanduíche, e pela disponibilidade e suporte contínuos.

À Dra Amanda Giroto pela amizade e parceria; por me orientar e acompanhar desde o começo dessa jornada, sempre oferecendo ideias, conselhos, apoio e palavras de incentivo. Obrigada por ser essa pessoa tão presente e disposta a ajudar, tanto na pesquisa como na minha vida pessoal.

Aos amigos da Embrapa Instrumentação e, principalmente, a todos que já fizeram parte do grupo de liberação controlada. Agradeço ao Gelton, Rodrigo, Ricardo, Marcela, Roger, Juliana, Camila e Raquel pelas contribuições, suporte e amizade.

À minha família por todo o amor. Agradeço a meus pais, Livia, Andrea, Lara e Marcelo; com vocês sempre me sentirei acolhida e cercada de carinho, sempre terei um lar.

A meu companheiro Mateus, por ser meu melhor amigo, por preencher meus dias com amor e risadas, e por me acompanhar e apoiar em todos os momentos.

À Embrapa Instrumentação pela excelente infraestrutura disponibilizada para a realização deste trabalho, e à equipe de funcionários por todo o suporte. Agradeço em especial à Adriana, Alice, Joana, Silviane, Viviane, Ana e Suzane pela disponibilidade e ajuda.

Ao Programa de Pós-Graduação em Química da Universidade Federal de São Carlos (PPGQ-UFSCar) pela oportunidade de realizar este trabalho de doutorado.

Ao CNPq pela bolsa de estudos concedida.

À CAPES/PrInt pela bolsa e oportunidade de realizar parte da minha pesquisa no exterior, durante o doutorado sanduíche.

A todos que de alguma forma contribuíram e torceram pelo sucesso deste trabalho, meus sinceros agradecimentos.

Table List

Figure List

Resumo

INVESTIGANDO O POTENCIAL DE POLISSULFETOS OBTIDOS VIA VULCANIZAÇÃO INVERSA COMO FERTILIZANTES SUSTENTÁVEIS. A segurança alimentar mundial é um dos maiores desafios atuais, sendo indispensável para tal estabelecer estratégias sustentáveis que tornem os insumos agrícolas mais eficazes e seguros. O enxofre (S) desempenha um importante papel agronômico para as colheitas como macronutriente secundário, e sua deficiência em solos agrícolas tem se tornado um problema crescente para a produtividade e a qualidade das plantações. O enxofre elementar (S_8) é um subproduto abundante do refino do petróleo que tem se destacado como fertilizante. Porém, o S_8 só pode ser absorvido pelas plantas após oxidação por microrganismos do solo a sulfato, um processo lento que restringe sua eficiência agronômica, especialmente quando aplicado na forma de pellets. Buscando otimizar a oxidação, investigamos recentemente a transformação da estrutura estável do S_8 em um novo material com cadeias lineares de S, usando a técnica de polimerização por vulcanização inversa. Os polissulfetos (PolyS) desenvolvidos demonstraram taxas de oxidação superiores ao S_8, além de exibirem características de processamento e conformação interessantes, ideais para veiculação de outros fertilizantes. Assim, este trabalho teve como objetivo principal avaliar o potencial do PolyS como material versátil e com maior eficiência como fertilizante multifuncional de enxofre. Pellets de PolyS com adição de porosidade à estrutura foram preparados visando aumentar a área superficial para a oxidação biológica. Foi estudada a interação desse sistema com a bactéria *Acidithiobacillus thiooxidans*, que obtém energia a partir da oxidação de S, além da aplicação combinada dos pellets com bactéria em solo, revelando uma oxidação

significativamente maior em comparação a pellets comerciais de S_8. O PolyS foi investigado também como matriz dispersora para liberação controlada de outros fertilizantes, com a vantagem de servir como fonte rica em S para as plantas. Compósitos contendo fontes sustentáveis de fósforo (P) com diferentes perfis de solubilidade – rocha fosfática e estruvita – foram sintetizados para estudar os efeitos físicos e químicos do PolyS como matriz. Foi verificado um efeito sinergético entre a oxidação do PolyS e a liberação de fosfato, com a acidez local da geração de sulfato favorecendo a solubilização de fósforo. A aplicação de compósitos de PolyS-estruvita para o cultivo da soja foi então testada em casa de vegetação, com estudo sistemático dos efeitos dos fertilizantes no perfil radicular e desenvolvimento vegetal. Comparado a fontes solúveis convencionais, o PolyS levou a uma maior eficiência na absorção de enxofre, e a liberação controlada de P estimulou a produção de raízes finas da soja. A partir dos resultados pôde-se concluir que os polissulfetos oferecem versatilidade para o design de diferentes produtos fertilizantes, com valor agregado como fonte de S eficiente.

Palavras-chave: polissulfeto; vulcanização inversa; fertilizante; enxofre; fósforo; liberação controlada.

Abstract

INVESTIGATING THE POTENTIAL OF POLYSULFIDES OBTAINED VIA INVERSE VULCANIZATION AS SUSTAINABLE FERTILIZERS. Global food security is one of the biggest challenges we face today, and to this end, establishing sustainable strategies towards the development of more efficient and safer agricultural products is indispensable. Sulfur (S) plays an important agronomic role for crops as a secondary macronutrient, and its deficiency in agricultural soils has become an increasing problem for crop productivity and quality. Elemental sulfur (S_8) is an abundant byproduct of petroleum refining that stands out as a S-fertilizer. However, S_8 can only be assimilated by plants after oxidation by soil microorganisms to sulfate, a slow process that restricts its agronomic efficiency, especially when applied as pellets. Aiming to optimize this conversion, we recently investigated the transformation of the stable S_8 structure into a new material with linear S chains using the polymerization technique of inverse vulcanization. The polysulfides (PolyS) showed superior oxidation rates to S_8, in addition to interesting processing and conformation characteristics, ideal for the incorporation of other fertilizers. Thus, the primary goal of this work was to evaluate the potential of PolyS as a versatile material with high efficiency as a multifunctional sulfur fertilizer. PolyS pellets were prepared with added porosity to the structure, aiming to increase the surface area for biological oxidation. A study was conducted to understand the interaction of this system with the bacterium *Acidithiobacillus thiooxidans*, which obtains energy from S oxidation. Moreover, compared to commercial S_8 pellets, oxidation in soil was significantly higher from the combined application of the porous PolyS with bacterium. PolyS was also investigated as a dispersant matrix for the

controlled-release of other fertilizers, with the advantage of serving as a rich source of S for plants. Composites containing sustainable phosphorus (P) sources with different solubility profiles - phosphate rock and struvite - were synthesized to study the physical and chemical effects of PolyS as a matrix. A synergistic effect between PolyS oxidation and phosphate release was verified, with the local acidity of sulfate generation favoring phosphorus solubilization. The application of PolyS-struvite composites for soybean cultivation was then tested in a greenhouse, with a systematic study of fertilizer effects on root profile and plant development. Compared to conventional soluble sources, PolyS led to higher sulfur uptake efficiency, and the controlled release of P stimulated the production of fine soybean roots. Based on the results it could be concluded that the polysulfides offer versatility for the design of different fertilizer products, with added value as an efficient S source.

Keywords: Polysulfide; Inverse vulcanization; Fertilizer; Sulfur; Phosphorus; Controlled-release.

Summary

1. Introduction

The growth of the world population is currently following an alarming trend that seriously threatens global food security, with predictions to reach up to 9.7 billion people by 2050. Many studies estimate the need to increase the current food production by 70% in order to meet this new global demand.[1,2] Nevertheless, the targeted agriculture productivity should be achieved in a sustainable way, prioritizing systems that allow greater efficiency while minimizing the expansion of cultivable area and the environmental impacts related to incorrect fertilizer use. Given this scenario, the search for technologies to support the development of new environmentally-friendly fertilizers is urgent, as crop yield directly depends on the provision of adequate and effective nutrition.

Agriculture represents a vital part of Brazilian economy and, consequently, the fertilizer industry is especially relevant for the country. Brazil was the third largest exporter of food products in 2016, exceeding 5% of the global exports. Brazil's consumption of fertilizers follows the same trend, being the fourth largest consumer of these products in 2013, reaching a consumption of 29.1 million tons. The country is still highly dependent on fertilizer imports, which represents 85% of the fertilizers consumed in Brazil.[3–5] The production and efficient use of fertilizers is, therefore, an essential tool to ensure the continued growth of national agriculture and economy.

Fertilizers are natural or synthetic compounds applied to soils to ensure the replacement of essential nutrients for plant growth.[6,7] The deficiency of any of these compounds becomes restrictive for plant development, even if the other nutrients are present in adequate levels, as

dictated by Liebig's Law of Minimums.[8,9] On the other hand, excessive fertilizer supply can also impair plant growth, reaching toxic and inhibitory levels for the plant. Moreover, if the fertilizer is delivered in excess, incompatible with the nutrient demands of the crop, it tends to accumulate in the medium and, consequently, it may escape and damage the environment through air emissions and soil leaching to underground waters.[3,7] Therefore, for greater efficiency and sustainability, fertilizer supply should be conducted in a balanced way, more synchronized with the nutritional needs and cycles of the crops.

In general, agricultural soils are more deficient in nitrogen (N), phosphorus (P), and potassium (K), however, over the past few years sulfur (S) deficiency has also reached concerning levels, thus becoming a limiting nutrient to crop development, which should be urgently addressed.[7,10,11]

1.1. Sulfur Fertilization and Oxidation

Sulfur plays an important role in the synthesis of amino acids and of compounds involved in photosynthesis, being essential for plant quality and yields.[12,13] Despite this, sulfur has been the most neglected macronutrient in current agronomic practices, with the increasing substitution of S-containing fertilizers by options with higher NPK contents that, on the other hand, do not provide sulfur itself, e.g., simple superphosphate (SSP) replaced by triple superphosphate (TSP).[13,14] In addition, the stricter control of SOx gas emissions over the last decades paradoxically led to the decrease in S atmospheric deposition, contributing to the lower availability of this element in soils.[10,15,16]

Commercial S fertilizers are usually based on sulfate (SO_4^{2-}) salts or elemental sulfur (S_8).[10,13] Sulfate sources have the advantage of being readily available for plant uptake, e.g.: ammonium sulfate and simple superphosphate. However, their high solubility implicates in a tendency of leaching, which can lead to serious environment damages.[12,17,18] Elemental sulfur is a concentrated source (>90% S) obtained as an abundant byproduct from petroleum hydrodesulfurization, thus presenting low production and transportation costs. Nevertheless, since plants only absorb S in the form of sulfate, to be assimilated S_8 needs to undergo a biological oxidation process in soils, which is a restrictive step for the fertilizer efficiency.[14,15,18,19] Commercial pellets have been reported to take more than 3 years for a conversion of only 50%, for instance.[14,18]

Sulfur oxidation into sulfate may involve the formation of different intermediates depending on the S source and on the microorganism, with thiosulfate ($S_2O_3^{2-}$) and tetrathionate ($S_4O_6^{2-}$) being reported as intermediates of S_8 bacterial oxidation.[20–22] The chemolithotrophic bacterium *Acidithiobacillus thiooxidans* is considered the main responsible for S oxidation, deriving its energy precisely from oxidizing reduced S forms, including elemental sulfur, polysulfides, and sulfide minerals.[12,22,23] *A. thiooxidans* uses atmospheric oxygen as an electron acceptor for this process, and CO_2 as its only carbon source.[23] A vast population of heterotrophic microorganisms also participates in S conversion in agricultural soils, such as the fungi species *Aspergillus* and *Penicillium*. Nevertheless, the oxidation rate by these microorganisms is still limited, depending on the availability of organic carbon to sustain their activity.[12,22,24] Studies indicate that, contrary to the fungi population, *A. thiooxidans* is not present in significant numbers in

most agricultural soils nowadays, which could contribute to a lower oxidation efficiency.[22,25]

Biological sulfur oxidation is influenced by numerous factors, including the soil properties and fertilizer characteristics.[12,20,22,26–28] Environmental conditions like soil temperature, moisture, aeration, pH, and organic matter content have a direct effect on oxidation and on the activity of microorganisms involved in this process. Most importantly, as a superficial process, oxidation rate is governed by the fertilizer surface area and sulfur atoms directly exposed to microbial activity, being highly favored when the particle size is reduced.[12,14,20,22] However, the application of S_8 as a powder is unfeasible due to its explosive nature. Moreover, fertilizers in general are usually applied as pellets or granules in field for management and safety purposes.[14,15,29]

There is also an influence of sulfur molecular form on the oxidation process,[22,30] which could change the pathway to sulfate formation. Therefore, an alternative to effectively optimize the use of elemental sulfur could be to modify its structure. The transformation from its crystalline and highly stable form to a linear and amorphous form could make the chains more susceptible to oxidation, a strategy that should be more investigated.

1.2. Structural Modification of Elemental Sulfur and its Effect on Oxidation

Elemental sulfur can assume a vast number of allotropic forms, occurring in nature predominantly as a yellow crystalline solid with orthorhombic geometry (α-S_8). Around 95.3 ºC it is converted to the monoclinic form (β-S_8), which melts at 119.6 ºC.[31,32] When heated above 159° C a ring opening polymerization (ROP) is initiated, with the homolytic generation of linear chains containing radicals at the end points. These

diradicals are extremely reactive, attacking other S_8 molecules successively and thus promoting the growth of polymeric sulfur chains, signaled by a pronounced and characteristic increase in the viscosity of the reaction medium.[19,33] Nevertheless, polymeric sulfur is chemically unstable in this form, with a tendency to depolymerize back to ring formation after a short period of time. Processing elemental sulfur itself can be quite challenging, since the behavior of the molten compound varies with temperature gradients, making its handling complex and dangerous. Upon cooling, the products tend to exhibit a brittle character, with poor mechanical properties.[19] This is mostly due to the solid state transformation of monoclinic crystals into the more stable orthorhombic form, which is more dense, thus resulting in a structure shrinkage.[32] Moreover, S_8 immiscibility with water and with most conventional organic solvents is also restrictive to its use industrially.[19]

To tackle these problems, Pyun and co-workers have recently developed the innovative inverse vulcanization method, obtaining stable polysulfide products as described in FIGURE 1.1.[34] The technique is based on the use of high contents of molten S_8 both as a reagent and non-traditional solvent, followed by the addition of an alkene as binding agent to stabilize the S diradicals. The method works around issues like S_8 incompatibility with traditional solvents, its difficult processing, and the polymerization reversibility. Another important aspect is that, unlike conventional vulcanization, here the sulfur chains are the backbone of the polymer, crosslinked by alkenes. These polysulfides have also been reported as able to be repaired, reprocessed, and recycled.[35,36] It is therefore a simple, inexpensive, and sustainable method, with the absence of solvent use, excellent atom economy, and valorization of an abundant residue as a feedstock.[37]

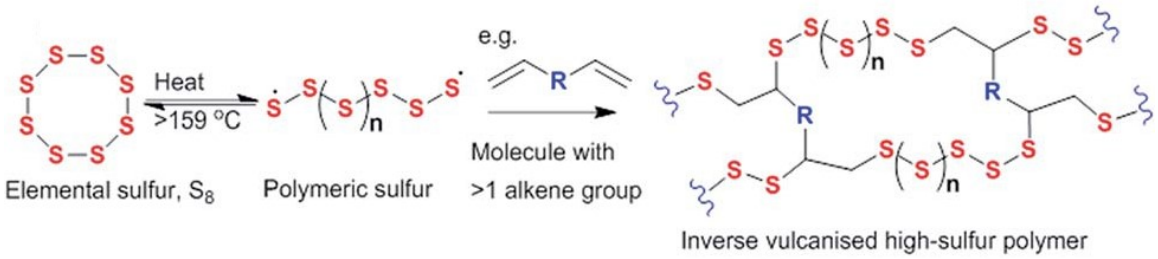

FIGURE 1.1: Inverse vulcanization chemical scheme. Source: Parker et al. (2017).[38]

A vast number of research on inverse vulcanization has been carried out exploring different alkenes and application areas.[37,39–42] Most of the studies have been focusing on its use in Li-S batteries [34,43–46] and as an adsorbent material for the removal of pollutants.[38,47–53] Polysulfides were also investigated as IR optical materials,[54–57] matrixes in nanocomposites with gold and lead,[58,59] adhesives,[35,60] and in composites with bio-based fillers.[61–63]

Recently, Valle and collaborators studied the effect of S_8 structural transformation on sulfur oxidation by using a polysulfide obtained *via* inverse vulcanization.[64,65] Up to that point, polysulfide application in agriculture had not been published yet. The polysulfides from our study were synthesized with soybean oil as the diene (FIGURE 1.2a), selected due to its high polyunsaturated fatty acid content and as a renewable raw material with low cost, non-toxic character, and abundant production.[66–68] The oxidation tests conducted in submerged culture medium with the fungus *Aspergillus niger* and in soil showed that the polymeric sulfur indeed achieved superior sulfate production from oxidation compared to elemental sulfur. Besides stabilizing the sulfur radicals, the use of soybean oil produced functional and malleable materials, as shown in FIGURE 1.2b, with physical characteristics that can allow versatility in processing and in product conformation, e.g.,

polysulfides molded into pellets in FIGURE 1.2c. Moreover, the organic fraction in the polysulfide (from the vegetable oil) appeared to contributed to the higher oxidation rate, possibly as a carbon source that stimulated the biological activity.

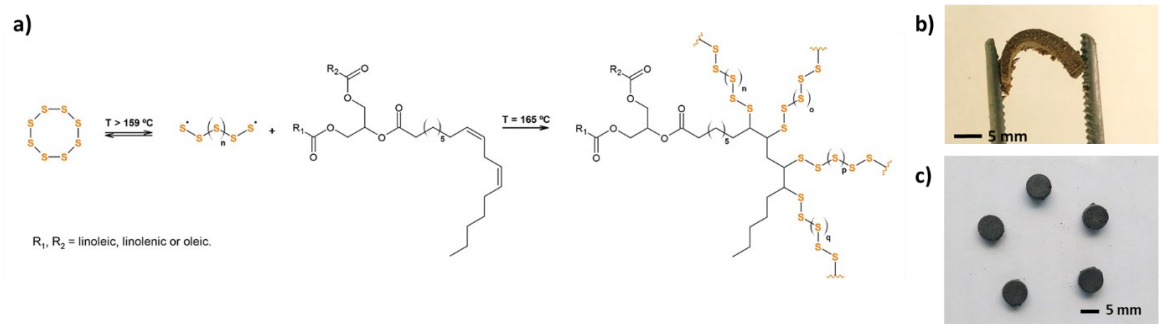

FIGURE 1.2: (a) Inverse vulcanization of elemental sulfur with soybean oil; (b) malleable polysulfide with 50 wt% S_8; and (c) molded polysulfide. Adapted from Valle et al. (2019).[65]

Therefore, the soybean oil polysulfide presents great potential to be used as a new class of multifunctional sulfur-based fertilizer, with improved agronomic efficiency and sustainability. Nevertheless, due to the recent development, some properties and dynamics are not yet known in detail. For polysulfide validation as a fertilizer for plant growth, its interactions with soil components and biota still needs to be thoroughly elucidated, as well as possible modifications to enhance nutrient availability to plants. Moreover, based on the observed physical characteristics of the synthesized polysulfide, this new material stands out as an alternative matrix for the controlled release of other fertilizers.

1.3. Controlled-Release Fertilizers

Controlled-release fertilizers (CRF) are designed to promote a gradual nutrient delivery, with a release rate more compatible with crop growth stages than the conventional soluble fertilizers. This strategy ensures superior agronomic efficiency and lower environmental impact, reducing fertilizer losses by leaching and volatilization, and eliminating the need for multiple fertilizer inputs.[3,69] The soybean oil polysulfide is a potential candidate to replace polymers conventionally used in CRFs, with the advantage of its intrinsic value as a S-fertilizer.

There are several mechanisms to promote the controlled release of nutrients, the most common being the use of a physical barrier for highly soluble compounds. This can be done by encapsulation with a hydrophobic material (coating) or by dispersion of the fertilizer in a matrix that restricts its dissolution. It is worth noting that elemental sulfur has been used as a mineral coating for urea granules, but due to its brittle nature and fractures, it provides an irregular release profile.[3,69,70] In the case of poorly soluble fertilizers, like phosphate rocks, the best strategy to control and facilitate nutrient availability is to reduce the particle size.[71–73] It is important to promote the dispersion of these particles in a matrix, not only because it is not feasible to use them directly as fertilizers in the field, but also to avoid their agglomeration.[29,74–78] Giroto et al. (2015) demonstrated that the solubility of the matrix is less relevant for composites than the porosity of the material, since the accessibility of water through the channels is fundamental for the solubilization of the phosphorus source.[74]

Mann et al. (2019) published the first work using a polysulfide from inverse vulcanization in controlled-release fertilizers.[79] The authors synthesized composites containing a polysulfide from canola oil and soluble

NPK salts. Nevertheless, the individual release profile of each nutrient was not demonstrated, and sulfate release from the polysulfide or the effects of its interaction with the other elements were not evaluated. More recently, Ghumman et al. (2022a) used a jatropha oil polysulfide as matrix for urea particles, investigating nitrogen release behavior.[80] Ghumman et al. (2021, 2022b) also investigated dissolving this polysulfide and a rubber seed oil polysulfide in THF to dip-coat urea granules, preventing a rapid N delivery.[81,82]

Polysulfides are thus emerging as innovative materials for the manufacture of fertilizers with intelligent design, great versatility, and improved efficiency. As a matrix in a fertilizer composite, it would be interesting to study its physical effect as a dispersing medium on the delivery of phosphorus sources with low solubility. Polysulfides increase the acidity of the medium after being oxidized to sulfate, which could favor P dissolution.[78,83] Research involving P composites should not be restricted, however, to investigating new matrices - it is essential to also evaluate alternatives to replace conventional P sources.

1.4. Phosphorus Fertilizers

Phosphorus is one of the most essential and limiting elements for plant development, being the main responsible for photosynthesis.[84] Tropical soils present low P availability due to the immobilization tendency of phosphate with aluminum and iron, requiring frequent fertilizer inputs to compensate for this effect and to ensure crop productivity.[71,85,86] The most common phosphate fertilizers are highly soluble, which often leads to the nutrient being released faster than the plant capacity to uptake it. Consequently, the fertilizer becomes more susceptible to soil fixation or to

leaching to nearby water bodies, where phosphate can cause their eutrophication.[87–89] The production of conventional P fertilizers can also be harmful to the environment as it depends on the treatment of the phosphate rocks (PR) with sulfuric acid, which generates significant amounts of residues.[90,91] PR can be used directly as a fertilizer, offering less environmental impact, however, their chemical stability implicates in a low solubility which should be improved for adequate nutrient supply.[77,86,88,92]

Nearly 90% of the phosphorus production is directed at agriculture use, and the current consumption rate of the non-renewable phosphate rocks has proven to be unsustainable and incompatible with the cycle of the element. It is estimated that the global demand for P will double by 2050 and, therefore, some studies predict the exhaustion of world reserves of phosphate rocks within 100 years. The geographic concentration of PR in only few countries - Morocco, China, and the USA - also means a great dependence on export and international policies. Given this scenario, technologies aimed at recycling phosphorus have been growing in interest, especially those that promote the recovery of P present in urban effluents.[91,93,94]

Struvite ($MgNH_4PO_4.6H_2O$) is a granular and concentrated crystal, easily obtained by treating urban wastewaters and other wastes under alkaline conditions. Besides recycling phosphate and reducing the P cycle gap, this prevents P from re-entering and damaging watercourses. In addition to a rich P content (with around 13% m/m P), struvite provides nitrogen and magnesium for plant fertilization, which are essential macronutrients.[95–102] Struvite solubility is strongly dependent on the pH, being insoluble in water and readily soluble in acidic medium.[103] Degryse et al. (2017) demonstrated that struvite can achieve the same agronomic efficiency as soluble fertilizers

when applied as a powder, however, it displayed an inferior performance in granular form.[104]

Therefore, phosphate rocks and struvite have the potential to provide a more eco-friendly and economically feasible option for P fertilization – the first by avoiding processing steps and the residues generated from it, and the latter for giving a destination to abundant wastes. For their efficient use in granular form, solubilization and release rates still need to be controlled. Combining the strategy of reducing P particle size with its dispersion in matrix system could achieve that sustainably, and polysulfides are ideal candidates for this purpose as easily processible materials with added value as S sources to plants.

2. Goals and Overview

The main goal of this thesis was to evaluate the effect of elemental sulfur chain modification on its biological oxidation to sulfate, under different conditions of application as a fertilizer. The present work proposes to use a polysulfide obtained by the inverse vulcanization of elemental sulfur with soybean oil as a model material to study the oxidation of linear sulfur chains, and compare it with elemental sulfur rings. The polysulfides were investigated as versatile materials for the development of sustainable fertilizers, motivated by their malleable and functional character, and their simple and green processing. This work proposes a systematic study of the structure and physicochemical properties of the polysulfides, focusing on their interaction with microorganisms that can directly oxidize sulfur and with other fertilizers, aiming to elucidate the potential of this new material as both a fertilizer and a vehicle for other fertilizers in controlled-release systems.

As specific goals, the present work aims to:

- Evaluate the combined application of the polysulfide with microorganisms that favor sulfur oxidation, which can optimize its efficiency;
- Evaluate the application of the polysulfide as a matrix in fertilizer composites for the controlled-release of phosphorus sources with different solubility behaviors;
- Study the polysulfide interaction with a soil-plant system, to verify its effect and viability as a fertilizer.

The research conducted for this thesis resulted in three published manuscripts. The following sections were adapted from those manuscripts, each corresponding to a different Chapter. The manuscripts were organized in Chapters I to III in the same order as the specific goals of the thesis, instead of the chronological order of their publication, aiming to highlight the progression of this investigation. Chapter I describes the preparation and characterization of polysulfide pellets, and their interaction with sulfur-oxidizing bacteria to improve the efficiency of sulfate supply. Based on the polysulfide potential in providing sulfur to plants and their versatile physical and processing characteristics, Chapter II presents the application of the polysulfide as a matrix to disperse and carry phosphate sources, in controlled-release fertilizer composites. The morphological, structural, and thermal characteristics of the materials were thoroughly elucidated, and the influence of the polysulfide on phosphorus availability was evaluated based on their interactions both physically and chemically. Finally, Chapter III describes a complete study of the effect of polysulfide-based composites on plant growth and nutrition, in a greenhouse experiment with soybean (*Glycine max L.*).

3. – Chapter I: A Study of Polysulfide Oxidation into Sulfate by *Acidithiobacillus thiooxidans*

The content of this chapter is an adaptation of the manuscript entitled "Co-Application of Porous Polysulfide Pellets with *Acidithiobacillus thiooxidans* Improves Sulfate Availability in Soil" by Valle et al. (2022), published in Journal of Polymers and the Environment (doi: 10.1007/s10924-022-02520-3).

Journal of Polymers and the Environment
https://doi.org/10.1007/s10924-022-02520-3

ORIGINAL PAPER

Check for updates

Co-Application of Porous Polysulfide Pellets with *Acidithiobacillus thiooxidans* Improves Sulfate Availability in Soil

Stella F. Valle[1,2] · Amanda S. Giroto[2] · Rodrigo Klaic[2] · Denise Bevilaqua[3] · Caue Ribeiro[2]

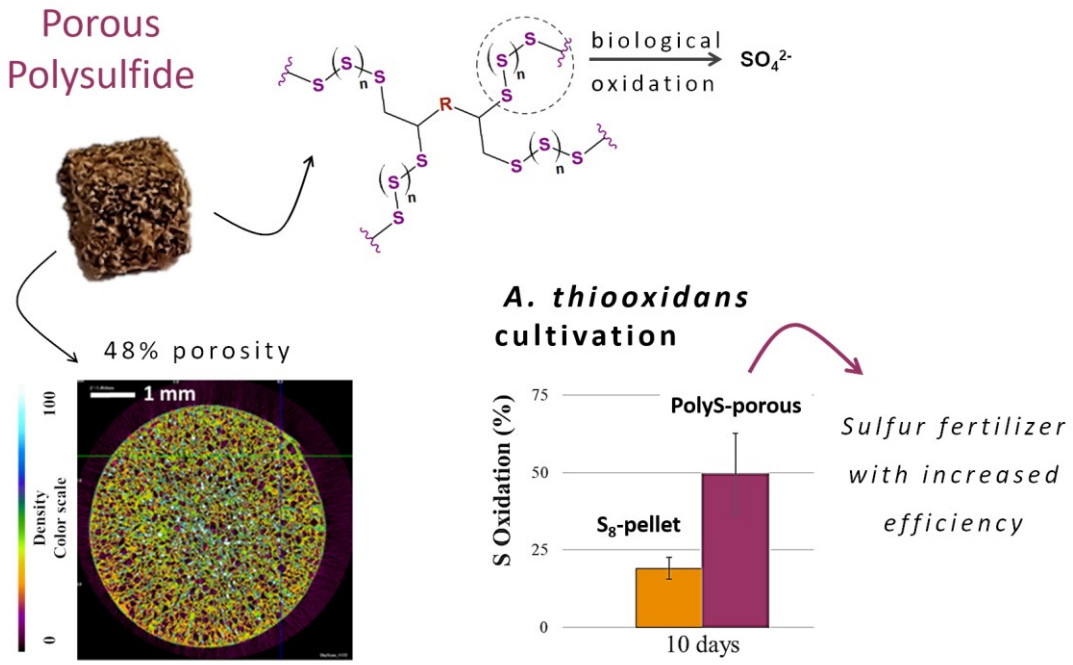

3.1. Abstract

Sulfur (S) fertilization is necessary to overcome the low availability of this essential nutrient in agricultural soils. Although elemental sulfur (S_8) pellets are often used, they tend to be poorly effective due to their low oxidation rate to sulfate, the form assimilated by plants. Here we designed highly porous polysulfide pellets (PolyS-porous) as S fertilizers with higher surface area for oxidation, aiming to improve sulfate delivery. A porosity of nearly 50% was achieved via inverse vulcanization of soybean oil and S_8 in the presence of a salt porogen. A culture medium test with S-oxidizing bacterium *Acidithiobacillus thiooxidans* revealed PolyS-porous had a faster initial oxidation than S_8-pellet, reaching respectively 57% and 20% at the end of 10 days. Sulfate released from PolyS-porous in soil was 3 times higher than from S_8-pellet in 30 days, and PolyS-porous co-application with *A. thiooxidans* achieved twice as much. Overall, the results from this study demonstrated the potential of porous polysulfide pellets as sulfur fertilizers with improved efficiency, especially when combined with *A. thiooxidans*.

3.2. Introduction

Sulfur (S) is a limiting macronutrient for plant metabolism, required for cysteine and methionine biosynthesis. While little attention has been directed at sulfur supply to crops over the past decades, its deficiency in agricultural soils has been increasingly frequent and thus a growing concern.[10,12,16] With population growth predictions and the need to increase food production,[1,2] optimizing fertilizer input practices is an urgent task – including better sulfur management.

Sulfate-based fertilizers provide readily available S to plants, however, they are usually susceptible to leaching due to their fast

solubilization.[18,105] Elemental sulfur (S_8) is an abundant waste from oil refineries, often used as S fertilizer for its lower water solubility, which reduces nutrient loss. Nevertheless, as plants can only uptake sulfate (SO_4^{2-}), the recovery of S_8-sulfur by crops depends on its biological oxidation in soil.[14,15] As a surface process, the oxidation rate is primarily affected by the fertilizer available surface area to microbial colonization, being favored by smaller particle sizes.[22,106] However, in field S_8 is usually handled in granules or pellets due to the explosive nature of its powder, considerably limiting the oxidation efficiency.[15,18] Oxidation rate of commercial S_8-bentonite pastilles was found to be only around 0.0006 d^{-1}, for instance.[14]

Polysulfides are a new class of S-fertilizer candidates recently studied by our group to optimize sulfur oxidation.[65,107,108] These materials are obtained with the inverse vulcanization of S_8 in the presence of an alkene, a method with no solvent use and excellent atom economy that transforms a residue (i.e., elemental sulfur) into useful materials.[34,37,39–41] The polysulfides prepared by our group displayed higher oxidation than elemental sulfur in a culture medium with the fungus *Aspergillus niger*.[24,65] The ring-opening polymerization of S_8 crystalline structure produces an amorphous material with less ordered S-chains, likely facilitating the conversion to sulfate. As malleable and functional materials, the polysulfides were also explored in previous works as matrices in multi-nutrient controlled-release fertilizers, featuring superior oxidation than S_8 in soil.[107] Moreover, soybean cultivation with the polysulfide composite achieved higher sulfur use efficiency and biomass than with a sulfate salt reference.[108] Other researches with polysulfides in agriculture have also been reported, aimed at the controlled release of soluble NPK sources and urea, but not on sulfur fertilization.[79,81]

The use of polysulfide pellets as sulfur fertilizers should be further explored, as our previous soil and plant experiments only evaluated the performance of ground composites. In the present work, polysulfide pellets were developed with added porosity and tested as S fertilizers with enhanced available surface area for S oxidation. Another specific goal was to assess polysulfide oxidation in the presence of the chemolithotrophic bacterium *Acidithiobacillus thiooxidans*, which is regarded as the most important S-oxidizing microorganism, deriving energy directly from the oxidation of mineral sulfur.[12,22,23] Since studies show that *A. thiooxidans* is mostly absent in agricultural soils nowadays,[12,25,106] we were interested in testing the potential of a combined application of the polysulfides with *A. thiooxidans* to optimize sulfate release.[109–111]

3.3. Materials and Methods

Preparation of Porous Polysulfide Fertilizer

The polysulfide materials were synthesized based on the inverse vulcanization of elemental sulfur (S_8) with soybean oil (SO), using a proportion of 50 wt% of the components.[65] Soybean oil was selected for the reaction for its advantages as a low-cost, renewable, and natural polyene. Sodium chloride (NaCl, < 0.150 mm) was used as a porogen, following an adapted method from Abraham et al., (2018).[112] Elemental sulfur, soybean oil, and NaCl were first mixed in a flask using a mass ratio of 0.6: 0.6: 1. The flask was then heated with an oil bath under constant agitation provided by a mechanical stirrer. The reaction progressed at 165 ºC until the formation of a brown solid material (PolyS-salt). After cooling, the polymeric material was hand-cut into small cubic pellets with an average side length of 2.1 mm.[50] The salt porogen was then washed off from the structure by placing the material in

a beaker flask filled with de-ionized water, keeping agitation with a magnetic bar stirrer overnight at room temperature. The resulting porous polysulfide (PolyS-porous) was rinsed with de-ionized water to remove residual salt particles from the surface, after which the pellets were dried in an oven at 50 ºC until constant weight.

Characterizations

Scanning Electron Microscopy (SEM) images were obtained using a microscope with a secondary electron detector (JEOL, JSM6510, Japan). Samples were prepared with gold coating in an ionization chamber (BalTec, Med. 020, Switzerland). X-Ray Microtomography (MicroCT) was conducted in a microtomography scanner (Bruker, SkyScan 1172, Germany), using the following parameters: unfiltered, 0.2 º step rotation, and 8 frames for the average process. A molded porous polysulfide was prepared for this analysis, as described in the "Synthesis of Molded Porous Polysulfide" section in Appendix A. Image reconstruction was obtained with the NRecon software. Fourier transform infrared spectroscopy (FTIR) of soybean oil, and PolyS-porous was performed with a spectrometer (Bruker, VERTEX 70, Germany). Differential scanning calorimetry (DSC) was recorded from −50 to 150 °C, at 10 °C/min, with nitrogen purge (50 mL/min) (TA Instruments, Q100, USA). CHNS elemental analysis was conducted with an elemental analyzer (Thermo Fisher Scientific FlashSmart, USA).

Porosity Estimation

The porosity (θ, %) of the prepared polysulfides was estimated based on the relation between real density (ρ *real*, g/mL) and apparent density (ρ *apparent*, g/mL), as described in equation (3.1). Real density of PolyS-

porous was obtained using a glass pycnometer, as described in the "Real Density Measurement" section of the Appendix A. The apparent density was calculated based on the average mass of PolyS-porous cubic pellets and their average volume (measured with a caliper).

$$\emptyset = \left(1 - \frac{\rho\ apparant}{\rho\ real}\right) \times 100 \quad (3.1)$$

Sulfur Oxidation in Culture Medium (*A. thiooxidans*)

Sulfur oxidation from the polysulfide material was investigated in liquid culture medium with the chemolithotrophic bacterium *Acidithiobacillus thiooxidans* (FG01 strain).[113,114]

Since particle size is one of the main factors influencing the oxidation rate, two forms of the polysulfide were examined: small porous pellets and ground polysulfide (PolyS-porous and PolyS-powder, respectively). For this, a dense polysulfide (PolyS) was synthesized and ground (< 0.5 mm), as described in the "Synthesis of Dense Polysulfide" section in Appendix A. Elemental sulfur was tested as a reference in both forms: as a powder (< 0.1 mm, Synth, Brazil) and in pellets (diameter of approximately 3.7 mm, ICL Fertilizantes, Brazil).

A pre-culture was first incubated during 10 days in an orbital shaker incubator at 30 °C and 150 rpm. An adapted 9K nutrient medium was used in the experiment, at pH 2.8 (adjusted with H_2SO_4), as detailed in Appendix A.[115] The oxidation experiment was then carried out in the same conditions, using 10% (v/v) of the pre-culture. The S^0 sources for bacterium growth were PolyS-powder, PolyS-porous, S_8-powder, or S_8-pellet. The treatments were analyzed in triplicates for each incubation time – 2, 6, and 10 days. A control with no

sulfur addition was also incubated to quantify sulfate traces from both the nutrient medium and the pre-culture.

Following each incubation period, the samples were filtered and sulfate concentration was determined by the turbidimetric method with UV-Vis spectrophotometry (FEMTO, 700 Plus, Brazil).[65,116] The data was treated with one-way statistical analysis (ANOVA), using Tukey's test at a $p < 0.05$ level of significance.

Sulfur Oxidation in Soil

Sulfur oxidation of the porous polysulfide was assessed in soil and compared with the co-application of the material with *A. thiooxidans*. In addition, S_8 pellets with and without bacteria were also tested as references.

Soil incubation of the materials was conducted using the top layer (0-20 cm) of an Oxisol soil from São Carlos, Brazil. Soil analysis results can be found in TABLE A1 (Appendix A). The soil was previously prepared by drying for 24 hours in an oven at 40 ºC, followed by sieving (< 2.0 mm), and acidity correction with limestone powder (3:1 wt%) [117]. Two soil controls with no fertilizer incorporation were also studied, with and without *A. thiooxidans* addition.

Polyethylene screw-cap bottles with perforated lids were filled with 50 g of soil, and the fertilizers were added to complete 50 mg of S per pot. In treatments without bacterium incorporation, the fertilizers were physically mixed with the soil and, after that, 10 mL of distilled water were added. For treatments with *A. thiooxidans* incorporation, the fertilizers were first placed at the soil surface and bacterium was added on the top (2.5×10^8 cells/g of S), followed by soil mixing and, lastly, water addition to complete 10 mL. The same volume of pre-culture and water were used in the controls

with no fertilizer. The pre-culture of *A. thiooxidans* was prepared in a 9K medium as described in the previous method section. Cell concentration was estimated turbidimetrically with a McFarland standard in a UV spectrophotometer (FEMTO, 700 Plus, Brazil) at 625 nm wavelength.

The experiment was conducted in an incubator with a controlled temperature of 25 °C, with the samples in triplicates. Soil humidity was maintained with water addition once a week, based on the estimated water weight loss. After each incubation time (15, 30, 45, and 60 days), the soil samples were immediately dried in an oven at 40 ºC. Sulfate was extracted with acid ammonium acetate solution, and the concentration was estimated turbidimetrically.[107,116] The data was subjected to one-way statistical analysis (ANOVA), using Tukey's test with a level of significance of $p < 0.05$.

3.4. Results and Discussion

Characterization of the Porous Polysulfide

A porous polysulfide (PolyS-porous) was prepared to be studied as a sulfur fertilizer with increased surface area (FIGURE 3.1), designed to improve S oxidation rate to sulfate. The porogenesis method highlights polysulfide materials' easy processability and versatility, especially in contrast to elemental sulfur (S_8). Elemental sulfur processing into useful forms is usually complex, as the molten phase tends to rapidly re-crystallize and produce fragile materials.[19] The polysulfide product obtained after the inverse vulcanization in the presence of NaCl, PolyS-salt, displayed a malleable character and was easily cut into the desired pellet size. The salt particles modified the mechanical behavior of the material, increasing brittleness compared to the pure PolyS. After salt removal, a porous structure was obtained, with a sponge-like appearance.

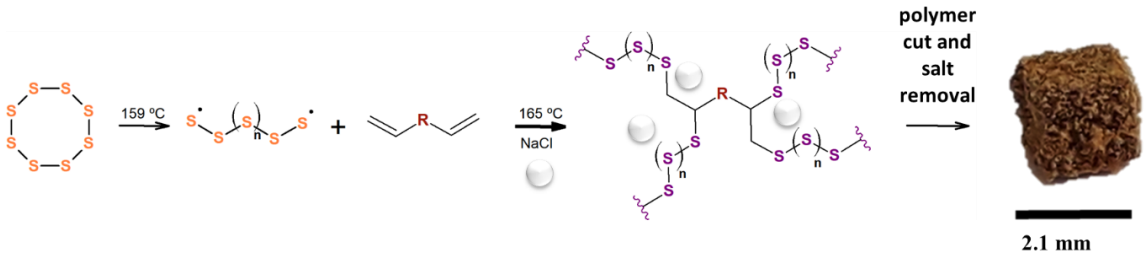

FIGURE 3.1: Scheme of the inverse vulcanization of elemental sulfur (S8) and soybean oil (R alkene structure) in the presence of a salt porogen (NaCl), producing PolyS-salt. The material was hand-cut and washed for salt removal, forming the porous polysulfide pellet (PolyS-porous).

Morphology changes of the polysulfide materials were investigated with SEM (FIGURE 3.2a-c). The NaCl salt used as porogen displays a mixture of particles with varying sizes and irregular shapes. PolyS-salt presents a heterogeneous surface comprising two distinct phases, with the polymer covering up the salt particles. PolyS-porous features a smooth material with no visible salt particles, indicating a satisfactory removal. Pores can be seen in different magnitudes, compatible with the different particle sizes of the salt. The porous surface is distinct from the dense polysulfide (PolyS) (FIGURE A2c, Appendix A), which exhibits a plain continuous surface. It should be noted that there was no effort to obtain smaller pores, as this was not needed for the purpose of this study and would involve more preparation steps.

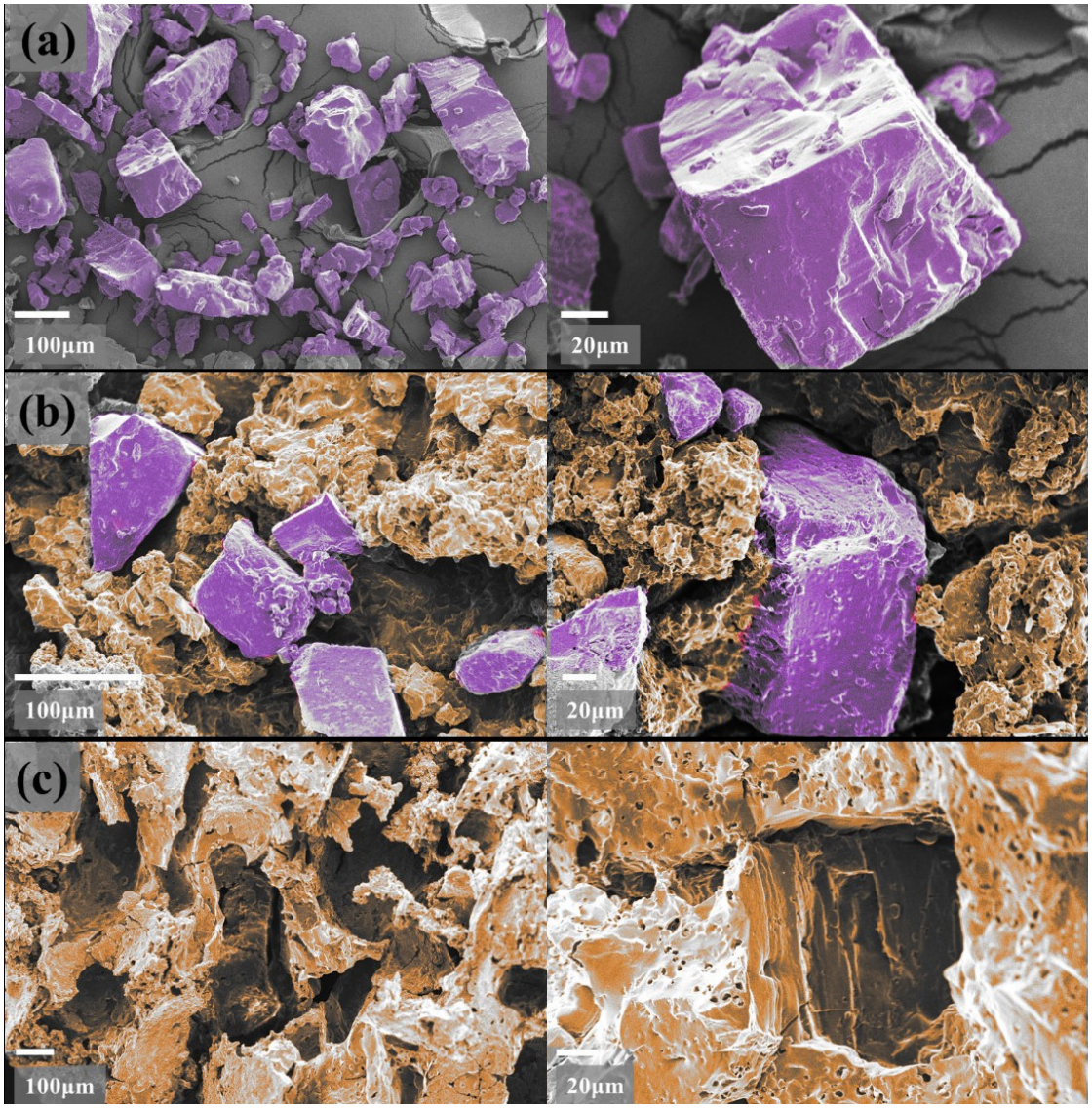

FIGURE 3.2: SEM images in different magnitude of (a) NaCl, (b) PolyS-salt, and (c) PolyS-porous. Salt particles and the polysulfide matrix are colored in purple and orange, respectively (software GIMP 2.10.14). Original images can be found in FIGURE A3 (Appendix A).

FIGURE 3.3a shows the Micro-CT image of a porous polysulfide. The polymer displays a completely porous structure, as verified in the SEM images, with pores vastly distributed and occupying a large area of the material. Some spots of higher density can be seen, possibly from

unreacted sulfur or NaCl residue. Moreover, the polymer itself displays a uniform density.

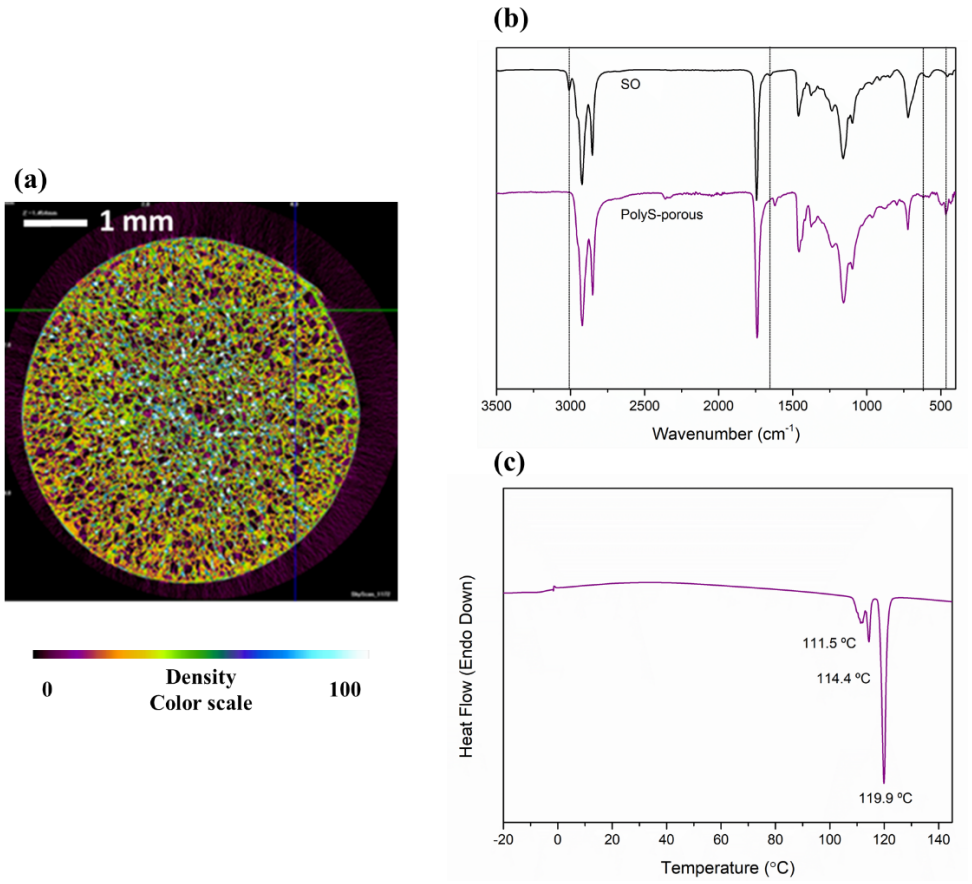

FIGURE 3.3: (a) Micro-CT image of the porous polysulfide; (b) FTIR patterns of soybean oil (SO) and PolyS-porous; (c) DSC thermogram of PolyS-porous.

FTIR spectra were analyzed to observe chemical changes in soybean oil (SO) structure after the reaction (FIGURE 3.3b). SO spectrum features typical triglyceride alkene bands at 3009 cm^{-1} (H-C=C stretching) and 1653 cm^{-1} (C=C stretching). These vibration modes were not present in the PolyS-porous spectrum, evidencing the polymerization occurred successfully.[38,44] A weak band appeared at 619 cm^{-1} attributed to C-S stretching, further confirming the reaction.[118] In addition, signals between 528

and 480 cm^{-1} and also at 467 cm^{-1} can be related to S-S stretching, consistent with polysulfides.[52]

The thermal behavior of the polysulfide material and the presence of unreacted elemental sulfur were investigated with DSC (FIGURE 3.3c). The DSC thermogram of PolyS-porous shows three endothermic peaks related to S_8 melting. The sharp endotherm at 119.9 ºC and the small one at 114.4 ºC correspond to the melting of the monoclinic phase β-S_8, while orthorhombic α-S_8 melting occurs at 111.5 ºC.[119] When cooled after the inverse vulcanization, unreacted sulfur was probably recrystallized in different phases due to the presence and interference of the polymer chains and salt particles.

CHNS elemental analysis showed the material contains 43.5% of S (TABLE 3.1), which is close to the theoretical ratio. An estimation of the free sulfur and polymeric sulfur contents was also conducted, using DSC thermograms. The percentage of unreacted sulfur present in the material was calculated based on S_8 melting peak area, according to Worthington et al. (2017).[48] The detailed method can be found on the Appendix A. The results revealed that more than half of the sulfur mass corresponds to residual S_8 (TABLE 3.1). The reaction between polymeric sulfur chains and soybean oil was probably disrupted by the significant amount of salt particles present in the reaction medium. Although sulfur was just partially converted into the polymeric form, it was sufficient to develop a functional structure, capable of being processed and modified into porous pellets. Moreover, the residual S_8 is finely dispersed within the polysulfide structure, favoring S_8 oxidation compared to a pellet.

TABLE 3.1: Estimated sulfur composition and porosity of PolyS-porous.

Polysulfide Composition		
Sulfur (wt%)	S_8 residual (wt% of S)	S polymeric (wt% of S)
43.5 ± 4.2	62.0 *	38.0 *
Polysulfide Porosity		
Apparent Density, $\rho_{apparent}$ (g/mL)	Real Density, ρ_{real} (g/mL)	Porosity (v%)
0.53 ± 0.14	1.04 †	48.5 ± 0.1

* Estimated by linear regression; † value assumed constant, estimated from > 10 pellet samples.

The porosity (%) of the PolyS-porous material was estimated based on the calculated apparent and real densities (TABLE 3.1), revealing the volume occupied by pores corresponds to almost 50% of the material. This result is consistent with the amount of salt used as porogen and with images from SEM and Micro-CT analysis.

Sulfur Oxidation by *Acidithiobacillus thiooxidans*

Once the morphological and chemical characteristics of the porous polysulfide pellets were elucidated, sulfur oxidation from this material in the presence of *Acidithiobacillus thiooxidans* and the effect of the porous structure on oxidation were studied. FIGURE 3.4 features the results from sulfur oxidation test in culture medium with *A. thiooxidans*. Sulfate detected in the control treatment was discounted from the other treatments. As expected, S_8-powder oxidation was significantly superior to that of S_8-pellet due to particle size effect on oxidation kinetics, as powders are more dispersed

and have higher available surface area. No sulfate formation was observed from elemental sulfur pellets within 6 days of incubation, while the powder achieved 20% of S oxidation in 2 days and nearly 90% after 10 days. Most importantly, the results confirmed the bacterium capacity to oxidize the soybean oil polysulfide, which is reported for the first time to the best of the author's knowledge. The ground polysulfide (PolyS-powder) displayed a comparable performance to S_8-powder despite having larger particles, reaching 25%, 57%, and 77% of S oxidation in 2, 6, and 10 days, respectively. Although PolyS-porous oxidation was lower than the ground material, it still proved to be more efficiently converted to sulfate than S_8-pellet. The porous polysulfide material initially achieved 11% of oxidation within 2 days of the experiment, and at the end, 50% of the S content was transformed into sulfate.

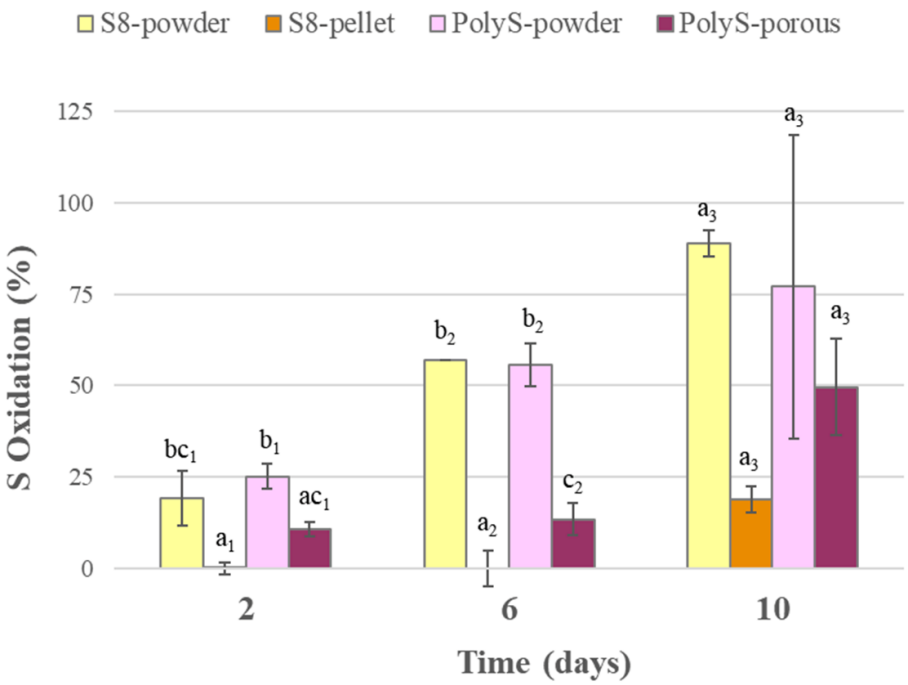

FIGURE 3.4: Sulfur oxidation to sulfate (%) over time in culture medium with *A. thiooxidans*, comparing the porous polysulfide pellets, the ground

polysulfide, and elemental sulfur powder and pellets. Bars show mean values ± standard deviations. Indexes a, b, c, and d signal the statistical differences for each group (i.e., each time of incubation, indexed with numbers).

Sulfur Oxidation in Oxisol Soil

Sulfur oxidation into sulfate was also studied in an Oxisol soil to simulate the performance of the PolyS-porous material as a fertilizer in real conditions. All treatments were tested with and without the incorporation of *A. thiooxidans*. Available sulfate in soil (mg of S/kg of soil) from each treatment over time can be seen in FIGURE 3.5. Over the first 15 days, *A. thiooxidans* addition improved sulfate production in all treatments, more significantly the fertilized ones. Both S_8-pellet and PolyS-porous with bacterium achieved more than 2 times the amount of sulfate from treatments with only the fertilizers. These results strongly indicate the S-oxidizing bacterium potential to boost sulfate release in soil, especially if blended with a S source. Other studies also explored supplying elemental sulfur with *A. thiooxidans* to increase sulfate production in soil.[109–111,120–123]

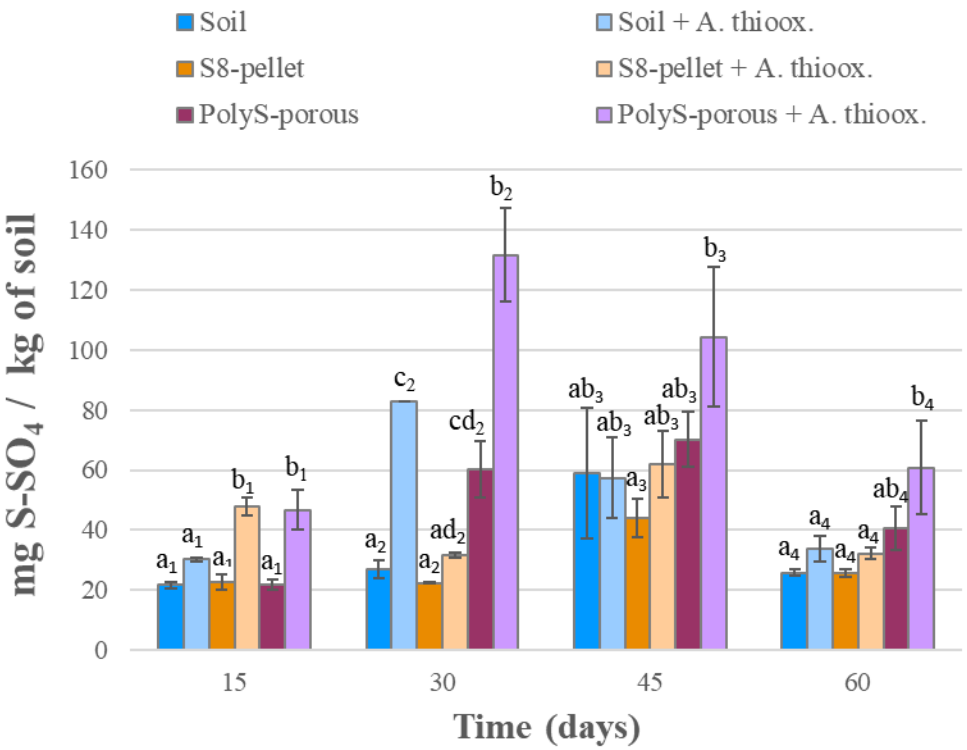

FIGURE 3.5: Sulfur as available sulfate (mg) per kg of soil, over the incubation time. The soil control, elemental sulfur pellets, and porous polysulfide were compared with and without the addition of *A. thiooxidans*. Bars show mean values ± standard deviations. Indexes a, b, c, and d signal the statistical differences for each group at $p < 0.05$ (i.e., each time of incubation, indexed with numbers).

After 30 days, sulfate concentration was practically unaltered in S_8-pellet, with and without bacterium. In contrast, a noticeable increase was observed in PolyS-porous treatments. S-sulfate formed with just PolyS-porous was nearly 3 and 2 times higher than, respectively, the pure S_8-pellet and its combination with *A. thiooxidans*. The co-application of PolyS-porous with S-oxidizing bacterium achieved the highest sulfate release, with twice the amount from PolyS-porous alone, representing approximately 10% of the applied S. These results are consistent with the dynamics observed in the

culture medium test, where S_8-pellet displayed a considerably lower oxidation rate than PolyS-porous. This can be attributed to the high porosity degree of the polymer in comparison to the dense elemental sulfur pellet, which allowed more accessibility to water and soil microorganisms and an increased available surface area for biochemical interactions. Moreover, this could be further indication of a faster oxidation of the polysulfide form compared to crystalline elemental sulfur.

After 45 days of incubation, S_8-pellet had the lowest performance, while PolyS-porous with bacterium continued to be the highest. By the end of the experiment at 60 days, available sulfate was reduced in all treatments, probably from soil precipitation and adsorption processes [105]. Moreover, it is likely that *A. thiooxidans* activity decreased after the first 30 days due to the unavailability of important nutrients. Nevertheless, PolyS-porous treatments were still significantly superior to the others. Sulfate from PolyS-porous was 25% and 54% higher than S_8-pellet with and without bacterium, respectively. FIGURE A5 (Appendix A) shows SEM images of the fertilizer materials after 60 days of soil incubation. Biofilm formation can be observed on the surface of S_8-pellet and PolyS-porous, however, the identification of *A. thiooxidans* specifically was not conclusive.

It is worth mentioning that S oxidation into sulfate may reduce the local soil pH and increase the availability of other nutrients (e.g., P, Mg, Zn, and K).[120] Therefore, *A. thiooxidans* application has the potential of improving the overall soil fertility, especially when combined with sulfur. Nevertheless, the bacterium performance in the experiment could have been negatively affected by low cell viability. Microbial survival after application in soil is one of the biggest challenges for the efficiency of inoculants, as they need to adapt to available nutrients and soil conditions.[124] Cell viability is also

highly affected by competing microorganisms already present in the soil. These issues could be addressed with the encapsulation of the bacterium within the porous polysulfide as a single biofertilizer.[78,109,125–127]

3.5. Conclusion

Porous polysulfide pellets (PolyS-porous) were prepared with a porosity of almost 50% of its volume, ideal for increasing the surface area available to S biological oxidation. In a culture medium with *Acidithiobacillus thiooxidans*, S_8-pellet was only oxidized after six days, while PolyS-porous displayed 11% of oxidation within just two days. Moreover, results at the end of ten days were respectively 20% and 57%. In soil PolyS-porous released 3 times the amount of sulfate achieved by S_8-pellet within 30 days, confirming the improved efficiency of the polysulfide. The incorporation of *A. thiooxidans* with PolyS-porous doubled its sulfate release, while for S_8-pellet the co-application was not significantly different. These results demonstrated the potential use of porous polysulfide pellets as S fertilizers with faster sulfate delivery in soil than dense elemental sulfur pellets. Moreover, the performance was significantly higher with the combined application of S-oxidizing bacterium *Acidithiobacillus thiooxidans*. Sulfur oxidation could be further improved with the direct incorporation of the bacterium in the polymer, which is currently under study.

4. - Chapter II: Polysulfide as a Multifunctional Matrix for the Controlled Release of Phosphate

The content of this chapter is an adaptation of the manuscript entitled “Synergy of Phosphate-Controlled Release and Sulfur Oxidation in Novel Polysulfide Composites for Sustainable Fertilization” by Valle et al. (2021), published in Journal of Agricultural and Food Chemistry (doi: 10.1021/acs.jafc.0c07333).

JOURNAL OF AGRICULTURAL AND FOOD CHEMISTRY

pubs.acs.org/JAFC Article

Synergy of Phosphate-Controlled Release and Sulfur Oxidation in Novel Polysulfide Composites for Sustainable Fertilization

Stella Fortuna do Valle, Amanda Soares Giroto, Heitor Pontes Gestal Reis, Gelton G. F. Guimarães, and Caue Ribeiro*

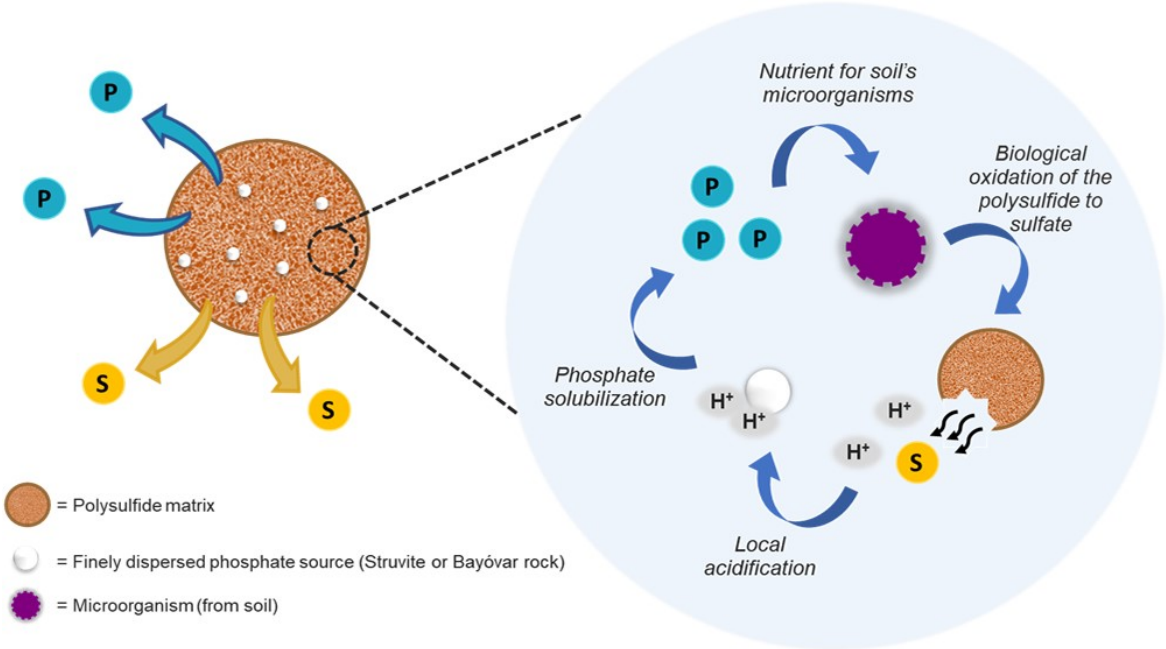

4.1. Abstract

The development of smart and ecofriendly fertilizers is pivotal to guarantee food security sustainably. Phosphate rock and struvite are promising alternatives for P fertilization, nevertheless, the solubility of these sources is a challenge for consistent use efficiency. Here we propose using a polysulfide obtained via inverse vulcanization as a novel controlled-release fertilizer matrix in a system containing either Bayóvar rock (Bay) or struvite (Str). The polysulfide provides S for plants after being biologically oxidized to sulfate in soil, generating local acidity for P solubilization. After 15 days of soil incubation, the composites with 75 wt% Str and 75 wt% Bay achieved, respectively, three and two times the S oxidation from the elemental sulfur reference. Results indicated that P contents stimulates the soil microorganisms' activity for S oxidation. The matrix had a physical role in improving Bay dissolution and regulating the rapid release from Str. Moreover, the available P in soil was 25 to 30 mg/dm^3 for Bay composites, while for pure Bay it was 9 mg/dm^3.

4.2. Introduction

By 2050 agriculture will face the challenge of feeding over 10 billion people worldwide and, to guarantee food security, food production is expected to increase at least 70 %.[1,2] To meet this growing demand, it is pivotal to promote sustainable agriculture systems, which can be achieved with the development of smart environmentally-friendly fertilizers for efficient plant nutrition.[71] Among the main fertilizers, phosphorous (P) is an essential element for crop growth and vital to photosynthesis. Nevertheless, it

is also the least available macronutrient in tropical soils as it tends to get immobilized by iron (Fe) and aluminum (Al), requiring frequent inputs.[71,85,86] Commercial P fertilizers are generally highly water-soluble and may lixiviate to water bodies, causing eutrophication and severe environmental impacts.[87–89] Moreover, their production involves the aggressive chemical treatment of mineral P with sulfuric acid, generating tons of residues.[90,91]

Thus, it is urgent to provide a portfolio of solutions for phosphatic fertilization through sustainable alternatives. The direct utilization of primary phosphate sources (ground phosphate rocks (PR)) reduces the environmental processing cost, although their low solubility results in limited agronomic efficiency.[88,92,128,129] Besides, phosphate recycling is another strategy, offering a sustainable source and closing the P cycle gap .[91,97] Phosphate can be recovered from wastes such as municipal wastewater, sewage, and manure, as struvite ($MgNH_4PO_4.6H_2O$).[95–97] Struvite also provides nitrogen (N), crop's most required macronutrient, and magnesium (Mg), which can provide a synergistic effect on P uptake and even maximize P absorption by more than 50 % in some crops.[95]

For the consistent use of both struvite and PR, new strategies should be developed to enhance their efficiency, facilitating nutrient supply in a responsible manner. Controlled-release fertilizers (CRF) are designed to promote a gradual delivery, more compatible with crop cycles.[3,69,71] The weak performance of fertilizers with low solubility, for instance, can be managed in a CRF by the dispersion of the ground nutrient in a matrix. Giroto studied the reduction of P particle size to accelerate the dissolution and, most importantly, demonstrated that it is essential to distribute the particles in a porous matrix (making a composite) to avoid their re-agglomeration and consequent loss of efficacy.[74,75] Furthermore, it is necessary to develop adequate matrices with

fertilizer role to increase the product functionality. Other nutrients should be delivered by the matrices, integrating the plant's needs. For instance, sulfur (S) is a secondary macronutrient and its deficiency in soils has been a growing concern, often managed with the use of elemental sulfur (S_8) as a matrix to other fertilizers.[12,105] However, crops can only assimilate sulfate, and S_8 slow oxidation to sulfate considerably limits its efficiency.[14,109] In addition, S_8 tends to form brittle and non-uniform matrices.[70,130] Recently, our research group has demonstrated that polysulfides formed by inverse vulcanization of elemental sulfur with soybean oil (SO) increase S oxidation, leading to superior sulfate release in comparison to pristine S_8.[65] Inverse vulcanization is an innovative copolymerization method, easily controllable and solvent-free process to obtain sulfur-rich polymers, making versatile, malleable and porous structures – ideal for application as composite matrices.[34,37,45,49]

The present work proposes to use this polysulfide as a matrix for the dispersion of sustainable phosphate sources in a controlled-release fertilizer composite and to evaluate the interaction of S and P in this system. The polysulfide is a multifunctional alternative to conventional CRF polymers for its physical characteristics and agronomic role in S supply. Mann recently demonstrated the use of a triglyceride-based polysulfide as a matrix for the controlled-release of NPK fertilizers with high solubility.[79] Nonetheless, the study did not address S supply from the polymer and the effects of its chemical interaction with the other components. Moreover, the polysulfide material can synergistically enhance P availability, as both the sulfate from matrix degradation and the organic acids produced from the carbonic domain simultaneously generate a local acidity that is ideal to favor phosphate dissolution.[78,83]

4.3. Materials and Methods

Materials

Elemental sulfur 98% (Synth, Brazil) and soybean oil (Liza, Brazil) were used to synthesize the polysulfide material. The phosphate sources for the composites' preparation were struvite (Ostara Crystal Green®) and Bayóvar rock, a sedimentary rock provided from Sechura (Peru). The oxide composition of both phosphate sources can be seen in TABLE B1 (Appendix B). Single superphosphate (Yara, Brazil) was also used in release tests.

Preparation of composites

The fertilizer composites were prepared based on the inverse vulcanization of elemental sulfur (S_8) with soybean oil (SO), in the presence of a phosphate source – Struvite (Str) or Bayóvar rock (Bay) (FIGURE 4.1). An equal mass ratio of S_8:SO was maintained for the formation of a 50 wt % polysulfide (PolyS), while the proportion of polymeric matrix and phosphate in the final products varied, with 25, 50, and 75 wt % of the ground mineral filler. The reactants were first mixed in an open recipient equipped with an overhead stirrer. The system was heated in an oil bath up to 160 ºC for S_8 ring-opening polymerization (ROP) and its inverse vulcanization with SO, keeping vigorous stirring to ensure proper homogenization.[65] The reaction progressed with a typical increase of viscosity until a brown rubbery solid was formed after approximately 45 minutes.

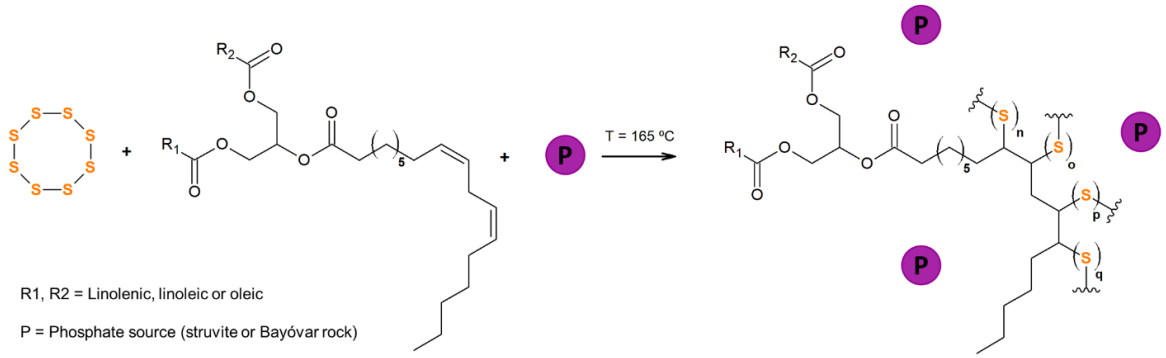

FIGURE 4.1 Chemical scheme of inverse vulcanization with elemental sulfur (S_8) and soybean oil (SO) in the presence of a phosphate source (struvite or Bayóvar rock) for the formation of fertilizer composites. The final polymer and SO are represented by generic structures.

Characterizations

The following characterizations were performed: CHNS Elemental Analysis (Thermo Scientific FlashSmart Elemental Analyzer); Scanning Electron Microscopy (SEM), with a JEOL microscope (JSM 6510); X-Ray Diffraction (XRD), on a Shimadzu XRD-6000 diffractometer with Cu Kα radiation (λ=1.54178 Å); Fourier-Transform Infrared (FTIR) Spectroscopy (Bruker VERTEX 70); Nuclear Magnetic Resonance (NMR): ^{1}H NMR spectra were obtained using a 600 MHz Avance III HD Bruker spectrometer ($CDCl_3$ (δ = 7.27 ppm) was used to solubilize soybean oil and pyridine-d5 (δ = 8.75 ppm) for the composites), Solid-state ^{31}P NMR MAS was conducted using a 10 kHz Avance III HD Bruker equipment; Thermogravimetric Analysis (TGA) was conducted in a TA Instruments TGA Q500 with nitrogen purge flow of 60 mL/min and 10 ºC/min heat flow at the range of 25 – 600 ºC; Differential Scanning Calorimetry (DSC) was performed in a Q100 instrument (TA Instrument) from -80 to 200 °C at 10 °C/min, with nitrogen purge (50 mL/min); Optical Microscopy (BEL Photonics, Brazil).

Release Test in Solution

Phosphate release from the composites was evaluated in a citric acid solution (2%) with pH 2.3.[117] The grounded composites and pure phosphate sources (struvite and Bayovar rock) were added in beaker flasks containing 300 mL of the critic acid solution. A fixed concentration of P from the materials in the citric acid solution was established as 200 mg/L. Triplicates were used, and the system was kept in an incubator under constant agitation (60 rpm) at 30 ºC for seven days, with aliquots being removed every 24 hours. Phosphate determination was conducted using the colorimetric method with absorbance measurements in a UV-spectrophotometer (FEMTO 700 Plus) at 880 nm wavelength, as described by Murphy and Riley.[131]

Release Test in Soil

The ground composites and starting materials (struvite, Bayóvar rock, and elemental sulfur) were incubated in an Oxisol soil from Brazil (see characterization and preparation in Appendix B) to evaluate phosphate and sulfate release. Bare soil was also used as a control, and single superphosphate (SSP; 10 wt % P and 8 wt % S) was studied as a soluble fertilizer reference. A fixed relation between the mass of P from the fertilizers and the mass of soil was used, as 100 mg of P added per 1 kg of soil. Elemental sulfur, which does not contain P, was added with the same S dose of SSP (80 mg of S added per kg of soil).

The fertilizers were mixed with 50 g of soil in a plastic recipient containing a perforated lid to allow aerobic conditions. The flasks were kept in an incubator under 25 ºC with 0.2 mL of distilled water per g of soil, and soil

humidity was maintained at this value. Incubation times were 15, 30, 45, and 60 days, in triplicates. After each period, the triplicates were removed, the soil was dried, and the nutrients (sulfate and phosphate) were extracted.

Based on standard procedure,[116] exchangeable sulfate was extracted from the soil with acid ammonium acetate solution (39 g of ammonium acetate per 1 L of 0.25 M acetic acid). Soil samples (10g) were added to erlenmeyer flasks with 25 mL of the solution, and were kept under agitation for 30 min. Then 0.25 g of activated charcoal was added and the recipients were agitated for three additional minutes. The samples were filtered with Whatman paper nº 42, and the solution was collected for analysis. Sulfate concentration was determined by the turbidimetric method.[116] Briefly, 5 mL of the samples (diluted when necessary) were added in test tubes, followed by the addition of 0.5 mL of acid solution (0.1087 g of K_2SO_4 per 1 L of HCl 6M) and agitation. Then, 0.25 g of $BaCl_2$ were added and agitated, and sulfate concentration was determined using an UV-spectrophotometer (FEMTO 700 Plus) at 420 nm.

The available phosphate (P in soil solution) was extracted with water and anionic resin, as proposed by Quaggio and Raij.[132] Phosphate determination was performed as described in the "*Release test in solution*" section. The soil pH was measured in $CaCl_2$ solution (0.01 mol/L). The results from S and P quantification, and also pH data, were subjected to statistical analysis (ANOVA) with Tukey's test at the level of significance $p < 0.05$.

4.4. Results and Discussion

Fertilizer composites were prepared based on a polysulfide matrix and a dispersed phosphate source in different mass ratios. The materials (FIGURE B1, Appendix B) appeared more brittle as their phosphate content increased, with PolyS-Str75 being the only material to form a powder. In this case, the volume occupied by struvite was superior to the polysulfide; thus, the polymer did not behave as a matrix. PolyS-Bay25 presented a rapid expansion during the reaction, which led to more gases trapped in the reaction medium, producing a highly porous structure. TABLE 4.1 describes the composition of composites and raw materials. CHNS elemental analysis was conducted, as well as P extraction and determination (details in Appendix B).[117,131] While PolyS-Bay products present S, P, and N contents close to the expected values, PolyS-Str materials display higher P and S percentages. It could be explained by the loss of water and NH_3 from struvite structure when subjected to the elevated temperature (equation 4.1)[133] like the one used during the preparation of the composites, thus changing the total mass balance.

$$Mg(NH_4)(PO_4).6H_2O \rightarrow MgHPO_4(amorphous) + NH_3\uparrow + 6H_2O\uparrow \quad (4.1)$$

A considerable amount of N on the struvite composites is observed, indicating that only a small portion of NH_3 has volatilized, i.e., a different decomposition product was formed.

TABLE 4.1: List of composites and raw materials with their respective elemental compositions (% m/m), based on CHNS analysis and total P extraction method (details in Appendix B).

Sample	%C	%H	%N	%P	%S
PolyS-Str25	32.1	5.5	1.4	3.4	40.8
PolyS-Str50	23.8	5.0	3.0	7.8	29.8
PolyS-Str75	15.0	5.1	5.4	10.7	15.1
PolyS-Bay25	29.5	4.6	0.2	2.9	37.5
PolyS-Bay50	20.8	3.6	0.4	6.8	25.3
PolyS-Bay75	11.8	2.6	0.5	9.2	14.2
Struvite	0.3	6.2	6.3	11.1	-
Bayovar	1.8	0.2	0.9	13.1	-
S8	-	-	0.2	-	98.0

The morphology of the composites was investigated with SEM, as shown in FIGURE 4.2. SEM images of the phosphate sources can be seen in FIGURE B2(a,b) from Appendix B. Struvite displays solid particles with irregular shapes and uneven surface, while Bayóvar rock particles are round and smooth. FIGURE B2(c,d) displays a picture of previously prepared pure polysulfide (50 wt% S_8, 50 wt% SO) and its SEM image, which features a material with continuous uniform surface. PolyS-Str25 and PolyS-Str50 (FIGURE 4.2a and b, respectively) show mineral particles dispersed throughout a homogeneous and polymeric material. PolyS-Str75 (FIGURE 4.2c), on the other hand, exhibits agglomerates of the two phases instead of a continuous composite. While PolyS-Bay50 (FIGURE 4.2e) is similar to PolyS-Str50, PolyS-Bay25 (FIGURE 4.2d) presents a less homogeneous

material with a lumpy surface, characteristics that might implicate in a more friable composite. PolyS-Bay75 (FIGURE 4.2f) features Bayóvar rock particles attached to the polymeric phase. Compared with the pure polysulfide, the composites present pores and cavities, which increases the surface area and might favor matrix oxidation and facilitate water access to solubilize the phosphate source.

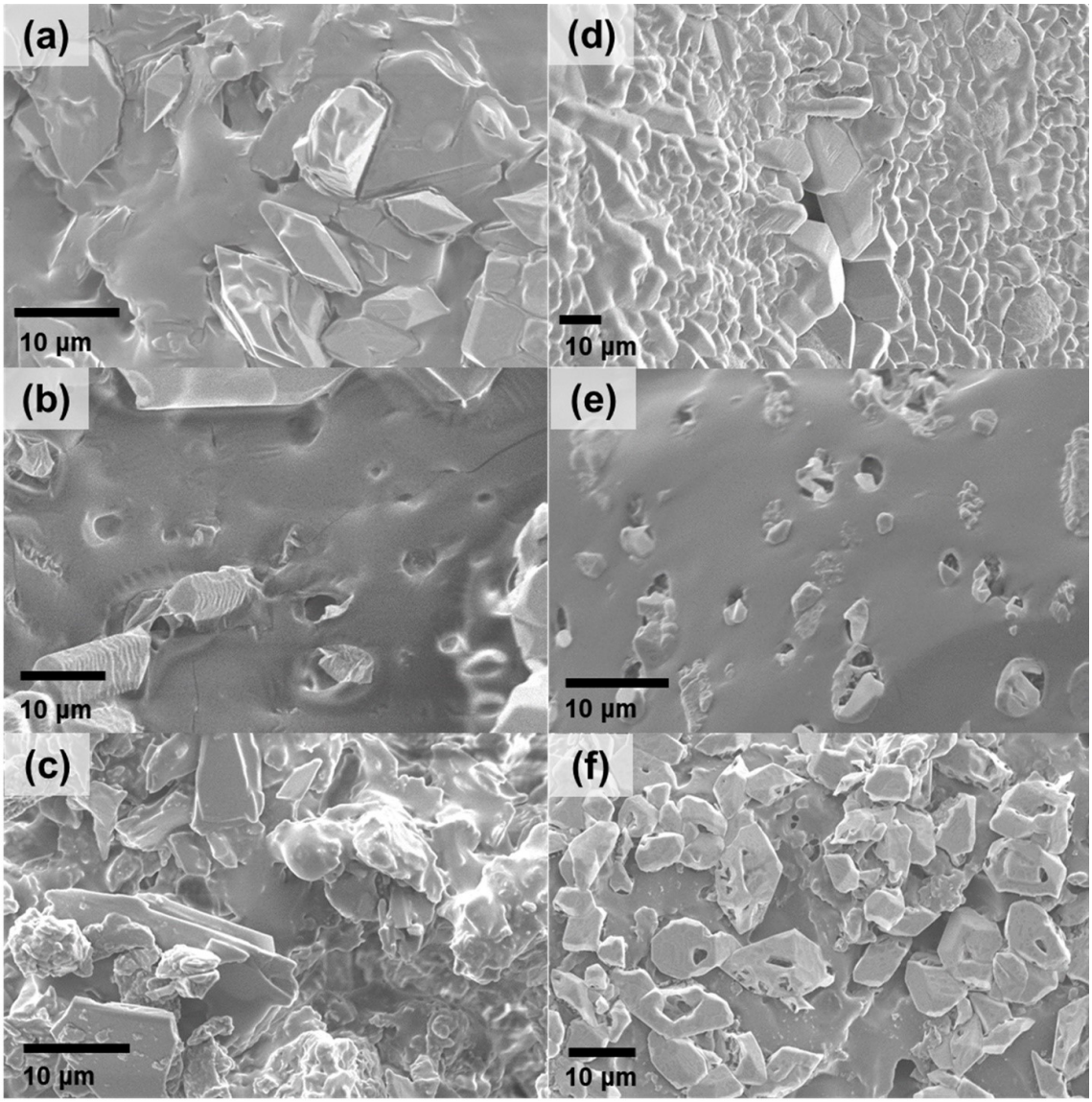

FIGURE 4.2: SEM images of (a) PolyS-Str25, (b) PolyS-Str50, (c) PolyS-Str75, (d) PolyS-Bay25, (e) PolyS-Bay50 and (f) PolyS-Bay75.

FIGURE 4.3 features the materials' structural elucidation with XRD (a,b) and FTIR (c,d). FIGURE 4.3a features XRD patterns of PolyS-Str25, PolyS-Str50, and PolyS-Str75. No peaks associated with pure struvite were detected in all composites, revealing the crystalline structure was completely disrupted after the reaction (the pure struvite pattern can be verified in Appendix B, FIGURE B3a). Besides, new peaks have matched with monohydrate form dittmarite ($Mg(NH_4)(PO_4).H_2O$) (ICDD 30-1491),[103] probably formed by releasing structural water and becoming more closely packed (equation 4.2). This phase transition was previously reported to occur in specific thermal treatment conditions, mainly when struvite is boiled in excess water.[133,134]

$$Mg(NH_4)(PO_4).6H_2O \rightarrow Mg(NH_4)(PO_4).H_2O + 5H_2O\uparrow \quad (4.2)$$

Accordingly, this clarifies why the N content of PolyS-Str products was still expressive after the composites' synthesis, as observed in TABLE 4.1. Dittmarite is also a valuable alternative for both N and P fertilization, and its higher nutrient concentration makes it more convenient for such application than struvite.[135] Despite this, few studies have explored dittmarite's role as fertilizer.

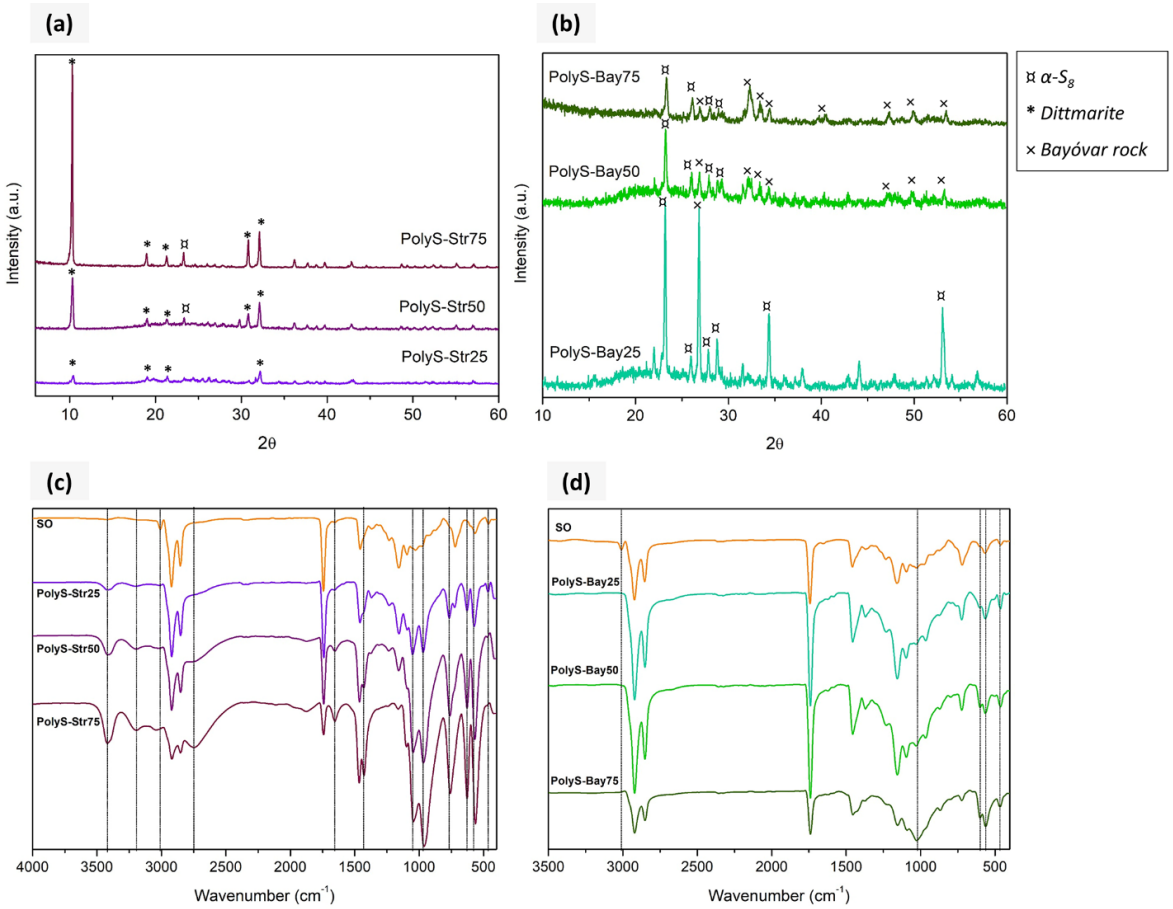

FIGURE 4.3: (a, b) XRD patterns of PolyS-Str and PolyS-Bay composites, respectively. (c, d) Normalized FTIR spectra of soybean oil (SO) compared with, respectively, PolyS-Str and PolyS-Bay composites.

PolyS-Bay materials (FIGURE 4.3b), on the other hand, display the same peaks of Bayóvar rock, as can be seen in FIGURE B3b (Appendix B). The signals are mostly attributed to carbonate apatite (ICDD 4-697) and quartz (ICDD 78-1254), proving the crystalline structure remains unaltered. Peaks associated with orthorhombic α-S_8 (ICDD 77-145) can also be observed in all the composites, indicating the presence of unreacted sulfur.

FIGURE 4.3 (c,d) presents normalized FTIR spectra of the composites in relation to soybean oil (SO). Struvite and Bayóvar results can be seen in FIGURE B4, Appendix B. As evidenced by XRD, the FTIR spectra of PolyS-Str products also show variations in bands attributed to the phosphate source, with no struvite signals, and new bands are consistent with dittmarite (TABLE B3, Appendix B).[136–140] Alkene vibration modes are observed in SO spectrum as weak stretching absorptions at 3010 cm^{-1} (H-C=C) and 1654 cm^{-1} (C=C), disappearing in the composites with C-S bond formation.[38,44,141] It is worth mentioning the increasing intensity of the 1655 cm^{-1} band in PolyS-Str is attributed to a characteristic low frequency H_2O bending signal of dittmarite instead of signaling the presence of unsaturation. Alkane bands appear around 2920 cm^{-1} and 2850 cm^{-1} (CH_2 stretching), and 1460 cm-1 (CH_2 bending).[142] PolyS-Bay spectra (FIGURE 4.3d) shows typical Bayóvar vibrations,[140] as well as the suppression of alkene bands. Furthermore, both struvite and Bayóvar composites display a polysulfide S-S stretching band near 465 cm^{-1}, confirming the polymeric structure's formation.

The fatty acid composition of soybean oil was estimated with ^1H NMR spectrum (FIGURE B5, Appendix B).[143] TABLE B4 shows that more than 83 % of the triglycerides' fatty acids are unsaturated, and the majority corresponds to linoleic acid. The percentage of unreacted alkene bonds can also be determined with ^1H NMR spectra of the materials.[50] To understand how the different P sources can affect the conversion of the polysulfide, two composites were investigated by ^1H NMR, PolyS-Str50, and PolyS-Bay50. The following signals are observed in PolyS-Str50 spectrum (FIGURE 4.4a): δ = 0.91 ppm (CH_3, h), δ = 1.32 and 1.72 ppm (CHS, g), δ = 2.09 and 2.15 ppm ($CH=CHCH_2$, f), δ = 2.45 and 2.51 ppm ($CH_2C=O$, e), δ = 4.54, 4.69 ppm (CH_2 glycerol, c/d), δ = 5.55 ppm (unreacted CH=CH, b), δ = 5.75 ppm

(CH glycerol, a). For PolyS-Bay50 composite (FIGURE 4.4b) the signals were: δ = 0.91 ppm (CH_3, h), δ = 1.32 and 1.72 ppm (CHS, g), δ = 2.08 and 2.15 ppm ($CH=CHCH_2$, f), δ = 2.45 and 2.51 ppm ($CH_2C=O$, e), δ = 4.54, 4.69 ppm (CH_2 glycerol, c/d), δ = 5.55 ppm (unreacted CH=CH, b), δ = 5.75 ppm (CH glycerol, a). Comparing the ratio of alkene to CH_3 peak areas of soybean oil (1.00:1.03) to those from PolyS-Str50 (1.70:7.27), it is revealed the reaction consumed 76% of the unsaturated bonds, while the data for PolyS-Bay50 (1.02:8.84) indicates 86 % of the alkenes reacted. PolyS-Str50 lower conversion is possibly related to the water released from struvite hindering the monomers.

Solid-state ^{31}P NMR elucidates the difference of phosphorous environment after the preparation of the composites (FIGURE 4.4c). Struvite shows a prominent narrow peak at the chemical shift +6.1 ppm. In addition, small shoulders at +5.1 and 4.8 ppm indicate another phase in low concentration, typically attributed to kovdorskite ($Mg_2PO_4(OH).3H_2O$), possibly formed after ammonia volatilization.[144] In PolyS-Str50 an intense peak also occurs at +6.1 ppm with a shoulder at +4.6 ppm, and a low intensity peak appeared at +2.8 ppm. Dittmarite is reported to show a chemical shift at +6.2 ppm, which is very close to the struvite signal since both species have similar P enviroments.[145] The new peak can be related to the formation of a poorly crystalline fragment, as the phosphate phase is mixed in the polymeric matrix. Bayóvar and PolyS-Bay50 display a single broad peak at +2.6 and 2.7 ppm, respectively, compatible with apatite patterns.[146]

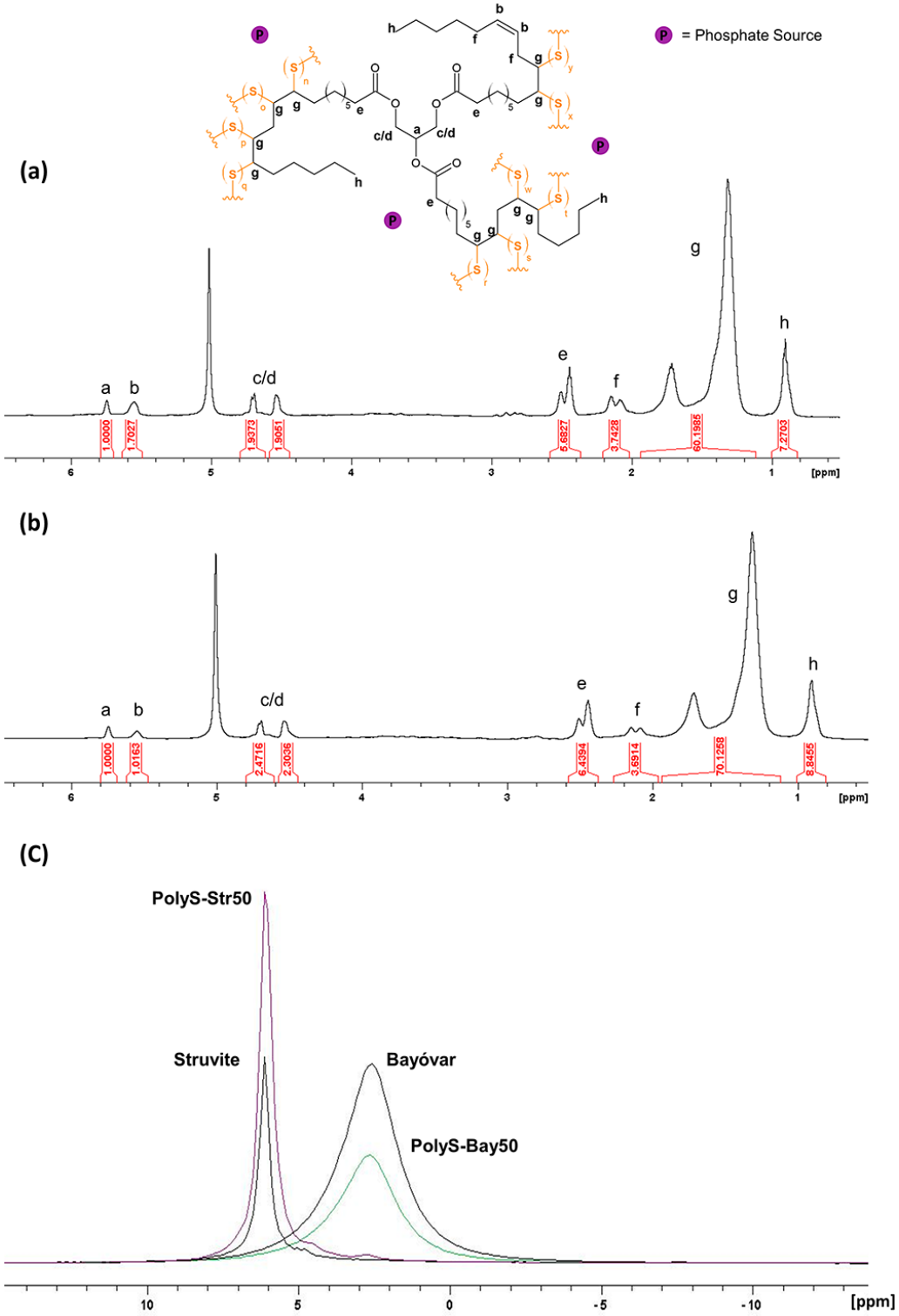

FIGURE 4.4: (a) ^{1}H NMR spectrum of PolyS-Str50, (b) ^{1}H NMR spectrum of PolyS-Bay50, (c) Solid state ^{31}P NMR spectra of Struvite, PolyS-Str50, Bayòvar and PolyS-Bay50.

FIGURE B6 from Appendix B features TGA and DTG profiles from the composites and their starting materials. Struvite presents a characteristic thermal behavior with 53 % weight loss from 40 to 100 ºC, mainly due to the elimination of structural water and ammonia.[133] The thermal decomposition of PolyS-Str products is mostly attributed to the polysulfide phase. The first stage represents the sulfur domain and the following step, the degradation of the triglyceride segment. The first weight loss is revealed to be superior to the amount of S of the material's composition, evidenced in TABLE B5. This additional mass corresponds to the decomposition of dittmarite structure, with simultaneous dehydration and release of NH_3 (equation 4.3).[147,148]

$$Mg(NH_4)(PO_4).H_2O \rightarrow MgHPO_4 + NH_3\uparrow + H_2O\uparrow \quad (4.3)$$

Dittmarite is more thermally stable than struvite, as ammonium ions are strongly bonded and trapped between much more packed layers, requiring higher temperatures for removal.[134] This event is also perceived by the shoulders at the DTG curves, and its contribution is more significant as the mineral content increases and is less hindered by the polymeric matrix. The thermogravimetric behavior of PolyS-Bay materials is more compatible with the polysulfide degradation, and the DTG peaks are less dislocated, suggesting a weaker interaction with the phosphate phase.

DSC thermograms are displayed in FIGURE 4.5. Since neither dittmarite nor Bayóvar present thermal events below 200 ºC, the peaks observed in all composites are attributed exclusively to unreacted S_8. Elemental sulfur typically shows three endothermic peaks: a solid phase transition around 105 ºC, melting at 119 ºC, and the formation of catena-sulfur at 175 ºC.[119] Likewise, melting peaks in the same region appear in the

composites' patterns.[45,48,65] The fraction of residual S_8 in the composites was estimated (TABLE 4.2) using a calibration curve obtained from the correlation of different pure S_8 masses and the area of their respective DSC endotherms (FIGURE B7).[48,65] Based on CHNS results for total sulfur, and the calculated free S_8 by DSC, S fraction from the polysulfide structure was also estimated. TABLE 4.2 shows a better conversion of the comonomers in the presence of Bayóvar than struvite. As discussed before, water from struvite dehydration can partially disturb the reaction, especially when it is trapped inside a larger volume of the mineral.

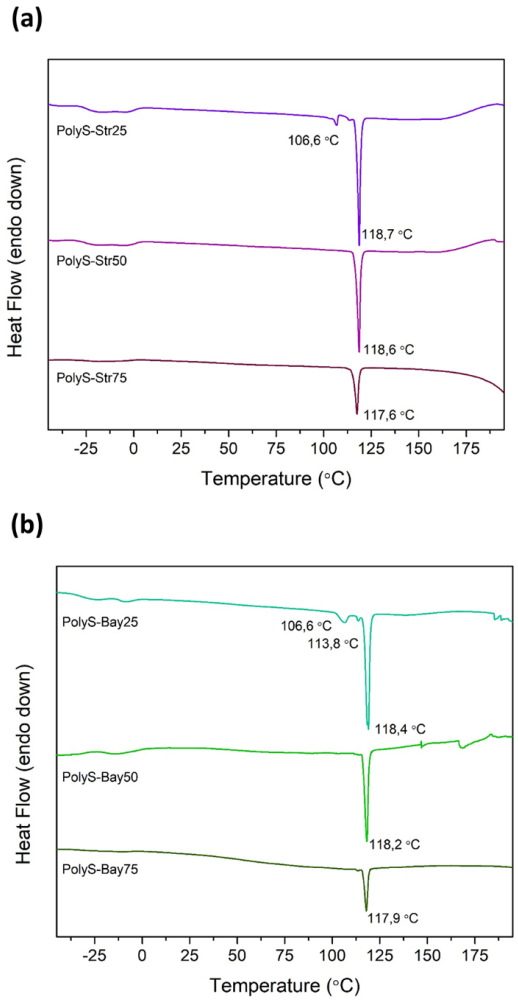

FIGURE 4.5: DSC patterns of (a) PolyS-Str and (b) PolyS-Bay composites.

TABLE 4.2: Residual sulfur in the composites, estimated with via DSC and predicted polymeric S.

Sample	Mass (g)	ΔH (J/g)	$S_{8\ free}$ (% of total)	$S_{8\ free}$ (% of S)	$S_{8\ poli}$ (% of S)
PolyS-Str25	0.0042	8.983	18	44	56
PolyS-Str50	0.0046	7.379	15	50	50
PolyS-Str75	0.0041	4.326	9	60	40
PolyS-Bay25	0.0040	7.298	14	37	63
PolyS-Bay50	0.0043	4.608	9	36	64
PolyS-Bay75	0.0046	1.865	4	28	72

Before the release tests in citric acid and in soil, all composites were ground in a blade grinder to be used in powdered form. Images from optical microscopy were recorded in order to verify the grain size of these ground materials (FIGURE B8 and B9 from Appendix B). The composites present a heterogeneous grain size distribution and, in general, are bigger than the pristine phosphate sources, elemental sulfur, and SSP. While elemental sulfur grains are mostly < 50 μm, PolyS-Str and PolyS-Bay composites are on average superior to this, with some particles even as large as 300 μm. PolyS-Str75 displays smaller particles than the other composites, as it has fewer polysulfide coverage.

Phosphorous release trends were evaluated in citric acid solution (2 %) for 7 days, as shown in FIGURE 4.6. The test simulates phosphate dissolution in a harsher environment than from what happens in agricultural soils, providing the release pattern in a shorter period, as the acidic condition

greatly favors the process.[117] The test is also useful to specifically evaluate the material's susceptibility to dissolution without interferences from other variables present in soil. The experiment does not evaluate the matrix's chemical effect on phosphate dissolution, since the solution is already acid (pH 2.3), with no microorganisms to oxidize the polysulfide; however, the test exhibits the physical role of the matrix.

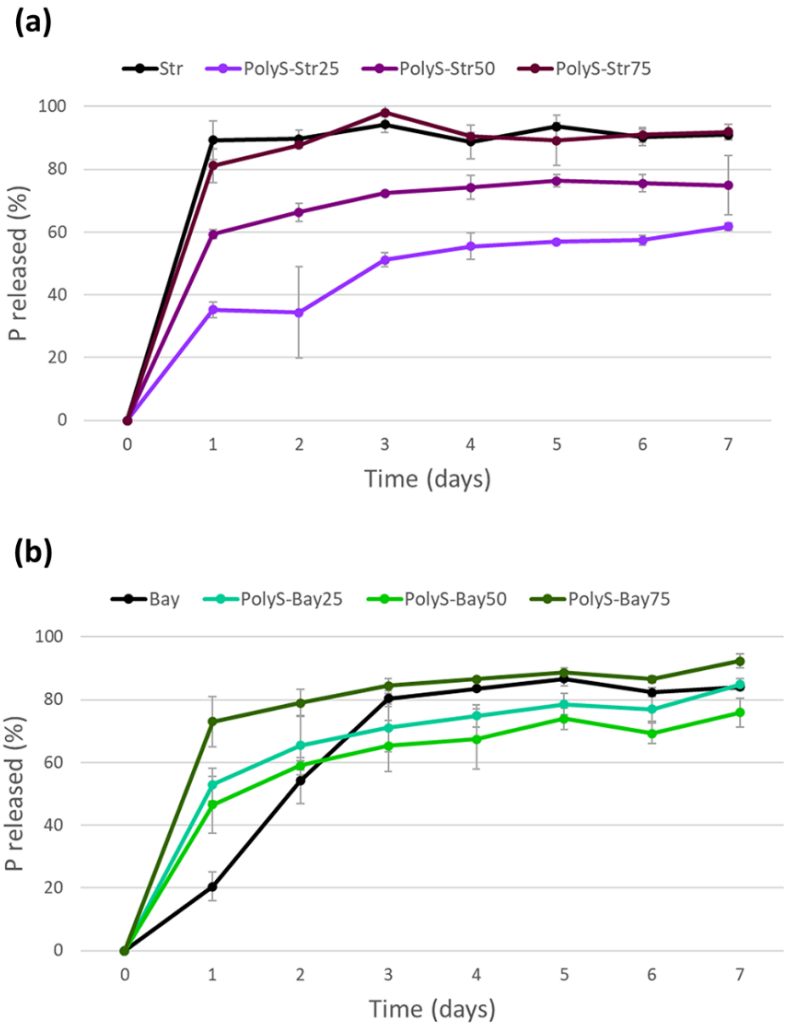

FIGURE 4.6: Phosphorous released over time in citric acid solution (2 wt %, pH 2.3) by (a) Struvite, PolyS-Str25, PolyS-Str50, and PolyS-Str75 and (b) Bayóvar rock, PolyS-Bay25, PolyS-Bay50 and PolyS-Bay75.

Analyzing both graphs, the polysulfide matrix displays a distinct function in each system, providing a physical barrier for the controlled-release of the highly soluble source (FIGURE 4.6a) and, at the same time, acting as a medium for dispersing particles with low P availability to enhance the release rate (FIGURE 4.6b). Struvite presents a fast initial P release, reaching 89 % in the first 24 hours, after which it enters an equilibrium. PolyS-Str75 features a similar behavior, releasing 81 % of P from dittmarite in 1 day. Dittmarite dissolution pattern is equivalent to struvite's, since once dittmarite is in solution, it rehydrates to struvite before dissolution.[135] It has been vastly reported in the literature that struvite solubility is strongly dependent on the pH, presenting insoluble behavior in water, similarly to PR, and high solubility in acidic environments, where it performs like commercial fertilizers (e.g., single superphosphate (SSP) and triple superphosphate (TSP)),[95,96,104] which explains the rapid trend observed for struvite and PolyS-Str75. PolyS-Str25 and PolyS-Str50 display a gradual release of P, with initial values of respectively 35 % and 59 %. These results are directly related to the amount of polysulfide, showing the matrix role as a physical barrier to regulate solution penetration and control the nutrient release. The moderate delivery can prevent fertilizer escape to the environment and its impacts. By the end of the experiment, the maximal P released was 94 %, 92 %, 76 %, and 62 % for Str, PolyS-Str75, PolyS-Str50, and PolyS-Str25, respectively.

Bayóvar rock presents only 20 % P release in the first 24 hours, and its dissolution stays lower than all composites until the third day. Similar behavior was observed by Giroto et al. (2015), in which hydroxyapatite was compared to composites containing the P source in a thermoplastic starch

matrix.[74] With increasing amounts of the polymer, the greater was P dissolution, attributed to the matrix effect in preventing particle agglomeration. The present results indicate that the polysulfide provides the same influence in Bayóvar rock solubilization. PolyS-Bay75 displays higher P release than the others, both in the initial and equilibrium points, with 73 % on the first day and 92 % on the last. PolyS-Bay50 and PolyS-Bay25 have a similar profile. However, unlike the struvite composites with the same ratio, PolyS-Bay25 values are slightly bigger than PolyS-Bay50. It could be due to the higher porosity of PolyS-Bay25, observed in SEM images (FIGURE 4.2d).

The behavior of the composites in soil dynamics was investigated with a fixed P dose at different times. FIGURE 4.7 shows the percentage of sulfur oxidation achieved by each composite in relation to elemental sulfur. Although the initial S concentration was not fixed (see the complete list in TABLE B6, Appendix B) and sulfate formation was primarily evaluated to establish a correlation with P dissolution, converting the data in terms of S oxidation gives an essential key to understanding the synergism of this system. Despite the smaller grain size of S_8, as evidenced in FIGURE B9, it still displayed inferior oxidation compared to the polysulfide in struvite composites (FIGURE 4.7a), except for PolyS-Str25. The polymeric-sulfur structure was fundamental to improve the oxidation rate; however, it is interesting to notice this performance grows, especially with increasing relative P contents in the materials, with PolyS-Str75 showing the best outcome throughout the experiment. After 15 days, PolyS-Str75 result was almost three times bigger than S_8, reaching nearly 50 % of S oxidation in 32 days. This boost in the oxidation demonstrates a direct relation between P availability and microbial activity. As a limiting nutrient for soil's biota, the

presence of P stimulates microorganism growth and activity, thus enhancing the potential for S oxidation. The polysulfide's carbonic fraction could have also contributed to the bioactivity as a source of energy to heterotrophic microorganisms that help the oxidation. It is valid to highlight that PolyS-Str25 initial S dose might be above the soil's capacity to oxidize, resulting in much lower efficiency. FIGURE B10 shows that PolyS-Str25 actually produced more sulfate than the others, probably reaching a point of saturation that interrupted sulfate formation and reduced the oxidation rate.[22]

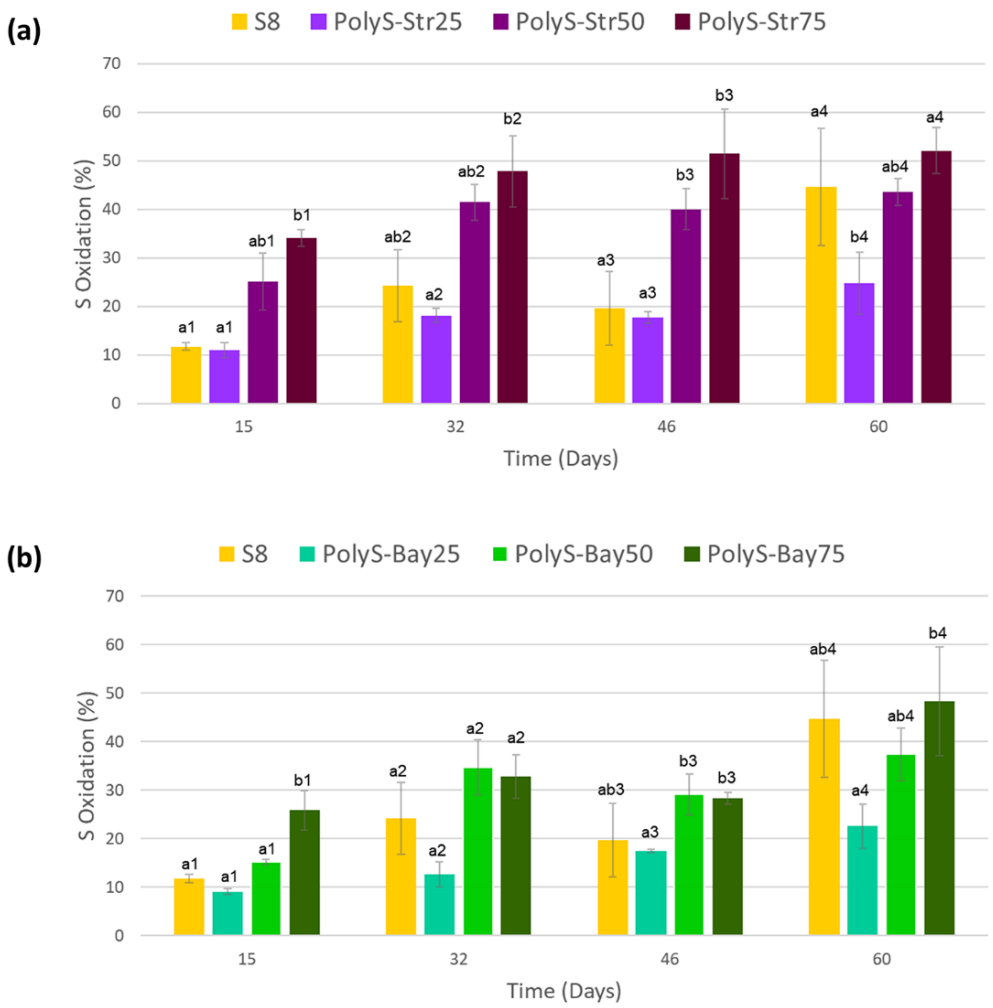

FIGURE 4.7: Sulfur oxidation (%) in soil over time of (a) struvite and (b) Bayóvar composites in relation to elemental sulfur. Statistical relevance was

analyzed for each group (index 1, 2, 3, and 4 for 15, 32, 46, and 60 days, respectively). Index a and b indicate the statistical differences.

Bayóvar composites (FIGURE 4.7b) follow the same trend regarding the P content effect. Given the apatite's low reactivity and solubility, the results are very compatible with those achieved with struvite, being an initial indicator of P availability.

FIGURE 4.8 displays the concentration of available P throughout time. Struvite, SSP, and the PolyS-Str composites were statistically identical in all periods evaluated, reaching around 40 mg/dm^3. In Bayóvar's case, the presence of the polysulfide had a clear influence in improving P dissolution, with PolyS-Bay composites performing similarly as the positive control SSP, in comparison to the low results of pure Bayóvar. As previously discussed, struvite becomes rapidly soluble in acidic environments and at soil pH as low as 6.5,[135] reflecting on the observed patterns of the pristine compound in contrast to the phosphate rock. It could explain why its dissolution behavior was not as affected as the Bayóvar rock by the presence of sulfate. The polymer's barrier effect to dittmarite featured in the citric acid test could have also played a role and balanced the acidity effect, with PolyS-Str25 leading to the highest sulfate formation and lowest pH (FIGURE B11), but also the largest polymer content to restrict the release. The enhanced performance of Bayóvar composites could also be related to the dispersion effect observed in the citric acid solution.

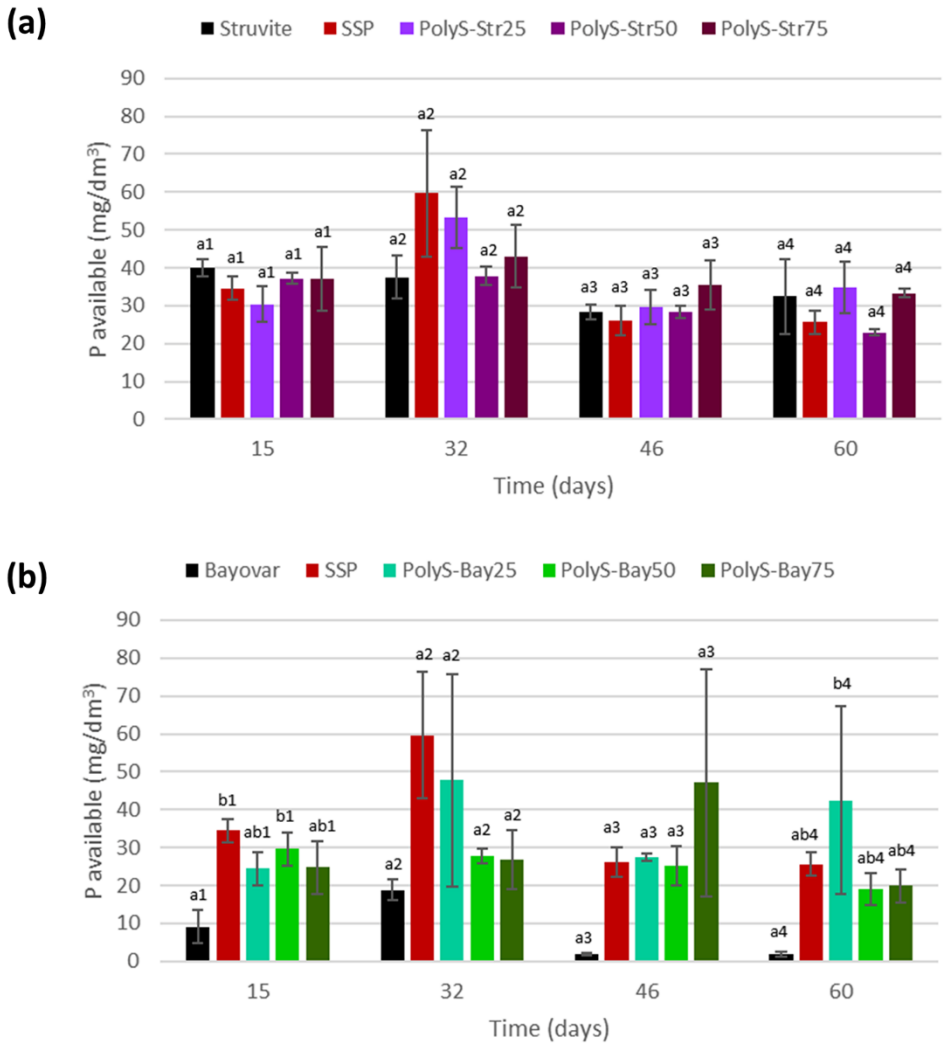

FIGURE 4.8: Fertilizer phosphorus recovery as P available in soil over time of (a) struvite composites, struvite, and SSP, and (b) Bayovar composites, Bayovar rock, and SSP. Statistical relevance was analyzed for each group of days (index 1, 2, 3, and 4 for 15, 32, 46, and 60 days, respectively). Index a and b indicate the statistical differences.

It is important to mention that P release is possibly slightly underestimated for the composites since a fraction of the available P was likely consumed by microorganisms that promote the polysulfide oxidation. Besides, the results could be underestimated because the phosphate

measurement with the resin method only shows the available P for plants. On the one hand, this simulates more accurately the fertilizer nutritional potential for plant uptake, but on the other hand, it does not show how much of the phosphate was actually solubilized, as part of it is precipitated with other soil components. This immobilization effect is evidenced by the general reduction of P availability after 32 days.

The results demonstrated that P and S interaction significantly improves nutrient delivery of both elements. Considering that all composites displayed a consistent P pattern to the soluble commercial source SSP, the use of the polysulfide matrix was efficient to significantly improve the performance of a more sustainable P source with low reactivity like Bayóvar rock, and can also produce great results when applied with the greener and more soluble struvite, with the additional benefit of providing sulfur with phosphorous.

4.5. Conclusion

In conclusion, composites based on the dispersion of environmentally-friendly phosphate sources – Bayóvar rock and struvite – on a polysulfide matrix were investigated for improving the delivery of both P and S. The materials were produced via inverse vulcanization between soybean oil and elemental sulfur in the presence of varying amounts of the P source. Chemical characterizations revealed struvite underwent a phase transition to dittmarite during the preparation of the composites, in which phosphate became more concentrated. Bayóvar composites displayed a porous structure, ideal for greater surface contact with soil microorganisms and other species. Phosphate release trends in acid solution showed the polymer

function as a physical barrier for struvite's fast release, while for Bayóvar the polysulfide improved P dissolution by reducing phosphate agglomeration. In soil, a positive dynamic was revealed between P and S. Sulfur oxidation was favored by the presence of higher P contents, which can be attributed to the fact that P is a vital element for microorganisms' development. Similarly to the citric acid test, P release in soil was greatly enhanced in Bayóvar composites, due to phosphate dispersion and local acidity from sulfate formation. As for struvite composites, the polysulfide barrier effect balanced out the acidity effect, performing similarly to the pure struvite and SSP. Overall, the composites displayed satisfactory results for S and P delivery, and the combination of the materials proved to be a useful strategy, which should be further explored in field conditions.

5. – Chapter III: A Soil-Plant Study with Soybean Cultivation under Polysulfide-Struvite Fertilization

The content of this chapter is an adaptation of the manuscript entitled “Co-fertilization of Sulfur and Struvite-Phosphorus in a Slow-Release Fertilizer Improves Soybean Cultivation” by Valle et al. (2022), published in Frontiers in Plant Science (doi: 10.3389/fpls.2022.861574).

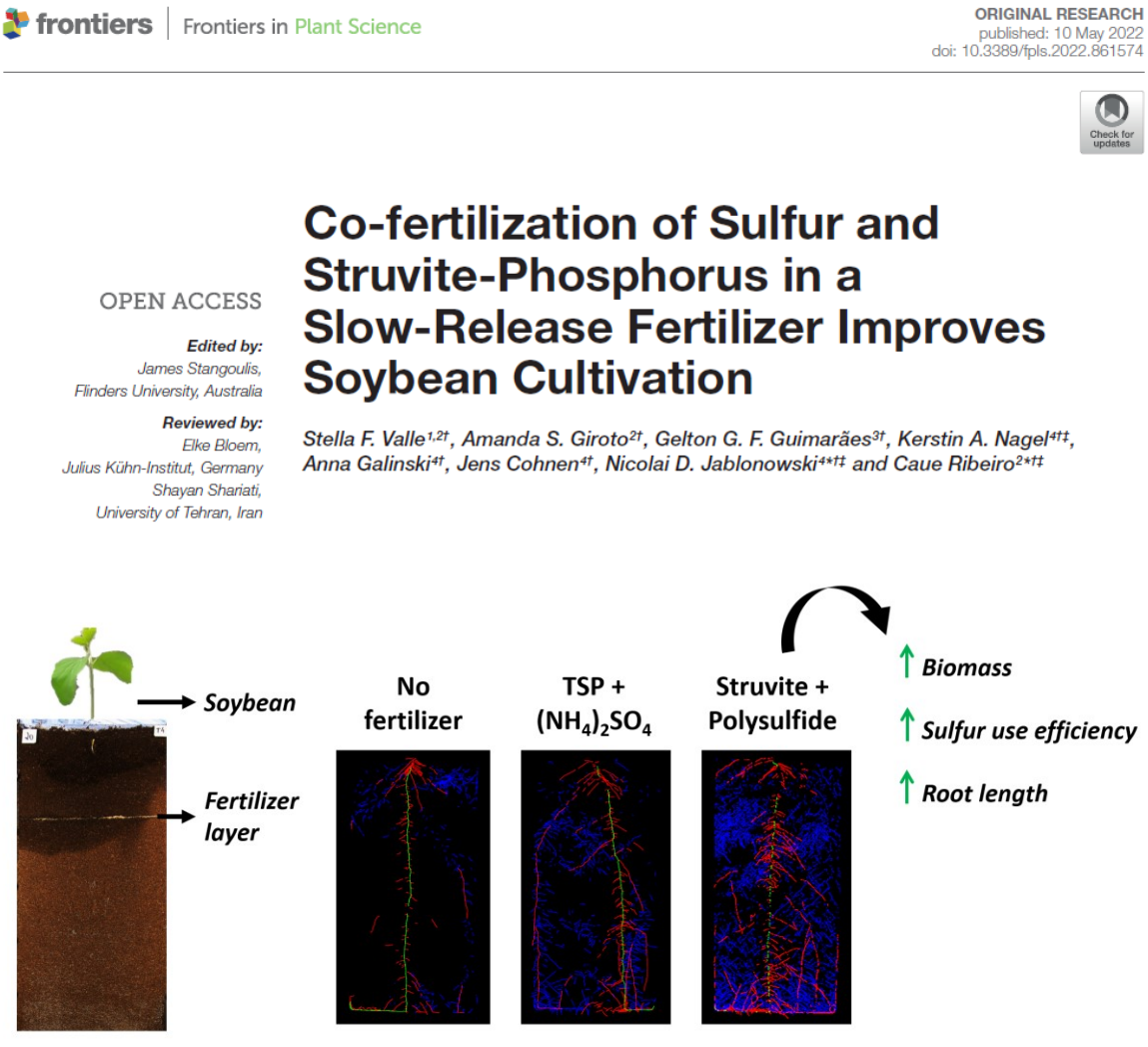

5.1. Abstract

In face of the alarming world population growth predictions and its threat to food security, the development of sustainable fertilizer alternatives is urgent. Moreover, fertilizer performance should be assessed not only in terms of yield but also root system development, as it impacts soil fertility and crop productivity. Fertilizers containing a polysulfide matrix (PS) with dispersed struvite (St) were studied for S and P nutrition due to their controlled-release behavior. Soybean cultivation in a closed system with St/PS composites provided superior biomass compared to a reference of triple superphosphate (TSP) with ammonium sulfate (AS), with up to 3 and 10 times higher mass of shoots and roots, respectively. Root system architectural changes may explain these results, with a higher proliferation of second order lateral roots in response to struvite ongoing P delivery. The total root length was between 1942 and 4291 cm for plants under St/PS composites and only 982 cm with TSP/AS. While phosphorus uptake efficiency was similar in all fertilized treatments (11-14%), St/PS achieved a 22% sulfur uptake efficiency against only 8% from TSP/AS. Overall, the composites showed great potential as efficient slow-release fertilizers for enhanced soybean productivity.

5.2. Introduction

Phosphorus (P) is vital for plant nutrition and growth, and one of the most limiting elements for crop production. Agriculture represents nearly 90% of P use worldwide, yet, its current consumption rate has been unsustainable and incompatible with natural cycle of the element, as phosphate rocks are non-renewable resources.[91,94,97] Moreover, the efficiency of P fertilizers is significantly restricted by soil immobilization processes of sorption and precipitation.[101] Conventional P fertilizers are readily soluble and

thus release P faster than plants can uptake, contributing to soil fixation. These sources are also highly susceptible to runoff losses, causing eutrophication of water bodies and associated environmental damages.[87,88]

Therefore, sustainable solutions for phosphorus fertilization are an urgent concern facing food security. Struvite ($MgNH_4PO_4 \cdot 6H_2O$) is a promising alternative, recovered from municipal wastewater streams, which could reduce the P cycle gap.[95,96,98–101] In addition, it serves as a source of nitrogen (N) and magnesium (Mg), essential macronutrients for plant development.[95,96] Moreover, struvite is considered as a slow-release fertilizer due to its low water solubility, which leads to reduced losses and a prolonged residual value to crops.[98] Nevertheless, low solubility may also result in an inadequate phosphorous supply to plants. Struvite dissolution can be significantly improved in acidic conditions and is highly affected by particle size, and it is solubilized at a much slower rate when in granular form than as a powder.[102–104,149] For field application, however, fertilizers are usually managed as granules or pellets, which are easier for handling and storage.[29]

Therefore, by controlling local acidity and particle size, struvite can provide P fertilization more efficiently and safely. Recently, our research group accomplished both of these criteria with the development of fertilizer composites based on a polysulfide matrix containing dispersed ground struvite.[107] Matrices are strategic for getting around the particle size problem, as they can be processed as granules, while simultaneously keeping small P particles from agglomerating.[71] At the same time, the matrix acts as a barrier, preventing a fast P delivery.[79] The studied polysulfide is an especially interesting material as it can provide sulfur to plants, an important macronutrient for plant growth that is frequently unavailable in agricultural soils.[10,12,65] The polysulfide structure contains polymeric sulfur chains,

obtained by inverse vulcanization of elemental sulfur (S_8), a residue from the oil industry.[34,39–42] For plant uptake, both the polysulfide and pure S_8 have to be oxidized in soil to sulfate, a slow rate process promoted by soil microorganisms.[14,22] The polysulfides from our previous studies displayed superior oxidation compared to S_8, especially when combined with struvite.[65,107] Additionally, sulfate formation lowered the local pH, assisting struvite dissolution.[107]

Despite its potential as an environmentally friendly fertilizer, the struvite-polysulfide effects on plants are still unknown, and its dynamics in a soil-plant system should be further investigated. Most importantly, we were interested in understanding the fertilizer's influence on root development and spatial distribution of roots in the growth medium, as an indication of how the fertilizer can be accessed by plants. In the current work we investigated the effect of struvite-polysulfide fertilizers on nutrient uptake, biomass formation, and root system architecture. Soybean (*Glycine max L.*) was selected for the study, as a plant with high protein content and high S demand.[150,151] We hypothesized that soybean would respond differently to the struvite-polysulfide composites compared to a soluble reference, due to the controlled delivery of P. In addition, we hypothesized that the S chemical structure from the fertilizers would affect S supply and soybean root system traits, as polysulfides need to be biologically converted to sulfate.

5.3. Materials and Methods

Preparation of Composites

Composite fertilizers containing a polysulfide matrix and dispersed struvite particles were prepared as described by Valle et al. (2021),[107] illustrated in FIGURE 5.1. Prior to the preparation of the

composites, struvite (Ostara Crystal Green®, United Kingdom) was pulverized in an orbital mill (Servitech CT 241, Brazil) with alumina balls, followed by sieving (<0.15 mm). The polysulfide structure was obtained using the inverse vulcanization between elemental sulfur (S_8; Synth, Brazil) and soybean oil (Liza, Brazil), each at 50 wt%. This method is solvent-free and has no byproduct formation. The reaction was conducted in the presence of ground struvite, with different mass ratios (25, 50, and 75 wt% of struvite in relation to the composite). All compounds were mixed in a flask and the system was kept under constant agitation and heat, using a mechanical stirrer and oil bath. The temperature was kept at approximately 165º C, allowing the ring-opening polymerization (ROP) of S_8, followed by the reaction between bi-radical polymeric sulfur chains and unsaturated bonds from soybean oil, until a light brown material was obtained. In order to compare the polysulfide-based composites with the struvite reference (1 mm granules) in the greenhouse experiment, the composites were roughly ground (< 1 mm) in a blade grinder (Philco, Brazil).

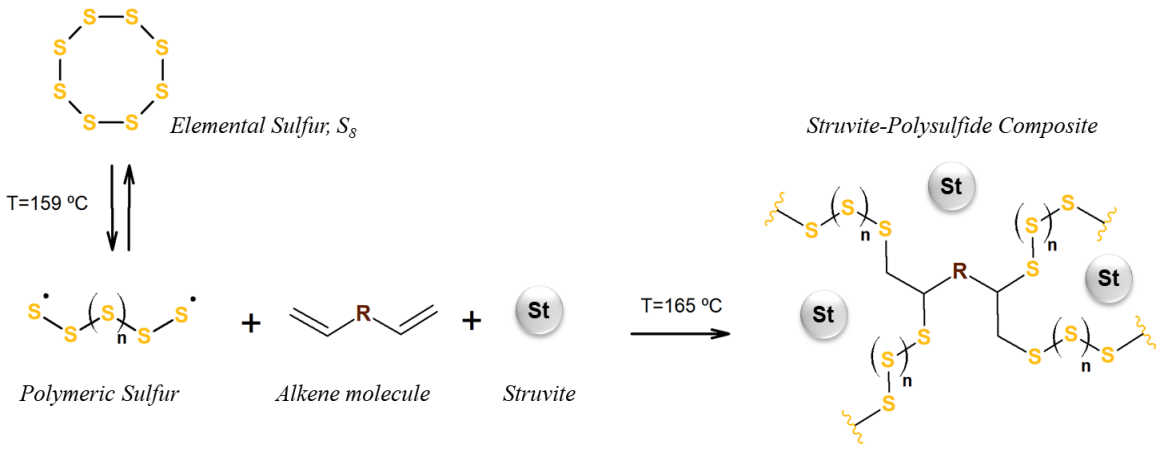

FIGURE 5.1: Preparation of the Struvite-Polysulfide fertilizer composite (generic structure). Elemental sulfur undergoes ring-opening polymerization

and reacts with alkene molecules (in this work, soybean oil), in the presence of ground struvite, producing the polysulfide matrix with dispersed phosphate particles.

Greenhouse Experiment

To test the agronomic efficiency of the St/PS composite fertilizers and their effect on root and shoot soybean plant performance, an experiment was conducted under controlled greenhouse conditions at the Institute of Bio- and Geosciences, IBG-2: Plant Sciences, *Forschungszentrum Jülich GmbH*, Germany (50°54′36″N, 6°24′49″E), from May to July 2020. An average temperature of 23º C and air humidity of 48% were maintained at the greenhouse over this period.

In order to evaluate the combined effect of struvite and polysulfide, the following treatments were applied: no fertilizer (control); a positive reference with the highly soluble sources triple superphosphate for P and ammonium sulfate for S (TSP/AS); mixed pure struvite and elemental sulfur powder (St/S8); and ground fertilizer composites with different mass ratios of struvite and polysulfide – St 25/PS, St 50/PS, and St 75/PS (respectively with 25, 50, and 75 wt% of struvite). A fixed ratio of 50 mg of S per kg of soil was established for all fertilized treatments. To achieve a P concentration of 200 mg per kg of soil, additional struvite was supplied with the composite treatments. Since the aim was to study P and S effects on plant development, a fixed dose of N was supplied to all fertilized treatments to make sure it was sufficiently provided and not a limiting factor to soybean growth. Nitrogen was supplemented with ammonium nitrate in all fertilized treatments to complete 300 mg of N/kg of soil. Potassium, zinc, and copper were also supplemented in concentrations of 200, 5, and 1.5 mg/kg,

respectively, using a nutrient solution containing KCl, ZnCl, and $CuSO_4$. Detailed information on nutrient content and supply can be found in Table C1.

Peat substrate ("Nullerde", Einheitserde/Patzer Erden, Germany) was selected as a growth medium due to an assumed high microbial activity of organic-rich environments, which is necessary to promote S oxidation from the polysulfide and S_8. The substrate consisted of a mixture of 30% clay and 70% white peat, with no prior addition of fertilizers. Detailed substrate characterization can be seen in TABLE C2, Appendix C. Before the experiment, the substrate was shredded and sieved (<0.7 cm) to remove coarse particles. Flat rhizotrons (60 x 30 x 2 cm)[152] were filled with 2 kg of the substrate (approximately 3.36 dm^3), with 10 replicates per treatment. Fertilizers were added 8 days before sowing, placed on a fixed layer at 40 cm from the bottom of the rhizotron (at approximately 16 cm from the substrate surface, 20 cm from the rhizotron top), as illustrated in FIGURE 5.2a. After completely filling up the rhizotrons, 100 mL of tap water was added to moisten the medium and allow initial solubilization of the fertilizers.

Soybean seeds (*Glycine max L.*, Eiko cultivar; Asgrow, United States) were pre-germinated in Petri dishes with moistened filter paper.[153] The Petri dishes were sealed and covered with aluminum foil, and kept incubated for 48 h in the greenhouse. Seedlings with equal radical sizes were then selected and transplanted, using one seedling per rhizotron.[153] The seedlings were placed in a centralized position close to the transparent plate of the rhizotrons, at a depth of approximately 2 cm from the substrate surface.[154] The rhizotrons were kept at 45º inclination in a fixed randomized position, with the transparent plates facing downwards, covered by black plastic sheets,[152,154] as shown in FIGURE 5.2b.

The growth medium was moistened throughout the experiment with 100-250 mL water supply two times per week, maintaining approximately 14-30 % of the substrate field capacity. All plants were treated against downy mildew contamination with Ortiva® (Syngenta, Germany), applied at 19 days from sowing. Images of the visible root system were recorded 2-3 times a week, along with measurements of the number of leaves and plant height. Harvest was conducted after 40 days of cultivation in the rhizotrons. Prior to shoot harvest, SPAD values were measured from trifoliate leaves at the uppermost node with a Chlorophyll Meter SPAD-502Plus (Konica Minolta). The growth medium and the roots were collected in layers, cut as illustrated in FIGURE 5.2c: A (top layer, between 0 and 10 cm depth), B (middle layer, between 10 and 30 cm depth), and C (bottom layer, below 30 cm depth). Roots were separated from the substrate samples with a sieve (9 x 5 mm mesh holes).

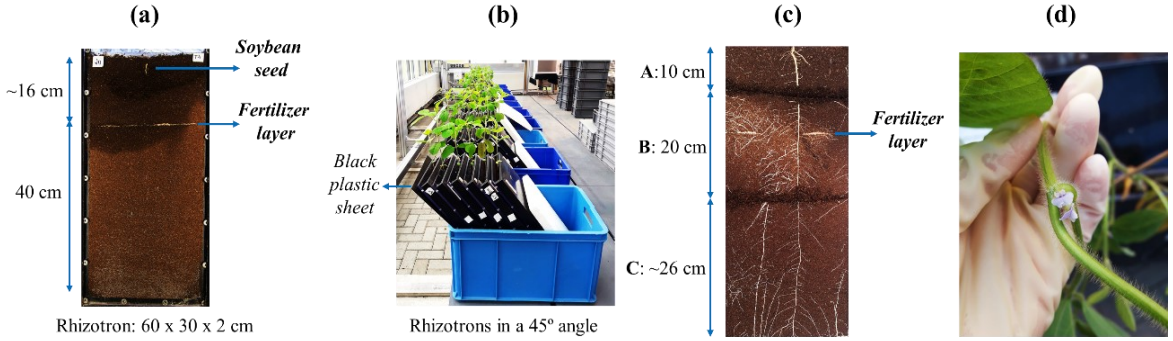

FIGURE 5.2: (a) Rhizotron with a fixed layer of fertilizer and pre-germinated soybean seedling; (b) Rhizotrons during cultivation; (c) Substrate and root sampling in layers A (top layer, 10 cm), B (middle layer, 20 cm, including the fertilizer layer), and C (bottom layer, ~26 cm); (d) Flower bloom 30 days after sowing.

Post-Harvest Analysis

After harvesting, leaf area was determined with a leaf area meter (LI-3100, LI-COR) and, subsequently, the shoots were dried in an oven at 60° C until constant weight to determine total dry biomass. Roots were immediately stored in flasks containing 50% v/v ethanol solution and kept in a dark cooling chamber at 4º C until further analysis. Roots were carefully washed and scanned (Epson Expression 10000 XL) for measurements of total root length, average root diameter, and root surface area, using WinRHIZO Pro V.2020a software, followed by drying in the same conditions as the shoots. Dry biomass of shoots and roots were measured, and shoot:root-ratio based on biomass was calculated.

Chemical analysis of the ground biomass was determined by inductively coupled plasma optical emission spectrometry (ICP-OES; Thermo Scientific iCAP6500) for P, S, Mg, and K, and via CHN elemental analysis (Leco TCH 600) for N. Based on the elemental analysis results, N:S ratio was calculated. Sulfur and phosphorus use efficiency (SUE and PUE, respectively) were estimated using the following equations:[155]

$$Uptake\ (g/pot) = Shoot\ Biomass\ (g/pot) \times \frac{Nutrient\ Concentration\ (\%)}{100} \quad (5.1)$$

$$SUE\ (\%) = \frac{S\ uptake\ (fertilized) - S\ uptake\ (control)\ (g/pot)}{S\ applied\ (g/pot)} \times 100 \quad (5.2)$$

$$PUE\ (\%) = \frac{P\ uptake\ (fertilized) - P\ uptake\ (control)\ (g/pot)}{P\ applied\ (g/pot)} \times 100 \quad (5.3)$$

Homogenized substrate samples from each layer were analyzed to determine nutrient concentrations. Available S (in sulfate form) was extracted with mono-calcium phosphate and the concentration was determined turbidimetrically with an UV-Vis spectrophotometer (Femto 600plus).[156]

Available P (phosphate in soil solution) was extracted with water and anionic resin, as proposed by Quaggio and Raij, and quantified in UV-Vis spectrophotometer (Femto 600plus).[132] Mg was extracted using a cationic resin and estimated with atomic absorption spectrophotometer (Perkin Elmer 2380). Nitrogen (total) was determined by CHN elemental analysis with a Perkin Elmer 2400 analyzer.

Rhizotron Image Analysis

Rhizotron images were analyzed using the software GrowScreen-Root, according to Nagel et al. (2012).[152] The roots were manually marked as primary roots or as first and second order lateral roots, labeled in green, red, or blue, respectively (FIGURES C2-C7 in Appendix C). The length of each root type, total root length, root length density, root system depth (representing the maximal vertical distribution of a root system), and convex hull area (representing the surface area of a rhizotron covered by the whole root system) were determined.

Statistical Analysis

All results were submitted to one-way statistical analysis (ANOVA) with Tukey's test at the significance level $p < 0.05$ (Origin Pro 9.0, USA).

5.4. Results and Discussion

Fertilizer composites with a controlled-release dynamic were obtained as sustainable alternatives to P and S fertilization, consisting of a polysulfide matrix (PS) as support to dispersed struvite particles (St). The fertilizers were produced with different contents of each component, namely

25, 50, and 75 wt% of the phosphate source. The different mass ratios were studied because the synergism and interactions between struvite particles and the polysulfide matrix may differ – e.g., the dispersion and barrier effects of the matrix on struvite dissolution and release may balance one another; S oxidation can be improved with higher P amounts and P solubilization can increase with higher polysulfide oxidation into sulfate. Therefore, we wanted to test different matrix-to-P configurations to observe if it could produce different outcomes regarding P release and S oxidations.

The same materials were studied in a previous work from our group, displaying a controlled-release behavior for phosphate in citric acid solution and a synergistic dynamic between S and P in soil.[107] Sulfur is partially polymerized in the composite, with a fraction remaining unreacted as re-crystallized elemental sulfur (S_8).[65,107] Nevertheless, the achieved polysulfide formation sufficiently provides functionality to the material, as an easily processible matrix to support struvite. Chemical characterizations of the materials in Valle et al. (2021) also revealed that, during the preparation of the composites, struvite crystalline phase is converted to dittmarite ($Mg(NH_4)(PO_4)\cdot H_2O$), losing structural water. This phase transition does not significantly impact the fertilizer's properties and, most importantly, it does not reduce the efficiency. Dittmarite has a similar P release profile to struvite, as it tends to rapidly re-hydrate when in solution, returning to struvite crystalline phase.[135] Dittmarite is more thermally stable than struvite, which could be favorable for processing purposes.[134] Moreover, dittmarite presents a higher nutrient concentration, which is more interesting for agronomic purposes.

Effect of different treatments on soybean development and root system architecture

Soybean (*Glycine max L.*) was cultivated in rhizotrons with different sources of S and P over 40 days. This crop was selected for the study due to its high demands on both P and S nutrition.[150,151,157] A substrate with low to moderate concentrations of P and S was used to favor the absorption of nutrients supplied *via* the fertilizers. It is worth mentioning that no phytotoxicity or micronutrient deficiency symptoms were observed over the course of the experiment. Plants grown with no additional fertilizer (control treatment) remained relatively small and did not evolve significantly over time, unlike the fertilized treatments (FIGURE C1). It was possible to observe a rapid development after around 30 days of plant growth for TSP/AS, St/S8, and the St/PS composites, corresponding to the appearance of flowers (FIGURE 5.2d). As the reproductive stage starts, soybean tends to rapidly accumulate biomass to complete the vegetative development.[158]

On the harvest day, measurements were carried out for the final plant height, number of leaves, total leaf area, and SPAD values (FIGURE 5.3). Plants under the unfertilized control achieved a significantly lower performance than the others in all measurements. It is interesting to notice that the treatments containing struvite (with S_8 or PS) were statistically superior to the positive control (TSP/AS), reaching more than double the leaf area, for instance. While TSP/AS featured on average 30 leaves per plant, St/S8 and St 50/PS displayed nearly 50 leaves. The SPAD values, which estimate the chlorophyll content of leaves, were less divergent among fertilized treatments, as expected by their development. The results indicate an increased development of soybean in the presence of struvite, demonstrating that phosphate can be efficiently provided to plants in this form. The results might

also be related to the co-management of struvite with sulfur (in S^0 oxidation state) or to the additional Mg supply. Moreover, the relatively higher application of NH_4NO_3 with water-soluble sources in TSP/AS probably elevated soil salinity, which is limiting to plant growth. The ammonium sulfate and nitrate sources have a saline index of 69 and 105%, respectively.[159] The rapid dissolution of these sources can increase the electrolyte concentration of the fertilized soil solution close to the roots. This high concentration of electrolytes near the seeds or roots can reduce or inhibit water absorption due to the increased osmotic pressure of the solution.[160]

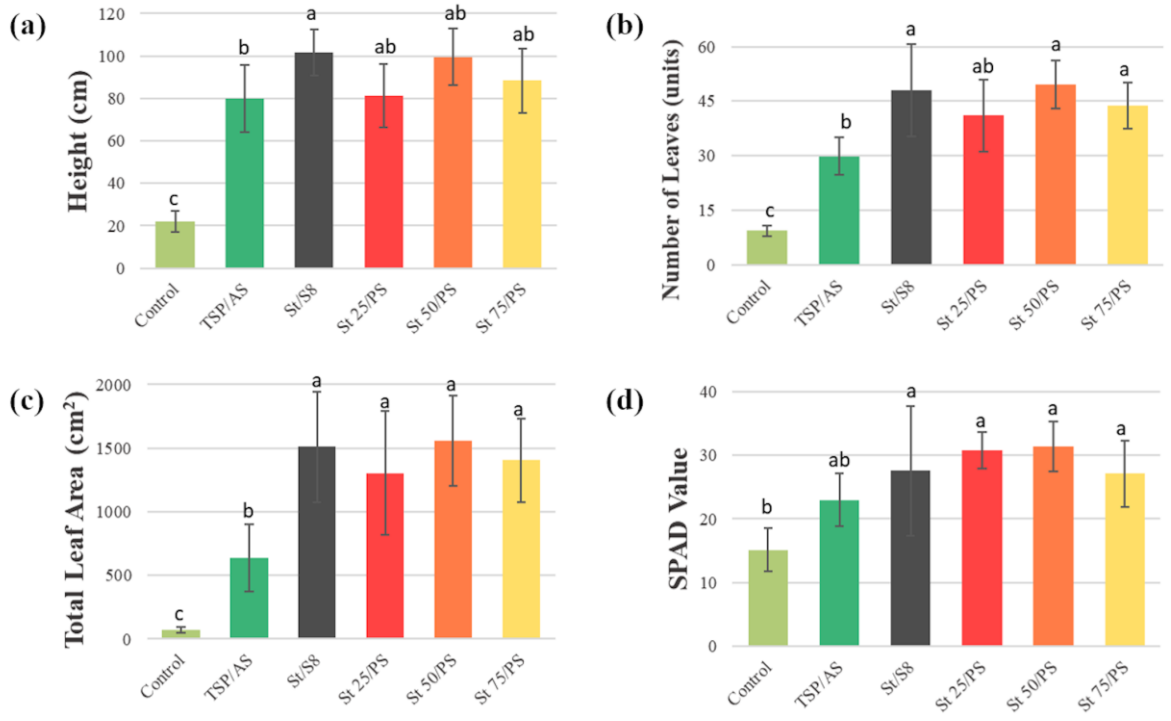

FIGURE 5.3: Average plant (a) height, (b) number of leaves, (c) total leaf area, and (d) SPAD value, measured before harvest, 40 days after sowing. Bars show mean values ± standard deviations. Indexes a, b, and c indicate significant differences between treatments ($p < 0.05$).

Root system architecture of unfertilized control plants strongly differed from the fertilized treatments, which presented pronounced second order lateral root development (FIGURE 5.4). Representative rhizotron images of all treatments over time can be found in FIGURES C2-C7. Plants that showed greater vegetative development (i.e., struvite-based treatments) also featured greater presence of thinner roots and a more homogeneous distribution throughout the substrate volume. It is known that lateral roots contribute the most to the absorption of water and nutrients by plants, due to their activity and capillarity in soil.

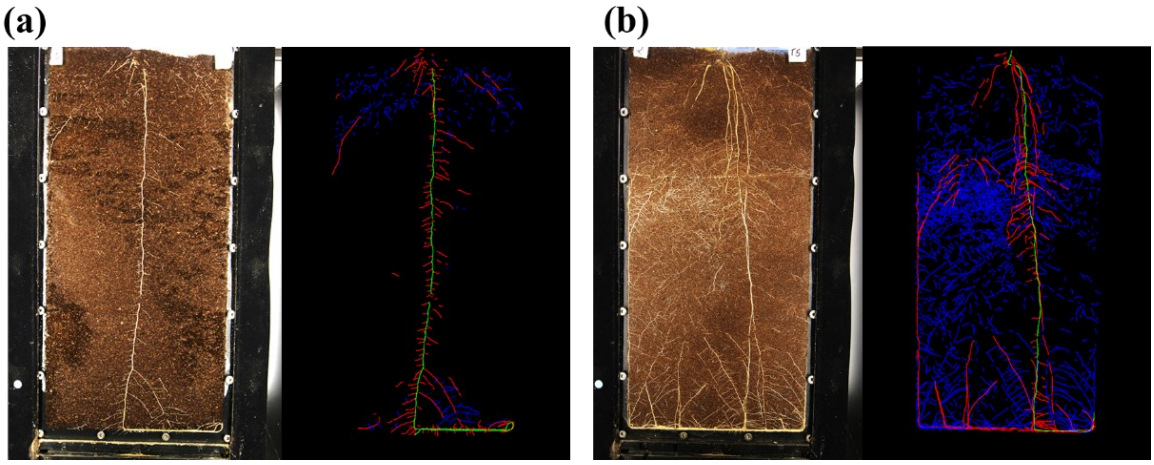

FIGURE 5.4: Original and analyzed color coded rhizotron images of (a) control with no fertilizer and (b) St 50/PS treatment, 40 days after sowing. Primary roots and first and second order lateral roots are represented by the colors green, red, and blue, respectively.

Visible root measurements from plants at 40 days of cultivation can be found in TABLE C3. While the final primary root length was similar among treatments, lateral root development was more affected by the fertilizer source. St 50/PS featured the largest first and second order lateral roots, with

respectively 565 cm and 1400 cm, which were significantly superior to TSP/AS (368 cm and 549 cm, respectively) and the unfertilized control (203 and 202, respectively). Moreover, struvite treatments achieved in general higher total root length than TSP/AS and control.

Plant response to nutrient availability or deficiency can be indicated by the differences in growth and in spatial distribution of roots within the soil. In some plants, like common wallcress (*Arabidopsis thaliana*) and alfalfa (*Medicago sativa*), S deficiency has relatively little effect on root morphology and affects more negatively shoot biomass production, decreasing shoot:root ratio.[161,162] Nevertheless, soybean plants treated with S_8 in Zhao et al. (2008) displayed an increase in lateral roots compared to a control with no S supply.[150] Phosphorus effect on root system architecture patterns is often more species-dependent. Gruber et al. (2013) reported that *A. thaliana* plants present shallower and branched root systems under insufficient P, for instance.[162] According to López-Bucio et al. (2003), their root system senses and responds to P deprivation locally.[163] Lyu et al., (2016) verified that P deficiency caused a more significant decrease in root length and increase of secondary lateral roots in fibrous root species (e.g., *Zea mays*) than in legumes (e.g., *Glycine max*).[164] Robles-Aguilar et al. (2020b) found that lupine (*Lupinus angustifolius L.*), a leguminous plant like soybean, increased primary root elongation in unfertilized treatments, compared to struvite fertilization.[165] On the other hand, in a study with soybean cultivation by Milton et al. (1991), P supply promoted an increase in total root length.[166] In Watt and Evans (2003), soybean produced more branched roots with P addition, which grew more concentrated around the area where the fertilizer was applied.[167] In contrast, Li et al., (2017) found that soybean root length density was smaller with higher P rates.[168]

FIGURE 5.5 illustrates the visible root length density profiles, indicating quite some variation in spatial root distributions across the different fertilizer treatments. A pronounced root development can be found in the region around the fertilizer layer (at 20 cm from the top), except for the unfertilized control, highlighting the relation between root growth and the presence of nutrients, also noticed by Watt and Evans.[167] It should be noted that all treatments displayed an increased root length in the lowest 10 cm of the rhizotrons. Roots started to reach the bottom of the rhizotrons 10 days after sowing and, thereafter, an enhanced root development could be found along the bottom part of the rhizotrons as a consequence of the experimental design.

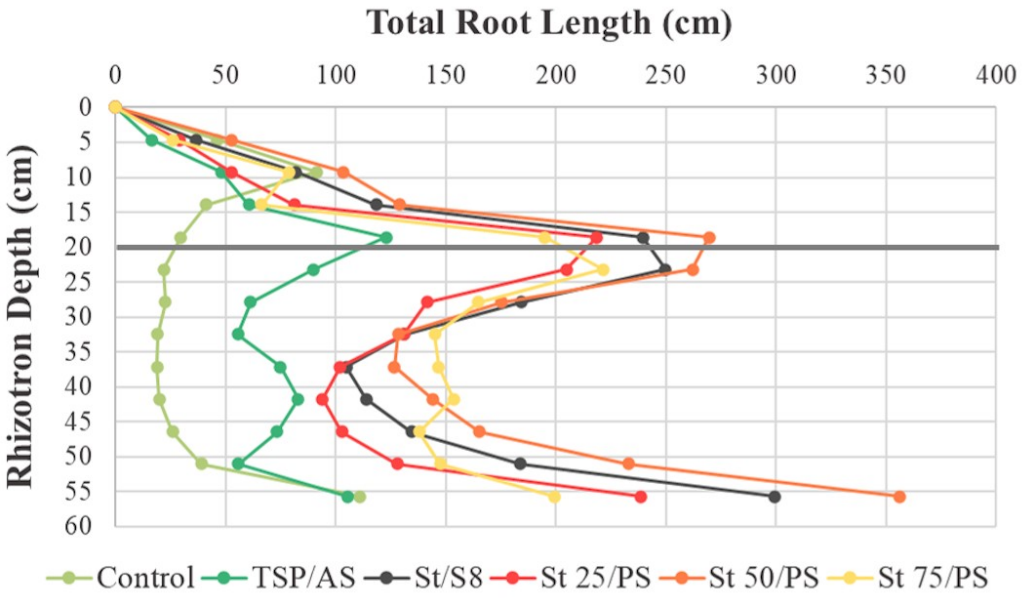

FIGURE 5.5: Effect of treatments on visible total root length. Trends of root length density over the rhizotron depth are shown at harvest time point (40 days after sowing). The applied fertilizer layer is at a depth of 20 cm from top (marked with the grey line). Dots represent mean values.

The lowest root length density is observed in the unfertilized control, compatible to its inferior shoot development. Unlike other treatments, the control presents a relatively larger root production closer to the substrate surface, which might be a response to P deficiency, as reported for *A. thaliana* plants.[162] Struvite-based treatments achieved a higher apparent root accumulation than TSP/AS over the rhizotron volume, especially composite St 50/PS. While the results clearly differed between struvite and TSP, plant behavior did not vary between S_8 and PS, indicating that soybean root distribution might be more strongly related to P supply than to differences between the S^0 sources.

Root production around the fertilizer layer corresponded mainly to second-order lateral roots, as can be seen in FIGURE 5.6. Primary root growth pattern was similar in all treatments, contributing less to the total root length density results (FIGURE 5.6a). First-order lateral roots showed a maximum around the fertilizer layer and a smaller peak of accumulation in the upper layer, probably from plant anchoring (FIGURE 5.6b). Second-order lateral roots occupied the largest volume of the rhizotron and could be found mainly in the fertilized region (FIGURE 5.6c). The profiles were consistent with the data found in TABLE C3, with a superior second-order lateral root production in struvite-treated plants than TSP/AS.

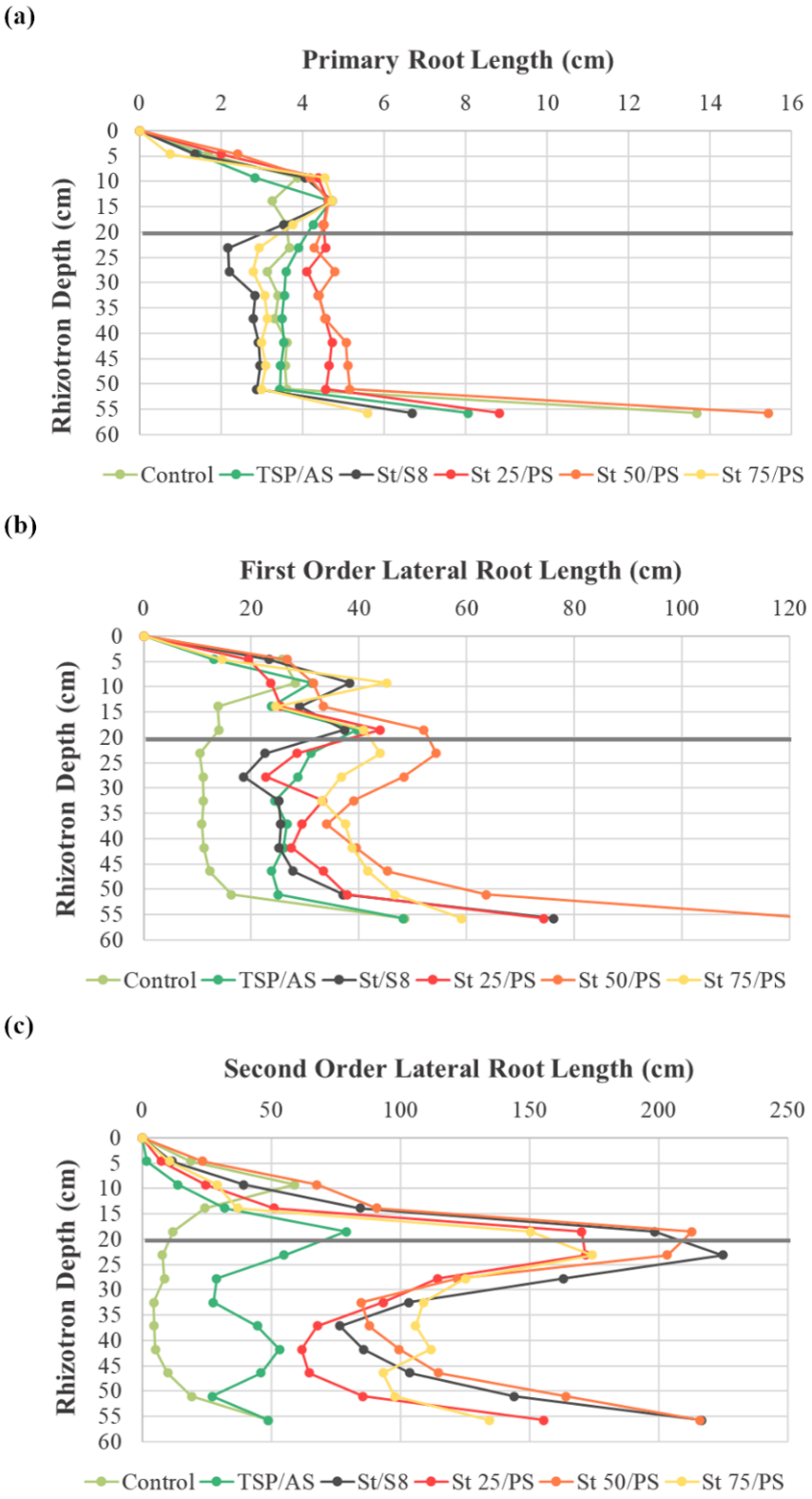

FIGURE 5.6: Effect of treatments on different root types: (a) primary roots and (b) first and (c) second order lateral roots. Trends of root length density

over the rhizotron depth are shown at harvest time point (40 days after sowing). The applied fertilizer layer is at a depth of 20 cm from top (marked with the grey line). Dots represent mean values.

Watt and Evans (2003) correlated soybean's high development of thinner branched roots to plant P uptake. The continuous root growth across the soil volume allows the interception of labile P from soil solution before it becomes soil-bound.[167] The different outcomes from TSP and struvite treatments could be related to their distinct phosphate release profiles. TSP has a fast initial release of P and, therefore, phosphate was probably highly available during the first days of soybean cultivation, before undergoing immobilization processes in the substrate. In contrast, struvite is a slow-release fertilizer with an ongoing dissolution. Phosphate from struvite treatments is delivered more steadily and may be accessed by roots over a longer period of time. The increased development of thinner lateral roots in struvite treatments, highly concentrated around the fertilizer layer, are strong indications that roots continued to grow and occupy the rhizotron as a response to phosphate prolonged delivery, especially in the case of the composites.

It is interesting to notice that St/S8 had a comparable second-order lateral root length to St 50/PS, but its first-order lateral root was inferior to all polysulfide treatments (TABLE C3 and FIGURE 5.6). This could be related to the differences in S structure. Zhao et al. (2008) showed that S supply to soybean as S_8 not only increased lateral root development, but also the amount of soil microorganisms and enzyme activity.[150] Both PS and S_8 require biological activity to be oxidized to sulfate, and roots may contribute to this by releasing organic compounds that stimulate soil microorganisms.[169]

Therefore, even though P supply appeared to contribute more significantly to soybean root system distribution, the S sources probably played a role in root traits as well.

The dynamic trend of root development over time revealed an increased rate of second-order lateral root growth after 30 days of cultivation (FIGURE C8). This result goes along with the enhanced plant height and number of leaves at the same period of time (FIGURE 5.3), corresponding to soybean reproductive period. Trends of root system depth and convex hull area can be found in Appendix C (FIGURE C9).

Since rhizotron images only provide information regarding visible roots, the complete root systems were measured after harvest by washing and scanning the roots (TABLE 5.1). It should be noted that the data corresponds mostly to primary and first-order lateral roots. The sampling method was not adequate to collect thinner roots, as a considerable portion of the second-order lateral roots was not separated from the soil during sieving, hence not contributing to the root measurements. Following the same trend from rhizotron images, St 50/PS achieved the largest total root length (4291 cm) and root surface area (593 cm^2, TABLE 5.1). The lowest values, however, were from TSP/AS, instead of unfertilized control plants, which could be attributed to the loss of second-order lateral roots, more prominent in the fertilized treatments (TABLE C3).

TABLE 5.1: Effect of treatment on average total root length, root diameter, and surface area. Indexes a and b signal significant differences between treatments ($p < 0.05$).

Root Measurements			
Treatment	Total Length (cm)	Diameter (mm)	Surface Area (cm^2)
Control	1592.2 *ab*	0.34 *b*	167.0 *b*
TSP/AS	982.2 *b*	0.42 *ab*	118.3 *b*
St/S8	1571.9 *ab*	0.50 *a*	215.4 *ab*
St 25/PS	1942.0 *ab*	0.48 *a*	256.1 *ab*
St 50/PS	4290.6 *a*	0.49 *a*	592.6 *a*
St 75/PS	3674.8 *ab*	0.48 *a*	481.5 *ab*

Control plants with no fertilizer displayed a smaller average root diameter than struvite treatments (TABLE 5.1), which goes along with the reduced root and shoot development and biomass accumulation. Root diameter was also analyzed in the three different layers (TABLE C4, Appendix C). The average root diameter of unfertilized control plants was constant in all layers (in the range of 0.33-0.35 mm). In contrast to the control, plants grown in fertilized treatments produced thicker roots in the top layer (top layer: 0.58-0.72 mm vs. bottom layer: 0.34-0.38 mm), possibly to support the higher biomass production. Plants under all treatments exhibited the highest proportion of roots in the root diameter class 0.2 and 0.3 mm (TABLE C5; around 30% of the total root length). In addition, plants treated with struvite had a high proportion of thicker roots (> 0.5 mm) which is less pronounced in control plants, reflecting the average results from TABLE 5.1.

Nevertheless, thinner roots could be underestimated, especially in struvite treatments, which had a high second-order lateral root development.

Dry biomass was measured both for shoots and roots (FIGURE 5.7). Shoot biomass was higher in treatments with struvite and significantly lower in the unfertilized control. Regarding root biomass, both plants under no fertilizer and TSP/AS treatments achieved inferior results. Plants treated with St 50/PS reached 10 times the root dry matter of TSP/AS grown plants, for instance. The fertilized treatments had comparable shoot:root ratios, superior to the unfertilized plants (FIGURE C10). The relation shows that plant biomass production was predominantly directed to shoot development when additional nutrients were supplied, indicating that struvite and polysulfide were able to properly provide P and S.

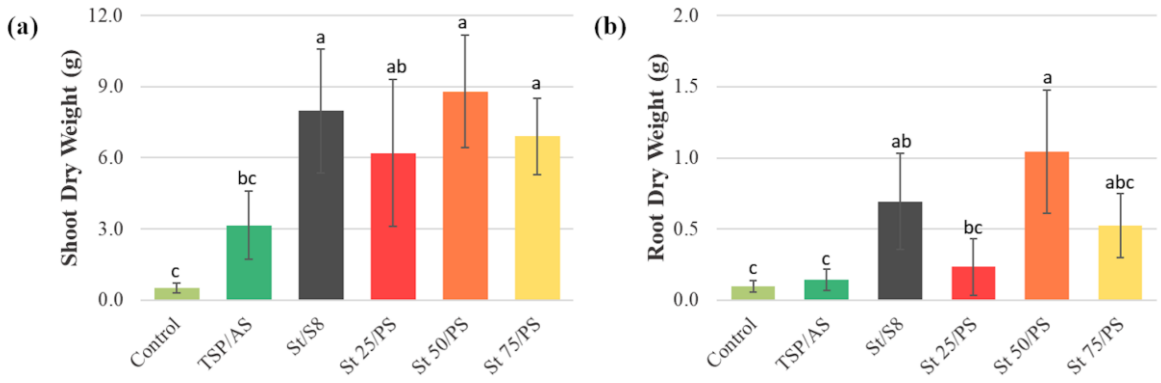

FIGURE 5.7: Effect of treatments on biomass from (a) shoots and (b) roots. Bars show mean values ± standard deviations. Indexes a, b, and c indicate significant differences between treatments ($p < 0.05$).

Soybean cultivation with the struvite-polysulfide composites not only displayed a significant biomass production, superior to the treatment with TSP and ammonium sulfate, but also a larger root proliferation. The intense

root growth could be a response to the prolonged availability of phosphate due to struvite slow-release character. Enhanced root growth can significantly benefit crop production, improving soil microstructure, soil porosity, and bulk density, among an overall enrichment of organic carbon in the soil. Most importantly, it implicates an increased soil rhizosphere, with a more diverse microbial community and better nutrient mobility and bioavailability. In field conditions this is especially favorable, benefiting the following crop cultivations.

Nutrient availability and uptake

For a more accurate understanding of the relationship between plant development and the fertilizers, it is essential to determine the nutrient recovery, as well as P and S final concentrations in the substrate. The control plants with no fertilizer displayed a lower relative concentration of all elements in shoots compared to the other treatments, except for sulfur (TABLE C6). Sulfur uptake by control plants was probably obtained from mineralization of organic S, promoted by enhanced root growth.[169] S plays a central role in the synthesis of proteins in plants, and also in symbiotic N_2 fixation, a process that soybean uses to assimilate nitrogen when this nutrient is deficient in soil.[170] However, nodule formation on roots was not observed, suggesting the unfertilized control plants did not fixate nitrogen. In addition, N uptake achieved by the control plant was critically low (0.74 wt%), possibly due to low availability of N and other essential nutrients.[7,154] Furthermore, the results indicate P deficiency in the unfertilized treatment (TABLE C6). Triple superphosphate provided the highest relative P concentration in shoots (1.15 wt%), although it did not outperform the other fertilized treatments for other

elements. Root elemental analysis of the complete root system and from the three rhizotron layers can be found in Appendix C (TABLE C6-C7).

All fertilized treatments resulted in adequate N:S ratios (TABLE 5.2), essential for protein synthesis and for crop yields.[151] The control plants with no fertilizer presented a low N:S relation due to insufficient nitrogen uptake. The highest sulfur use efficiency (SUE) was achieved by St 50/PS (22%), while the lowest efficiency was from the soluble form TSP/AS (8%). Furthermore, the triple superphosphate treatment featured the lowest phosphorus use efficiency (PUE), although at $p < 0.05$ it was comparable to the other treatments. The results indicate an efficient S oxidation from the polysulfide and sufficient struvite solubilization.

TABLE 5.2: Nutrient uptake efficiency parameters from plant biomass: average N:S ratio, sulfur use efficiency (SUE, %), and phosphorus use efficiency (PUE, %). Nutrient concentration in the substrate after soybean harvest: available phosphate (mg/dm^3), available sulfate (mg/dm^3), total nitrogen (mg/dm^3), and magnesium (mg/dm^3). Indexes a, b, c, and d indicate significant differences between treatments ($p < 0.05$).

	Nutrient Uptake Efficiency			**Nutrient Concentration in Soil**			
Treatment	N:S	SUE (%)	PUE (%)	P available (mg/dm^3)	S available (mg/dm^3)	N total (mg/dm^3)	Mg (mg/dm^3)
Control	2.2 *b*	-	-	16.5 *b*	14.3 *d*	2790.4 *a*	211.5 *bc*
TSP/AS	15.5 *a*	8.1 *b*	10.7 *a*	74.5 *a*	53.1 *a*	3949.5 *a*	177.9 *c*
St/S8	16.2 *a*	16.0 *ab*	11.4 *a*	95.7 *a*	37.4 *c*	3647.7 *a*	255.7 *a*
St 25/PS	15.2 *a*	11.8 *b*	11.5 *a*	85.5 *a*	39.4 *bc*	3128.7 *a*	232.0 *ab*
St 50/PS	15.8 *a*	22.0 *a*	14.1 *a*	93.9 *a*	51.3 *a*	2588.9 *a*	214.3 *bc*
St 75/PS	16.2 *a*	16.2 *ab*	13.6 *a*	86.4 *a*	47.7 *ab*	3125.9 *a*	241.8 *ab*

The concentration of available phosphate in the rhizotron was statistically similar between the different fertilized treatments, ranging from 75 to 96 mg/dm^3 (TABLE 5.2). Considering that TSP/AS is readily soluble, this result indicates the immobilization or loss of P from this source, reducing the expected fertilizer efficiency. Struvite treatments, on the other hand, have a controlled-release behavior, and may have not fully solubilized up to that point. In a long-term assessment with ryegrass, Bogdan et al. (2021) found that significant struvite dissolution and phosphate release was only observed after 4 months of cultivation.[171]

In the unfertilized control, available P presented no distinction between the three soil layers (TABLE C8). This shows that phosphate mobilization from the substrate by root exudates occurred equally over the rhizotron profile, as root length was relatively similar in all layers of the unfertilized control. In contrast, the middle layer (B) from TSP/AS and struvite treatments featured a significantly higher available P concentration, ranging from 164 to 237 mg/dm^3, while values from the top and bottom layers (A and C) were closer to the unfertilized control (around 20 mg/dm^3). This result shows the typical low mobility and diffusion of phosphate, observed in agricultural soils in general. Furthermore, it is consistent with the assumption that root proliferation in the middle layer (FIGURES 5.5 and 5.6) was associated to struvite ongoing dissolution.

The highest available sulfur concentration in the substrate was from TSP/AS and St 50/PS, while St/S8 achieved the lowest (TABLE 5.2). Since phosphate presence tends to block soil SO_4^{2-} adsorption sites, this explains why sulfate from the soluble source (AS) remains highly available.[10] The results also reveal that S oxidation into sulfate was more effective from PS in the composites than from S_8, which is compatible to the hypothesis that

S_8 and PS different S forms could have altered effects on the substrate microbial activity and plant growth dynamics. Sulfate concentration in the unfertilized control indicates S mineralization by root exudates, as discussed in the shoot recovery results. Contrary to phosphate, the middle and bottom layers have similar soil S contents (TABLE C8), indicating sulfate had a better transportation over the substrate depth.

High N values in the substrate reveal a low incidence of N volatilization and high organic N content (TABLE 5.2). St/S8 achieved a superior Mg concentration in the substrate by the end, which was expected from struvite composition. The other treatments displayed significant Mg concentrations, including the unfertilized control and TSP/AS, indicating a great mobilization from the organic fraction of the substrate. Moreover, this suggests Mg content in struvite was not decisive for the better performance and vegetative development of St/S8 and St/PS treatments. Based on these results, the lower Mg and N uptake by the unfertilized control plant was mostly related to insufficient P on the substrate.

5.5. Conclusion

The elucidation of plant-soil dynamics and roots growth patterns under struvite-polysulfide fertilization is important to understand and validate the agronomic efficiency of this new class of slow-release fertilizers. Hence, sustainable fertilizers with a polysulfide matrix and dispersed struvite (containing 25, 50, or 75 wt% of struvite) were prepared, using the simple and green method of inverse vulcanization. The effect of P and S supply from this system on soybean cultivation was compared both to the co-management of soluble commercial sources (TSP and $(NH_4)_2SO_4$) and to pure struvite mixed with S_8. The results revealed a significantly higher biomass production from

the combined application of struvite with S^0 sources (polysulfide or S_8) than with the TSP/$(NH_4)_2SO_4$ treatment. Struvite achieved a similar phosphorus use efficiency as the TSP reference, proving its controlled-release behavior can properly provide P to plants in the studied conditions. The composite St 50/PS displayed the greatest sulfur use efficiency, superior to the fine particles from S_8 powder and to ammonium sulfate, which reached the lowest SUE. Root system architecture analysis using rhizotrons revealed an intense accumulation of second-order lateral roots around the fertilizer layer, especially in struvite treatments. The higher development of thinner roots was attributed to the slow-release and continuous availability of phosphate from struvite, in contrast to TSP quick solubilization and P losses. Although root traits were more significantly influenced by the P source, differences in first-order lateral root lengths from PS and S_8 could be related to the S structure and its influence in the local microbial activity. The final concentration of sulfate in the growth medium also indicated a superior oxidation of S from the polysulfide than S_8. In summary, the slow-release struvite-polysulfide composites proved to be efficient fertilizer alternatives to soluble commercial sources, and beneficial to soybean development.

6. General Conclusions and Perspectives

In this thesis, it was demonstrated that it is possible to produce different fertilizer designs with polysulfides from inverse vulcanization, achieving superior oxidation to sulfate than elemental sulfur. Based on the discussed results and proposed goals, it can be concluded that the studied polysulfide provides a viable alternative not only as an efficient sulfur fertilizer, but also as a matrix to incorporate other fertilizers and promote their controlled-release. It should be highlighted that:

- The results showed that it was possible to adapt the simple method of inverse vulcanization to obtain materials with high S contents with particular characteristics and application purposes, such as composite and porous materials. This demonstrated the versatility of polysulfides compared to the more restrictive properties of elemental sulfur;
- Overall, the polysulfides displayed a faster oxidation than elemental sulfur in the different fertilizer forms and environments it was tested;
- Besides the structural modification of sulfur, the insertion of pores in the polysulfide material was a key strategy to increase the oxidation rate, reaching significantly higher results than the dense elemental sulfur pellets commercially available;
- The results showed that sulfur-oxidizing bacterium *Acidithiobacillus thiooxidans* is able to convert the polysulfide structure into sulfate, and that its incorporation with the fertilizer can optimize sulfate delivery efficiency in soil;
- As a matrix for the dispersion of P sources in fertilizer composites, the polysulfide demonstrated a multifunctionality, hindering the fast release of struvite in acidic conditions while also increasing P dissolution and

availability of the phosphate rock, thus allowing the controlled-release of phosphate. As hypothesized, phosphorus solubilization was favored by the increased acidity from sulfate formation and by the effect of physical dispersion of the particles;

- In the greenhouse conditions tested in this work, the controlled-release system from polysulfide-struvite composites produced different outcomes compared to soluble P and S fertilizers in soybean cultivation. Phosphate gradual release probably reduced P immobilization in soil and stimulated fine root proliferation, while the polysulfide was more efficient for plant sulfur uptake. The composites proved to be beneficial to soybean growth, promoting higher biomass production and adequate nutrition.

Therefore, these results support the development of further studies in the future, especially focusing on the following perspectives:

- The polysulfide characteristics could be manipulated by substituting soybean oil by other alkene candidates. It would be interesting to investigate alternatives that could increase the hydrophilicity of the material, for more compatibility with soil biochemical processes. Moreover, a compound with a more homogeneous composition than the vegetable oil could favor the reaction and decrease the amount of residual elemental sulfur;
- Strategies to inoculate *A. thiooxidans* in the polysulfide as a single material should be studied for improved oxidation efficiency;
- Finally, the demonstrated barrier and dispersing effects from the polysulfide, as well as the local acidity it generates, could be explored in other controlled release systems, with different nutrient sources or even in a different configuration (i.e., as a coating material).

7. References

1. FAO - FOOD AND AGRICULTURE ORGANIZATION OF THE UNITED NATIONS. The Future Of Food And Agriculture - Trends And Challenges.

2. GODFRAY, H. C. J.; BEDDINGTON, J. R.; CRUTE, I. R.; HADDAD, L.; LAWRENCE, D.; MUIR, J. F.; PRETTY, J.; ROBINSON, S.; THOMAS, S. M.; TOULMIN, C. "Food Security: The Challenge of Feeding 9 Billion People". Science (80-.)., 327 (February), p. 812–819, 2010.

3. PEREIRA, E. I.; GIROTO, A. S.; BORTOLIN, A.; YAMAMOTO, C. F.; MARCONCINI, J. M.; CARLOS DE, A.; BERNARDI, C.; RIBEIRO, C. "Perspectives in nanocomposites for the slow and controlled release of agrochemicals: Fertilizers and pesticides". Nanotechnologies Food Agric., p. 241–265, 2015.

4. WTO - WORLD TRADE ORGANIZATION. "Trade Policy Review: Brazil 2017"

5. ANDA - ASSOCIAÇÃO NACIONAL PARA DIFUSÃO DE ADUBOS. "RELATÓRIO SOBRE O MERCADO DE FERTILIZANTES – JANEIRO A AGOSTO/2022".

6. IFA; UNEP; ANDA. O Uso De Fertilizantes Minerais E O Meio Ambiente.

7. IFA; WFO; GACSA. "Nutrient Management Handbook", 2016.

8. HIGNETT, T. P. Fertilizer Manual.

9. KOPRIVA, S. "Plant sulfur nutrition : From Sachs to Big Data". Plant Signal. Behav., 10 (9), 2015.

10. SCHERER, H. W. "Sulphur in crop production". Eur. J. Agron., 14 (2), p. 81–111, 2001.

11. HANEKLAUS, S.; BLOEM, E.; SCHNUG, E. "History of Sulfur Deficiency in Crops Sulfur". IN: Sulfur: A Missing Link between Soils, Crops, and Nutrition. v. 50p. 45–58.

12. LUCHETA, A. R.; LAMBAIS, M. R. "Sulfur in Agriculture". Rev. Bras. Ciência do Solo, **36**, p. 1369–1379, 2012.

13. KANWAR, J. S.; MUDAHAR, M. S. Fertilizer Sulfur And Food Production. Dordrecht: Springer Netherlands, 1986.

14. DEGRYSE, F.; AJIBOYE, B.; BAIRD, R.; SILVA, R. C.; MCLAUGHLIN, M. J. "Oxidation of Elemental Sulfur in Granular Fertilizers Depends on the Soil-Exposed Surface Area". Soil Sci. Soc. Am. J., 80 (2), p. 294–305, 2016.

15. BOSWELL, C. C.; FRIESEN, D. K. "Elemental sulfur fertilizers and their use on crops and pastures". Fertil. Res., 35 (1–2), p. 127–149, fev. 1993.

16. BOURANIS, D. L.; MALAGOLI, M.; AVICE, J. C.; BLOEM, E. "Advances in plant sulfur research". Plants, 9 (2), p. 4–9, 2020.

17. HOROWITZ, N.; MEURER, E. J. "Oxidação do enxofre elementar em solos tropicais". Ciência Rural, 36 (3), p. 822–828, 2006.

18. DEGRYSE, F.; AJIBOYE, B.; BAIRD, R.; DA SILVA, R. C.; MCLAUGHLIN, M. J. "Availability of fertiliser sulphate and elemental sulphur to canola in two consecutive crops". Plant Soil, 398 (1–2), p. 313–325, 2016.

19. GRIEBEL, J. J.; GLASS, R. S.; CHAR, K.; PYUN, J. "Polymerizations

with elemental sulfur: A novel route to high sulfur content polymers for sustainability, energy and defense". Prog. Polym. Sci., **58**, p. 90–125, jul. 2016.

20. GRIFFITH, C. M.; WOODROW, J. E.; SEIBER, J. N. "Environmental behavior and analysis of agricultural sulfur". Pest Manag. Sci., 71 (11), p. 1486–1496, 2015.

21. BEVILAQUA, D.; LEITE, A. L. L. C.; GARCIA, O.; TUOVINEN, O. H. "Oxidation of chalcopyrite by Acidithiobacillus ferrooxidans and Acidithiobacillus thiooxidans in shake flasks". Process Biochem., 38 (4), p. 587–592, 2002.

22. GERMIDA, J. J.; JANZEN, H. H. "Factors affecting the oxidation of elemental sulfur in soils". Fertil. Res., 35 (1–2), p. 101–114, fev. 1993.

23. YANG, L.; ZHAO, D.; YANG, J.; WANG, W.; CHEN, P.; ZHANG, S.; YAN, L. "Acidithiobacillus thiooxidans and its potential application". Appl. Microbiol. Biotechnol., 103 (19), p. 7819–7833, 2019.

24. GRAYSTON, S. J.; NEVELL, W.; WAINWRIGHT, M. "Sulphur oxidation by fungi". Trans. Br. Mycol. Soc., 87 (2), p. 193–198, set. 1986.

25. YANG, Z. H.; STÖVEN, K.; HANEKLAUS, S.; SINGH, B. R.; SCHNUG, E. "Elemental Sulfur Oxidation by Thiobacillus spp. and Aerobic Heterotrophic Sulfur-Oxidizing Bacteria". Pedosphere, 20 (1), p. 71–79, 2010.

26. SUZUKI, I.; CHAN, C. W.; TAKEUCHI, T. L. "Oxidation of elemental sulfur to sulfite by Thiobacillus thiooxidans cells". Appl. Environ. Microbiol., 58 (11), p. 3767–3769, 1992.

27. LUCHETA, A. R. Oxidação Microbiológica Do Enxofre Elementar No

Solo.

28. SUZUKI, I.; LEE, D.; MACKAY, B.; HARAHUC, L. "Effect of Various Ions , pH , and Osmotic Pressure on Oxidation of Elemental Sulfur by Thiobacillus thiooxidans". Appl. Environ. Microbiol., 65 (11), p. 5163–5168, 1999.

29. GIROTO, A. S.; DO VALLE, S. F.; GUIMARAES, G. G. F.; MOLINA, A.; REIS, H. P. G.; FERNANDES, D. M.; BERNARDI, A. C. C.; MATTOSO, L. H. C.; RIBEIRO, C. "Tailoring efficient materials for NPK all-in-one granular fertilization". Ind. Eng. Chem. Res., 59 (41), p. 18387–18395, 2020.

30. KLEINJAN, W. E.; DE KEIZER, A.; JANSSEN, A. J. H. "Kinetics of the chemical oxidation of polysulfide anions in aqueous solution". Water Res., 39 (17), p. 4093–4100, 2005.

31. MEYER, B. "Solid allotropes of sulfur". Chem. Rev., 64 (4), p. 429–451, 1964.

32. OMER, H. "Sulfur". IN: Chemistry of the Elements. v. 1p. 645–746.

33. CHUNG, W. J.; GRIEBEL, J. J.; KIM, E. T.; YOON, H.; SIMMONDS, A. G.; JI, H. J.; DIRLAM, P. T.; GLASS, R. S.; WIE, J. J.; NGUYEN, N. A.; GURALNICK, B. W.; THEATO, P.; MACKAY, M. E.; SUNG, Y.; PARK, J.; CROCKETT, M. P.; EVANS, A. M.; WORTHINGTON, M. J. H.; ALBUQUERQUE, I. S.; et al. "Sulfur and Its Role In Modern Materials Science". Angew. Chemie - Int. Ed., 99 (50), p. 349–357, 2016.

34. CHUNG, W. J.; GRIEBEL, J. J.; KIM, E. T.; YOON, H.; SIMMONDS, A. G.; JI, H. J.; DIRLAM, P. T.; GLASS, R. S.; WIE, J. J.; NGUYEN, N. A.;

GURALNICK, B. W.; PARK, J.; SOMOGYI, Á.; THEATO, P.; MACKAY, M. E.; SUNG, Y.-E.; CHAR, K.; PYUN, J. "The use of elemental sulfur as an alternative feedstock for polymeric materials". Nat. Chem., 5 (6), p. 518–524, 14 jun. 2013.

35. TONKIN, S. J.; GIBSON, C. T.; CAMPBELL, J. A.; LEWIS, D. A.; KARTON, A.; HASELL, T.; CHALKER, J. M. "Chemically induced repair, adhesion, and recycling of polymers made by inverse vulcanization". Chem. Sci., 11 (21), p. 5537–5546, 2020.

36. LUNDQUIST, N. A.; TIKOALU, A. D.; WORTHINGTON, M. J. H.; SHAPTER, R.; TONKIN, S. J.; STOJCEVSKI, F.; MANN, M.; GIBSON, C. T.; GASCOOKE, J. R.; KARTON, A.; HENDERSON, L. C.; ESDAILE, L. J.; CHALKER, J. M. "Reactive Compression Molding Post-Inverse Vulcanization: A Method to Assemble, Recycle, and Repurpose Sulfur Polymers and Composites". Chem. - A Eur. J., 26 (44), p. 10035–10044, 2020.

37. WORTHINGTON, M. J. H.; KUCERA, R. L.; CHALKER, J. M. "Green chemistry and polymers made from sulfur". Green Chem., 19 (12), p. 2748–2761, 2017.

38. PARKER, D. J.; JONES, H. A.; PETCHER, S.; CERVINI, L.; GRIFFIN, J. M.; AKHTAR, R.; HASELL, T. "Low cost and renewable sulfur-polymers by inverse vulcanisation, and their potential for mercury capture". J. Mater. Chem. A, 5 (23), p. 11682–11692, 2017.

39. PARK, K. W.; LEITAO, E. M. "The link to polysulfides and their applications". Chem. Commun., 57 (26), p. 3190–3202, 2021.

40. CHALKER, J. M.; WORTHINGTON, M. J. H.; LUNDQUIST, N. A.; ESDAILE, L. J. "Synthesis and Applications of Polymers Made by Inverse

Vulcanization". Top. Curr. Chem., 377 (3), p. 1–27, 2019.

41. ZHANG, Y.; GLASS, R. S.; CHAR, K.; PYUN, J. "Recent advances in the polymerization of elemental sulphur, inverse vulcanization and methods to obtain functional Chalcogenide Hybrid Inorganic/Organic Polymers (CHIPs)". Polym. Chem., 10 (30), p. 4078–4105, 2019.

42. ABBASI, A.; NASEF, M. M.; YAHYA, W. Z. N. "Copolymerization of vegetable oils and bio-based monomers with elemental sulfur: A new promising route for bio-based polymers". Sustain. Chem. Pharm., 13 (March), p. 100158, 2019.

43. GRIEBEL, J. J.; LI, G.; GLASS, R. S.; CHAR, K.; PYUN, J. "Kilogram Scale Inverse Vulcanization of Elemental Sulfur to Prepare High Capacity Polymer Electrodes for Li-S Batteries". J. Polym. Sci., p. 173–177, 2015.

44. GOMEZ, I.; LEONET, O.; BLAZQUEZ, J. A.; MECERREYES, D. "Inverse Vulcanization of Sulfur using Natural Dienes as Sustainable Materials for Lithium-Sulfur Batteries". ChemSusChem, 9 (24), p. 3419–3425, 20 dez. 2016.

45. HOEFLING, A.; LEE, Y. J.; THEATO, P. "Sulfur-Based Polymer Composites from Vegetable Oils and Elemental Sulfur: A Sustainable Active Material for Li-S Batteries". Macromol. Chem. Phys., 218 (1), p. 1600303, jan. 2017.

46. WU, F.; CHEN, S.; SROT, V.; HUANG, Y.; SINHA, S. K.; VAN AKEN, P. A.; MAIER, J.; YU, Y. "A Sulfur–Limonene-Based Electrode for Lithium–Sulfur Batteries: High-Performance by Self-Protection". Adv. Mater., 30 (13), p. 1–8, 2018.

47. CROCKETT, M. P.; EVANS, A. M.; WORTHINGTON, M. J. H.; ALBUQUERQUE, I. S.; SLATTERY, A. D.; GIBSON, C. T.; CAMPBELL, J. A.; LEWIS, D. A.; BERNARDES, G. J. L.; CHALKER, J. M. "Sulfur-Limonene Polysulfide: A Material Synthesized Entirely from Industrial By-Products and Its Use in Removing Toxic Metals from Water and Soil". Angew. Chemie Int. Ed., 55 (5), p. 1714–1718, 26 jan. 2016.

48. WORTHINGTON, M. J. H.; KUCERA, R. L.; ALBUQUERQUE, I. S.; GIBSON, C. T.; SIBLEY, A.; SLATTERY, A. D.; CAMPBELL, J. A.; ALBOAIJI, S. F. K.; MULLER, K. A.; YOUNG, J.; ADAMSON, N.; GASCOOKE, J. R.; JAMPAIAH, D.; SABRI, Y. M.; BHARGAVA, S. K.; IPPOLITO, S. J.; LEWIS, D. A.; QUINTON, J. S.; ELLIS, A. V; et al. "Laying Waste to Mercury: Inexpensive Sorbents Made from Sulfur and Recycled Cooking Oils". Chem. - A Eur. J., 23 (64), p. 16219–16230, 16 nov. 2017.

49. LUNDQUIST, N. A.; WORTHINGTON, M. J. H.; ADAMSON, N.; GIBSON, C. T.; JOHNSTON, M. R.; ELLIS, A. V; CHALKER, J. M. "Polysulfides made from re-purposed waste are sustainable materials for removing iron from water". RSC Adv., (8), p. 1232–1236, 2017.

50. WORTHINGTON, M. J. H.; SHEARER, C. J.; ESDAILE, L. J.; CAMPBELL, J. A.; GIBSON, C. T.; LEGG, S. K.; YIN, Y.; LUNDQUIST, N. A.; GASCOOKE, J. R.; ALBUQUERQUE, I. S.; SHAPTER, J. G.; ANDERSSON, G. G.; LEWIS, D. A.; BERNARDES, G. J. L.; CHALKER, J. M. "Sustainable Polysulfides for Oil Spill Remediation: Repurposing Industrial Waste for Environmental Benefit". Adv. Sustain. Syst., **1800024**, p. 1–7, 2018.

51. PARKER, D. J.; CHONG, S. T.; HASELL, T. "Sustainable inverse-vulcanised sulfur polymers". RSC Adv., 8 (49), p. 27892–27899, 2018.

52. LIMJUCO, L. A.; NISOLA, G. M.; PAROHINOG, K. J.; VALDEHUESA, K. N. G.; LEE, S. P.; KIM, H.; CHUNG, W. J. "Water-insoluble hydrophilic polysulfides as microfibrous composites towards highly effective and practical Hg2+ capture". Chem. Eng. J., 378 (122216), 2019.

53. TIKOALU, A. D.; LUNDQUIST, N. A.; CHALKER, J. M. "Mercury Sorbents Made By Inverse Vulcanization of Sustainable Triglycerides: The Plant Oil Structure Influences the Rate of Mercury Removal from Water". Adv. Sustain. Syst., 4 (3), p. 1–9, 2020.

54. KLEINE, T. S.; GLASS, R. S.; LICHTENBERGER, D. L.; MACKAY, M. E.; CHAR, K.; NORWOOD, R. A.; PYUN, J. "100th Anniversary of Macromolecular Science Viewpoint: High Refractive Index Polymers from Elemental Sulfur for Infrared Thermal Imaging and Optics". ACS Macro Lett., 9 (2), p. 245–259, 2020.

55. GRIEBEL, J. J.; NAMNABAT, S.; KIM, E. T.; HIMMELHUBER, R.; MORONTA, D. H.; CHUNG, W. J.; SIMMONDS, A. G.; KIM, K. J.; VAN DER LAAN, J.; NGUYEN, N. A.; DERENIAK, E. L.; MACKAY, M. E.; CHAR, K.; GLASS, R. S.; NORWOOD, R. A.; PYUN, J. "New infrared transmitting material via inverse vulcanization of elemental sulfur to prepare high refractive index polymers". Adv. Mater., 26 (19), p. 3014–3018, 2014.

56. GRIEBEL, J. J.; NGUYEN, N. A.; NAMNABAT, S.; ANDERSON, L. E.; GLASS, R. S.; NORWOOD, R. A.; MACKAY, M. E.; CHAR, K. "Dynamic Covalent Polymers via Inverse Vulcanization of Elemental Sulfur for Healable Infrared Optical Materials". ACS Macro Lett., (4), p. 862–866, 2015.

57. ANDERSON, L. E.; KLEINE, T. S.; ZHANG, Y.; PHAN, D. D.; NAMNABAT, S.; LAVILLA, E. A.; KONOPKA, K. M.; DIAZ, L. R.; MANCHESTER, M. S.; SCHWIEGERLING, J.; GLASS, R. S.; MACKAY, M. E.; CHAR, K.; NORWOOD, R. A. "Chalcogenide Hybrid Inorganic/Organic Polymers: Ultrahigh Refractive Index Polymers for Infrared Imaging". 2017.

58. BEAR, J. C.; PEVELER, W. J.; MCNAUGHTER, P. D.; PARKIN, I. P.; BRIEN, P. O.; DUNNILL, C. W. "Nanoparticle–sulphur ‘“inverse vulcanisation”’ polymer composites". Chem. Commun., (51), p. 10467–10470, 2015.

59. MARTIN, T. R.; MAZZIO, K. A.; HILLHOUSE, H. W.; LUSCOMBE, C. K. "Synthesis of Ligand-free CdS Nanoparticles within a Sulfur Copolymer Matrix". J. Vis. Exp., (111), p. 1–9, 2016.

60. HERRERA, C.; YSINGA, K. J.; JENKINS, C. L. "Polysulfides Synthesized from Renewable Garlic Components and Repurposed Sulfur Form Environmentally Friendly Adhesives". ACS Appl. Mater. Interfaces, 11 (38), p. 35312–35318, 2019.

61. LIU, Y.; CHEN, Y.; ZHANG, Y.; CHEN, Y.; WANG, L.; ZAN, X.; ZHANG, L. "Density-adjustable bio-based polysulfide composite prepared by inverse vulcanization and bio-based fillers". Polymers (Basel)., 12 (9), p. 10–14, 2020.

62. LAUER, M. K.; KARUNARATHNA, M. S.; TENNYSON, A. G.; SMITH, R. C. "Robust, remeltable and remarkably simple to prepare biomass-sulfur composites". Mater. Adv., 1 (7), p. 2271–2278, 2020.

63. KARUNARATHNA, M. S.; LAUER, M. K.; THIOUNN, T.; SMITH, R.

C.; TENNYSON, A. G. "Valorisation of waste to yield recyclable composites of elemental sulfur and lignin". J. Mater. Chem. A, 7 (26), p. 15683–15690, 2019.

64. VALLE, S. F. DO. Avaliação Do Processo De Vulcanização Inversa Visando A Aplicação Na Produção De Fertilizantes.

65. VALLE, S. F.; GIROTO, A. S.; KLAIC, R.; GUIMARÃES, G. G. F.; RIBEIRO, C. "Sulfur fertilizer based on inverse vulcanization process with soybean oil". Polym. Degrad. Stab., **162**, p. 102–105, 2019.

66. HAMMOND, E. G.; JOHNSON, L. A.; SU, C.; WANG, T.; WHITE, P. J. "Soybean Oil". IN: Bailey's Industrial Oil and Fat Products. 6. ed.

67. MONTERO DE ESPINOSA, L.; MEIER, M. A. R. "Plant oils: The perfect renewable resource for polymer science?!". Eur. Polym. J., 47 (5), p. 837–852, maio 2011.

68. HIRAKURI, M. H.; LAZZAROTTO, J. J. "O agronegócio da soja nos contextos mundial e brasileiro"

69. TRENKEL, M. E. Slow- And Controlled-Release And Stabilized Fertilizers: An Option For Enhancing Nutrient Use Efficiency In Agriculture.

70. AZEEM, B.; KUSHAARI, K.; MAN, Z. B.; BASIT, A.; THANH, T. H. "Review on materials & methods to produce controlled release coated urea fertilizer". J. Control. Release, 181 (1), p. 11–21, 2014.

71. RIBEIRO, C.; CARMO, M. "Why nonconventional materials are answers for sustainable agriculture". MRS Energy Sustain. A Rev. J., 6 (9), p. 1–15, 2019.

72. PLOTEGHER, F.; RIBEIRO, C. "Characterization of single

superphosphate powders - A study of milling effects on solubilization kinetics". Mater. Res., 19 (1), p. 98–105, 2016.

73. LIM, H. H.; GILKES, R. J.; MCCORMICK, P. G. "Beneficiation of rock phosphate fertilisers by mechano-milling". Nutr. Cycl. Agroecosystems, 67 (2), p. 177–186, 2003.

74. GIROTO, A. S.; FIDÉLIS, S. C.; RIBEIRO, C. "Controlled release from hydroxyapatite nanoparticles incorporated into biodegradable, soluble host matrixes". RSC Adv., 5 (126), p. 104179–104186, 2015.

75. GIROTO, A. S.; GUIMARÃES, G. G. F.; FOSCHINI, M.; RIBEIRO, C. "Role of Slow-Release Nanocomposite Fertilizers on Nitrogen and Phosphate Availability in Soil". Sci. Rep., 7 (October 2016), p. 46032, 2017.

76. GIROTO, A. S.; GUIMARÃES, G. G.; COLNAGO, L. A.; KLAMCZYNSKI, A.; GLENN, G.; RIBEIRO, C. "Controlled release of nitrogen using urea-melamine-starch composites". J. Clean. Prod., **217**, p. 448–455, 2019.

77. KLAIC, R.; GIROTO, A. S.; GUIMARÃES, G. G. F.; PLOTEGHER, F. "Nanocomposite of starch-phosphate rock bioactivated for environmentally-friendly fertilization". Miner. Eng., 128 (June), p. 230–237, 2018.

78. GUIMARÃES, G. G. F.; KLAIC, R.; GIROTO, A. S.; MAJARON, V. F.; AVANSI, W.; FARINAS, C. S.; RIBEIRO, C. "Smart Fertilization Based on Sulfur–Phosphate Composites: Synergy among Materials in a Structure with Multiple Fertilization Roles". ACS Sustain. Chem. Eng., p. 1–10, 3 ago. 2018.

79. MANN, M.; KRUGER, J. E.; ANDARI, F.; MCERLEAN, J.; GASCOOKE, J. R.; SMITH, J. A.; WORTHINGTON, M. J. H.;

MCKINLEY, C. C. C.; CAMPBELL, J. A.; LEWIS, D. A.; HASELL, T.; PERKINS, M. V.; CHALKER, J. M. "Sulfur polymer composites as controlled-release fertilisers". Org. Biomol. Chem., 17 (7), p. 1929–1936, 2019.

80. MANZOOR GHUMMAN, A. S.; SHAMSUDDIN, R.; NASEF, M. M.; MAUCIERI, C.; REHMAN, O. U.; ROSMAN, A. A.; HAZIQ, M. I.; ABBASI, A. "Degradable Slow-Release Fertilizer Composite Prepared by Ex Situ Mixing of Inverse Vulcanized Copolymer with Urea". Agronomy, 12 (1), 2022.

81. GHUMMAN, A. S. M.; SHAMSUDDIN, R.; NASEF, M. M.; KRIVOBORODOV, E. G.; AHMAD, S.; ZANIN, A. A.; MEZHUEV, Y. O.; ABBASI, A. "A degradable inverse vulcanized copolymer as a coating material for urea produced under optimized conditions". Polymers (Basel)., 13 (22), 2021.

82. GHUMMAN, A. S. M.; SHAMSUDDIN, R.; NASEF, M. M.; YAHYA, W. Z. N.; ABBASI, A.; ALMOHAMADI, H. "Sulfur enriched slow-release coated urea produced from inverse vulcanized copolymer". Sci. Total Environ., 846 (August 2021), 2022.

83. BRAHIM, S.; NIESS, A.; PFLIPSEN, M.; NEUHOFF, D.; SCHERER, H. "Effect of combined fertilization with rock phosphate and elemental sulphur on yield and nutrient uptake of soybean". Plant, Soil Environ., 63 (2), p. 89–95, 2017.

84. SCHACHTMAN, D. P.; REID, R. J.; AYLING, S. M. "Phosphorus Uptake by Plants: From Soil to Cell". Plant Physiol., 116 (2), p. 447–453, 1998.

85. JOHNSTON, A. E.; STEÉN, I. Understanding Phosphorous And Its Use In Agriculture.

86. VILAR, C. C.; COSTA, A. C. S. DA; ALLAN, H.; JUNIOR, I. G. DE S. "CAPACIDADE MÁXIMA DE ADSORÇÃO DE FÓSFORO RELACIONADA A FORMAS DE FERRO E ALUMÍNIO EM SOLOS SUBTROPICAIS". R. Bras. Ci. Solo, (1), p. 1059–1068, 2010.

87. CHIEN, S. H.; PROCHNOW, L. I.; TU, S.; SNYDER, C. S. "Agronomic and environmental aspects of phosphate fertilizers varying in source and solubility: An update review". Nutr. Cycl. Agroecosystems, 89 (2), p. 229–255, 2011.

88. INTERNATIONAL PLANT NUTRITION INSTITUTE (IPNI). "Better Crops With Plant Food"

89. HART, M. R.; QUIN, B. F.; NGUYEN, M. L. "Phosphorus Runoff from Agricultural Land and Direct Fertilizer Effects: A Review". J. Environ. Qual., 33 (6), p. 1954–1972, 2004.

90. MANNING, D. A. C. "Phosphate Minerals, Environmental Pollution and Sustainable Agriculture". Elements, 4 (2), p. 105–108, 2018.

91. CORDELL, D.; DRANGERT, J.; WHITE, S. "The story of phosphorus: Global food security and food for thought". Glob. Environ. Chang., **19**, p. 292–305, 2009.

92. CHIEN, S. H.; MENON, R. G. "Factors affecting the agronomic effectiveness of phosphate rock for direct application". Fertil. Res., 41 (3), p. 227–234, 1995.

93. PANTANO, G.; GROSSELI, G. M.; MOZETO, A. A.; QUÍMICA, D. DE;

FEDERAL, U.; CARLOS, D. S.; LUÍS, R. W.; SP, C. "SUSTENTABILIDADE NO USO DO FÓSFORO: UMA QUESTÃO DE SEGURANÇA HÍDRICA E ALIMENTAR". Quim. Nova, 39 (6), p. 732–740, 2016.

94. SCHOLZ, R. W.; ULRICH, A. E.; EILITTÄ, M.; ROY, A. "Sustainable use of phosphorus: A finite resource". Sci. Total Environ., **461**–**462**, p. 799–803, 2013.

95. KATAKI, S.; WEST, H.; CLARKE, M.; BARUAH, D. C. "Phosphorus recovery as struvite : Recent concerns for use of seed , alternative Mg source , nitrogen conservation and fertilizer potential". Resour. Conserv. Recycl., **107**, p. 142–156, 2016.

96. RAHMAN, M.; AMRAN, M.; SALLEH, M.; RASHID, U.; AHSAN, A.; MUJAFFAR, M.; SIX, C. "Production of slow release crystal fertilizer from wastewaters through struvite crystallization – A review". Arab. J. Chem., 7 (1), p. 139–155, 2014.

97. CHOWDHURY, R. B.; MOORE, G. A.; WEATHERLEY, A. J.; ARORA, M. "Key sustainability challenges for the global phosphorus resource, their implications for global food security, and options for mitigation". J. Clean. Prod., **140**, p. 945–963, 2017.

98. TALBOYS, P. J.; HEPPELL, J.; ROOSE, T.; HEALEY, J. R.; JONES, D. L.; WITHERS, P. J. A. "Struvite: a slow-release fertiliser for sustainable phosphorus management?". Plant Soil, 401 (1–2), p. 109–123, 2016.

99. YETILMEZSOY, K.; ILHAN, F.; KOCAK, E.; AKBIN, H. M. "Feasibility of struvite recovery process for fertilizer industry: A study of financial and economic analysis". J. Clean. Prod., **152**, p. 88–102, 2017.

100. MEHTA, C. M.; HUNTER, M. N.; LEONG, G.; BATSTONE, D. J. "The Value of Wastewater Derived Struvite as a Source of Phosphorus Fertilizer". Clean - Soil, Air, Water, 46 (7), 2018.

101. RECH, I.; WITHERS, P. J. A.; JONES, D. L.; PAVINATO, P. S. "Solubility, diffusion and crop uptake of phosphorus in three different struvites". Sustain., 11 (1), 2018.

102. HERTZBERGER, A. J.; CUSICK, R. D.; MARGENOT, A. J. "A review and meta-analysis of the agricultural potential of struvite as a phosphorus fertilizer". Soil Sci. Soc. Am. J., 84 (3), p. 653–671, 2020.

103. TANSEL, B.; MONJE, O. "Struvite formation and decomposition characteristics for ammonia and phosphorus recovery: A review of magnesium-ammonia- phosphate interactions". Chemosphere, **194**, p. 504–514, 2018.

104. DEGRYSE, F.; BAIRD, R.; SILVA, R. C.; MCLAUGHLIN, M. J. "Dissolution rate and agronomic effectiveness of struvite fertilizers – effect of soil pH, granulation and base excess". Plant Soil, (410), p. 139–152, 2017.

105. SCHERER, H. W. "Sulfur in soils". J. Plant Nutr. Soil Sci., 172 (3), p. 326–335, 2009.

106. MCCASKILL, M. R.; BLAIR, G. J. "Particle Size and Soil Texture Effects on Elemental Sulfur Oxidation". Agron. J., 79 (6), p. 1079–1083, 1987.

107. VALLE, S. F. DO; GIROTO, A. S.; REIS, H. P. G.; GUIMARAES, G. G. F.; RIBEIRO, C. "Synergy of Phosphate-Controlled Release and Sulfur Oxidation in Novel Polysulfide Composites for Sustainable Fertilization". J.

Agric. Food Chem., **69**, p. 2392–2402, 2021.

108. VALLE, S. F.; GIROTO, A. S.; GUIMARÃES, G. G. F.; NAGEL, K. A.; GALINSKI, A.; COHNEN, J.; JABLONOWSKI, N. D.; RIBEIRO, C. "Co-fertilization of Sulfur and Struvite-Phosphorus in a Slow-Release Fertilizer Improves Soybean Cultivation". Front. Plant Sci., 13 (May), p. 1–12, 2022.

109. MATTIELLO, E. M.; DA SILVA, R. C.; DEGRYSE, F.; BAIRD, R.; GUPTA, V. V. S. R.; MCLAUGHLIN, M. J. "Sulfur and Zinc Availability from Co-granulated Zn-Enriched Elemental Sulfur Fertilizers". J. Agric. Food Chem., 65 (6), p. 1108–1115, 2017.

110. MAJARON, V. F.; DA SILVA, M. G.; BORTOLETTO-SANTOS, R.; KLAIC, R.; RIBEIRO, S. J. L.; POLITO, W. L.; BEVILAQUA, D.; FARINAS, C. S.; RIBEIRO, C. "Bioactive Material with Microorganisms can Enhance the Micronutrients Solubilization and Sulfate Availability from Low Reactive Sources: Insight for Application as Coating Fertilizer Granules". J. Polym. Environ., 30 (6), p. 2602–2613, 20 jun. 2022.

111. STAMFORD, N. P.; RIBEIRO, M. R.; CUNHA, K. P. V.; FREITAS, A. D. S.; SANTOS, C. E. R. S.; DIAS, S. H. L. "Effectiveness of sulfur with Acidithiobacillus and gypsum in chemical attributes of a Brazilian sodic soil". World J. Microbiol. Biotechnol., 23 (10), p. 1433–1439, 2007.

112. ABRAHAM, A. M.; KUMAR, S. V.; ALHASSAN, S. M. "Porous sulphur copolymer for gas-phase mercury removal and thermal insulation". Chem. Eng. J., **332**, p. 1–7, jan. 2018.

113. GARCIA JR, O. "Isolation and purification of Thiobacillus ferrooxidans and Thiobacillus thiooxidans from some coal and uranium mines of Brazil".

Rev. Microbiol., **20**, p. 1–6, 1991.

114. PAULINO, L. C.; BERGAMO, R. F.; DE MELLO, M. P.; GARCIA, O.; MANFIO, G. P.; OTTOBONI, L. M. M. "Molecular characterization of Acidithiobacillus ferrooxidans and A. thiooxidans strains isolated from mine wastes in Brazil". Antonie van Leeuwenhoek, Int. J. Gen. Mol. Microbiol., 80 (1), p. 65–75, 2001.

115. SILVERMAN, M. P.; LUNDGREN, D. G. "Studies on the chemoautotrophic iron bacterium Ferrobacillus ferrooxidans. I. An improved medium and a harvesting procedure for securing high cell yields.". J. Bacteriol., 77 (5), p. 642–647, 1959.

116. CAMARGO, O. A.; MONIZ, A. C.; JORGE, J. A.; VALADARES, J. M. A. . "Métodos de Análise Química, Mineralógica e Física de Solos". Inst. Agronômico Campinas, p. 77, 2009.

117. MINISTÉRIO DA AGRICULTURA PECUÁRIA E ABASTECIMENTO (MAPA). MANUAL DE MÉTODOS ANALÍTICOS OFICIAIS PARA FERTILIZANTES E CORRETIVOS.

118. RAO, C. N. R.; VENKATARAGHAVAN, R.; KASTURI, T. R. "Contribution to the Infrared Spectra of Organosulphur Compounds". Can. J. Chem., **42**, p. 36–42, 1964.

119. MEYER, B. "Elemental sulfur". Chem. Rev., 76 (3), p. 367–388, jun. 1976.

120. ANSORI, A.; GHOLAMI, A. "Improved Nutrient Uptake and Growth of Maize in Response to Inoculation with Thiobacillus and Mycorrhiza on an Alkaline Soil". Commun. Soil Sci. Plant Anal., 46 (17), p. 2111–2126, 2015.

121. STAMFORD, N. P.; SANTOS, P. R.; SANTOS, C. E. S.; FREITAS, A. D. S.; DIAS, S. H. L.; LIRA, M. A. "Agronomic effectiveness of biofertilizers with phosphate rock, sulphur and Acidithiobacillus for yam bean grown on a Brazilian tableland acidic soil". Bioresour. Technol., 98 (6), p. 1311–1318, 2007.

122. ARIA, M. M.; LAKZIAN, A.; HAGHNIA, G. H.; BERENJI, A. R.; BESHARATI, H.; FOTOVAT, A. "Effect of Thiobacillus, sulfur, and vermicompost on the water-soluble phosphorus of hard rock phosphate". Bioresour. Technol., 101 (2), p. 551–554, 2010.

123. KHAN, A.; JILANI, G.; ZHANG, D.; AKBAR, S.; MALIK, K. M.; RUKH, S.; MUJTABA, G. "Acidithiobacillus thiooxidans IW16 and Sulfur Synergistically with Struvite Aggrandize the Phosphorus Bioavailability to Wheat in Alkaline Soil". J. Soil Sci. Plant Nutr., 20 (1), p. 95–104, 2020.

124. ZVINAVASHE, A. T.; MARDAD, I.; MHADA, M.; KOUISNI, L.; MARELLI, B. "Engineering the Plant Microenvironment to Facilitate Plant-Growth-Promoting Microbe Association". J. Agric. Food Chem., 69 (45), p. 13270–13285, 2021.

125. KLAIC, R.; GUIMARÃES, G. G. F.; GIROTO, A. S.; BERNARDI, A. C. C.; ZANGIROLAMI, T. C.; RIBEIRO, C.; FARINAS, C. S. "Synergy of Aspergillus niger and Components in Biofertilizer Composites Increases the Availability of Nutrients to Plants". Curr. Microbiol., 78 (4), p. 1529–1542, 2021.

126. VEJAN, P.; KHADIRAN, T.; ABDULLAH, R.; ISMAIL, S.; DADRASNIA, A. "Encapsulation of plant growth promoting Rhizobacteria—prospects and potential in agricultural sector: a review". J. Plant Nutr., 42 (19),

p. 2600–2623, 2019.

127. NÚÑEZ-RAMÍREZ, D. M.; LÓPEZ-MARTÍNEZ, A.; MEDINA-TORRES, L.; CALDERAS, F.; MARTÍNEZ-PRADO, M. A.; LARA, R. H.; HERRERA-VALENCIA, E. E.; ANGUIANO-VEGA, G. A.; MANERO, O. "Microencapsulation of Acidithiobacillus thiooxidans by spray drying using biopolymers as wall materials: A potential alternative for its application in the mining industry". Miner. Eng., 166 (April), 2021.

128. KLAIC, R.; PLOTEGHER, F.; RIBEIRO, C.; ZANGIROLAMI, T. C.; FARINAS, C. S. "A novel combined mechanical-biological approach to improve rock phosphate solubilization". Int. J. Miner. Process., **161**, p. 50–58, 2017.

129. HUANG, Z.; FU, W.; ZHANG, S.; WANG, H.; LIU, R.; CHENG, C.; LIU, Z.; GUO, Z.; YU, X.; HE, G.; AI, G. "“umbrella” structure trisiloxane surfactant: Synthesis and application for reverse flotation of phosphorite ore in phosphate fertilizer production". J. Agric. Food Chem., 68 (40), p. 11114–11120, 2020.

130. NAZ, M. Y.; SULAIMAN, S. A. "Slow release coating remedy for nitrogen loss from conventional urea: A review". J. Control. Release, **225**, p. 109–120, 2016.

131. J.MURPHY; J.P.RILEY. "A modified single solution method for the determination of phosphate in natural waters". Anal. Chim. Acta, **27**, p. 31–36, 1962.

132. VAN RAIJ, B.; QUAGGIO, J. A.; DA SILVA, N. M. "Extraction of phosphorus, potassium, calcium, and magnesium from soils by an ion-exchange resin procedure". Commun. Soil Sci. Plant Anal., 17 (5), p. 547–

566, 1986.

133. BHUIYAN, M. I. H.; MAVINIC, D. S.; KOCH, F. A. "Thermal decomposition of struvite and its phase transition". Chemosphere, 70 (8), p. 1347–1356, 2008.

134. FARHANA, S. Thermal Decomposition Of Struvite: A Novel Approach To Recover Ammonia From Wastewater Using Struvite Decomposition Products.

135. MASSEY, M. S.; DAVIS, J. G.; IPPOLITO, J. A.; SHEFFIELD, R. E. "Effectiveness of recovered magnesium phosphates as fertilizers in neutral and slightly alkaline soils". Agron. J., 101 (2), p. 323–329, 2009.

136. SILVERSTEIN, R. M.; WEBSTER, F. X.; KIEMLE, D. J. Spectrometric Identification Of Organic Compunds.

137. ZHENYU, L.; JUESHI, Q.; ZHONGYUAN, L.; QIAN, L.; QIULIN, Z. "Rapid synthesis of dittmarite by microwave-assisted hydrothermal method". Adv. Mater. Sci. Eng., **2012**, p. 1–5, 2012.

138. ŠOPTRAJANOV, B.; STEFOV, V.; KUZMANOVSKI, I.; JOVANOVSKI, G.; LUTZ, H. D.; ENGELEN, B. "Very low H-O-H bending frequencies. IV. Fourier transform infrared spectra of synthetic dittmarite". J. Mol. Struct., 613 (1–3), p. 7–14, 2002.

139. KOLEVA, V. G. "Vibrational behavior of the phosphates ions in dittmarite-type compounds M′M″PO4·H2O (M′ = K+, NH4+; M″ = Mn2+, Co2+, Ni2+)". Spectrochim. Acta - Part A Mol. Biomol. Spectrosc., 66 (2), p. 413–418, 2007.

140. MALUF, H. J. G. M.; SILVA, C. A.; DE MORAIS, E. G.; DE PAULA,

L. H. D. "Is composting a route to solubilize low-grade phosphate rocks and improve MAP-based composts?". Rev. Bras. Cienc. do Solo, **42**, p. 1–17, 2018.

141. SMITH, J. A.; WU, X.; BERRY, N. G.; HASELL, T. "High sulfur content polymers: The effect of crosslinker structure on inverse vulcanization". J. Polym. Sci. Part A Polym. Chem., 56 (16), p. 1777–1781, 2018.

142. CHENG, C.; HUANG, Z.; ZHANG, R.; ZHOU, J.; LIU, Z.; ZHONG, H.; WANG, H.; KANG, Z.; HE, G.; YU, X.; REN, Z.; QIU, T.; HU, Y.; FU, W. "Synthesis of an emerging morpholine-typed Gemini surfactant and its application in reverse flotation carnallite ore for production of potash fertilizer at low temperature". J. Clean. Prod., **261**, p. 121121, 2020.

143. BARISON, A.; DA SILVA, C. W. P.; CAMPOS, F. R.; SIMONELLI, F.; LENZ, C. A.; FERREIRA, A. G. "A simple methodology for the determination of fatty acid composition in edible oils through 1H NMR spectroscopy". Magn. Reson. Chem., 48 (8), p. 642–650, 2010.

144. MA, N.; ROUFF, A. A.; PHILLIPS, B. L. "A 31P NMR and TG/DSC-FTIR investigation of the influence of initial pH on phosphorus recovery as struvite". ACS Sustain. Chem. Eng., 2 (4), p. 816–822, 2014.

145. KONGSHAUG, K. O.; FJELLVAG, H.; LILLERUD, K. P. "Synthesis and ab-initio structure determination of organically templated magnesium phosphates from powder diffraction data". J. Mater. Chem., 10 (8), p. 1915–1920, 2000.

146. SUTTER, B.; TAYLOR, R. E.; HOSSNER, L. R.; MING, D. W. " Solid State 31 Phosphorus Nuclear Magnetic Resonance of Iron-, Manganese-, and

Copper-Containing Synthetic Hydroxyapatites ". Soil Sci. Soc. Am. J., 66 (2), p. 455–463, 2002.

147. SARKAR, A. K. "Hydration / dehydration characteristics of struvite and dittmarite pertaining to magnesium ammonium phosphate cement systems". J. Mater. Sci., **26**, p. 2514–2518, 1991.

148. NEGREA, A.; LUPA, L.; NEGREA, P.; CIOPEC, M.; MUNTEAN, C. "Simultaneous Removal of Ammonium and Phosphate Ions from Wastewaters and Characterization of the resulting Product". Chem. Bull. “POLITEHNICA” Univ., 55 (69), p. 136–142, 2010.

149. ROBLES-AGUILAR, A. A.; PANG, J.; POSTMA, J. A.; SCHREY, S. D.; LAMBERS, H.; JABLONOWSKI, N. D. "The effect of pH on morphological and physiological root traits of Lupinus angustifolius treated with struvite as a recycled phosphorus source". Plant Soil, 434 (1–2), p. 65–78, jan. 2019.

150. ZHAO, Y.; XIAO, X.; BI, D.; HU, F. "Effects of sulfur fertilization on soybean root and leaf traits, and soil microbial activity". J. Plant Nutr., 31 (3), p. 473–483, 2008.

151. IBAÑEZ, T. B.; SANTOS, L. F. DE M.; LAPAZ, A. DE M.; RIBEIRO, I. V.; RIBEIRO, F. V.; REIS, A. R. DOS; MOREIRA, A.; HEINRICHS, R. "Sulfur modulates yield and storage proteins in soybean grains". Sci. Agric., 78 (1), p. 1–9, 2020.

152. NAGEL, K. A.; PUTZ, A.; GILMER, F.; HEINZ, K.; FISCHBACH, A.; PFEIFER, J.; FAGET, M.; BLOSSFELD, S.; ERNST, M.; DIMAKI, C.; KASTENHOLZ, B.; KLEINERT, A.-K.; GALINSKI, A.; SCHARR, H.; FIORANI, F.; SCHURR, U. "GROWSCREEN-Rhizo is a novel phenotyping

robot enabling simultaneous measurements of root and shoot growth for plants grown in soil-filled rhizotrons". Funct. Plant Biol., 39 (11), p. 891, 2012.

153. HERZEL, H.; DOMBINOV, V.; VOGEL, C.; WILLBOLD, S.; LEVANDOWSKI, G. V.; MEILLER, M.; MÜLLER, F.; ZANG, J. W.; FONSECA-ZANG, W. A.; JABLONOWSKI, N. D.; SCHREY, S. D.; ADAM, C. "Soybean Fertilized by P-Phases from Bagasse-Based Materials: P-Extraction Procedures, Diffusive Gradients in Thin Films (DGT), and X-ray Diffraction Analysis (XRD)". Agronomy, 10 (895), p. 1–25, 2020.

154. ROBLES-AGUILAR, A. A.; GRUNERT, O.; HERNANDEZ-SANABRIA, E.; MYSARA, M.; MEERS, E.; BOON, N.; JABLONOWSKI, N. D. "Effect of Applying Struvite and Organic N as Recovered Fertilizers on the Rhizosphere Dynamics and Cultivation of Lupine (Lupinus angustifolius)". Front. Plant Sci., **11**, p. 1–17, 2020.

155. CHOWDHURY, M. A. H.; SULTANA, T.; RAHMAN, M. A.; SAHA, B. K.; CHOWDHURY, T.; TARAFDER, S. "Sulphur fertilization enhanced yield, its uptake, use efficiency and economic returns of Aloe vera L.". Heliyon, 6 (12), p. e05726, 2020.

156. RAIJ, B. V.; ANDRADE, J. C. DE; CANTARELLA, H.; QUAGGIO, J. A. Análise Química Para Avaliação Da Fertilidade De Solos Tropicais.

157. SOARES, M. M.; SEDIYAMA, T.; NEVES, J. C. L.; DOS SANTOS JÚNIOR, H. C.; DA SILVA, L. J. "Nodulation, Growth and Soybean Yield in Response to Seed Coating and Split Application of Phosphorus". J. Seed Sci., 38 (1), p. 30–40, 2016.

158. MCWILLIAMS, D. A.; BERGLUND, D. R.; ENDRES, G. J. "Soybean Growth and Management". NDSu Ext. Circ., p. 1–8, 1999.

159. VITTI, G. C.; BOARETTO, A. E.; PENTEADO, S. R. "Fertilizantes e fertirrigação". IN: VITTI, G. C.; BOARETTO, A. E. (org.). Fertilizantes fluidos. Piracicaba: . p. 262–281.

160. TAIZ, L.; ZEIGER, E.; MØLLER, I. M.; MURPHY, A. Plant Physiology & Development.

161. WANG, Y. F.; WANG, S. P.; CUI, X. Y.; CHEN, Z. Z.; SCHNUG, E.; HANEKLAU, S. "Effects of sulphur supply on the morphology of shoots and roots of alfalfa (Medicago sativa L.)". Grass Forage Sci., 58 (2), p. 160–167, 2003.

162. GRUBER, B. D.; GIEHL, R. F. H.; FRIEDEL, S.; VON WIRÉN, N. "Plasticity of the Arabidopsis root system under nutrient deficiencies". Plant Physiol., 163 (1), p. 161–179, 2013.

163. LÓPEZ-BUCIO, J.; CRUZ-RAMÍREZ, A.; HERRERA-ESTRELLA, L. "The role of nutrient availability in regulating root architecture". Curr. Opin. Plant Biol., 6 (3), p. 280–287, 2003.

164. LYU, Y.; TANG, H.; LI, H.; ZHANG, F.; RENGEL, Z.; WHALLEY, W. R.; SHEN, J. "Major crop species show differential balance between root morphological and physiological responses to variable phosphorus supply". Front. Plant Sci., 7 (DECEMBER2016), p. 1–15, 2016.

165. ROBLES-AGUILAR, A. A.; SCHREY, S. D.; POSTMA, J. A.; TEMPERTON, V. M.; JABLONOWSKI, N. D. "Phosphorus uptake from struvite is modulated by the nitrogen form applied". J. Plant Nutr. Soil Sci., 183 (1), p. 80–90, 2020.

166. MILTON, N. M.; EISWERTH, B. A.; AGER, C. M. "Effect of

phosphorus deficiency on spectral reflectance and morphology of soybean plants". Remote Sens. Environ., 36 (2), p. 121–127, 1991.

167. WATT, M.; EVANS, J. R. "Phosphorus acquisition from soil by white lupin (Lupinus albus L.) and soybean (Glycine max L.), species with contrasting root development". Plant Soil, **248**, p. 271–283, 2003.

168. LI, H.; MOLLIER, A.; ZIADI, N.; SHI, Y.; PARENT, L. É.; MOREL, C. "Soybean root traits after 24 years of different soil tillage and mineral phosphorus fertilization management". Soil Tillage Res., **165**, p. 258–267, 2017.

169. VAN VEELEN, A.; KOEBERNICK, N.; SCOTSON, C. S.; MCKAY-FLETCHER, D.; HUTHWELKER, T.; BORCA, C. N.; MOSSELMANS, J. F. W.; ROOSE, T. "Root-induced soil deformation influences Fe, S and P: rhizosphere chemistry investigated using synchrotron XRF and XANES". New Phytol., 225 (4), p. 1476–1490, 2020.

170. BECANA, M.; WIENKOOP, S.; MATAMOROS, M. A. "Sulfur transport and metabolism in legume root nodules". Front. Plant Sci., 9 (October), p. 1–10, 2018.

171. BOGDAN, A.; DONNELL, C. O.; ALEJANDRA, A.; AGUILAR, R.; SIGURNJAK, I.; POWER, N.; MICHELS, E.; HARRINGTON, J.; MEERS, E. "Impact of time and phosphorus application rate on phosphorus bioavailability and efficiency of secondary fertilizers recovered from municipal wastewater". Chemosphere, 282 (131017), p. 2–11, 2021.

172. RAIJ, B. VAN; CANTARELLA, H. .; QUAGGIO, J. A. .; FURLANI, A. M. C. Recomendacoes De Adubacao E Calagem Para O Estado De Sao Paulo.

Appendix A

Supporting Information from Section 3 - Chapter I.

Synthesis of Molded Porous Polysulfide

Porous polysulfide pellets (5 mm diameter) were prepared in a silicon mold for the X-Ray Microtomography (MicroCT) characterization. Elemental sulfur (S_8) and sodium chloride (NaCl) (< 0.150 mm) were first pre-homogenized at a mass ratio of 7:3 NaCl/S_8.[112] The system was heated in an oil bath to 165°C and soybean oil was added (1:1 mass ratio of S_8/OS) under constant magnetic agitation. As soon as the reaction medium appeared completely homogeneous, without phase separation, it was cast into a silicone mold and kept in a furnace (EDG 3000) at 140 ºC over 12 hours to complete the reaction termination step. After cooling, the materials were immersed in a beaker containing de-ionized water for salt removal, kept in room temperature under magnetic stirring for around 24 hours. Finally, the pellets were dried overnight in an oven at 50 ºC.

FIGURE A1: (a) Molded porous polysulfide pellets; (b) SEM image of the molded material.

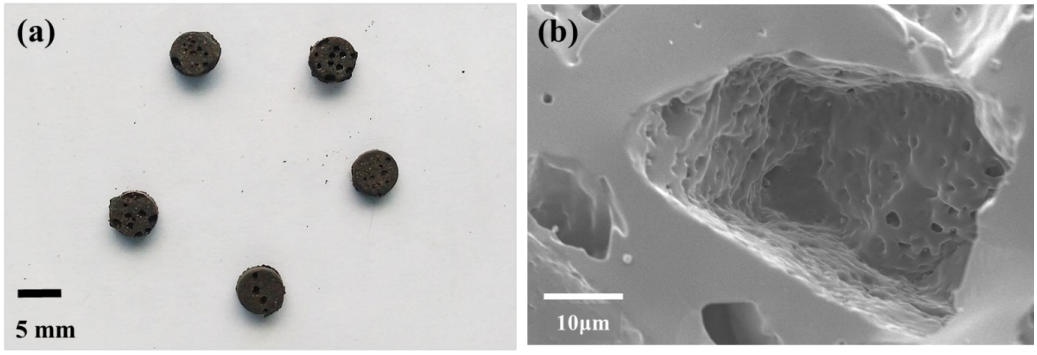

Synthesis of Dense Polysulfide

To obtain a powdered polysulfide (PolyS-powder) for the oxidation test, a dense polysulfide was synthesized without salt addition, with 50 wt% of S_8 and soybean oil, as described by Valle et a. (2019).[65] Briefly, S_8 was heated under constant agitation, using an oil bath equipped with an overhead mechanical stirrer. After ring opening polymerization (ROP) of the elemental sulfur structure at 159 ºC, soybean oil was slowly added. The system was kept at approximately 165 ºC under constant stirring, until the brown polymer was obtained (PolyS) and cooled in room temperature. Before use the material was ground in a blade grinder (< 0.5 mm).

FIGURE A2: (a) Dense polysulfide (PolyS); (b) the ground polysulfide (PolyS-powder; (c) SEM image of PolyS.

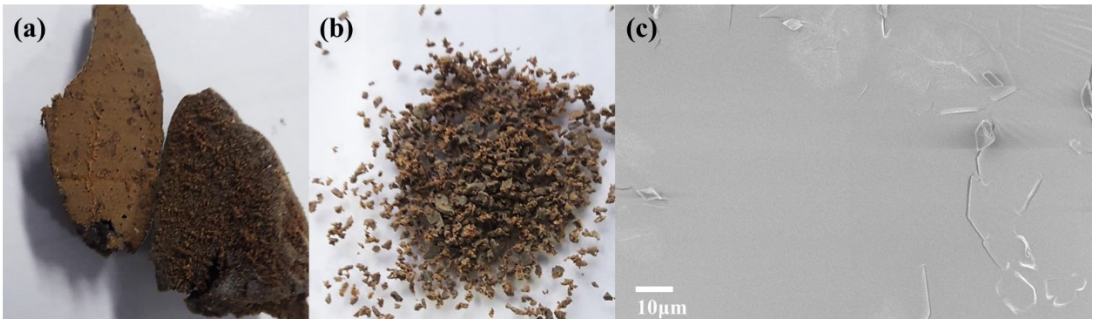

Real Density Measurement

Real density of PolyS-porous was calculated according to the equation below, using a glass pycnometer (50 mL) and mineral oil. Prior to the measurements, the equipment was calibrated with distilled water for the determination of the actual volume (V_{pyc}, mL).

$$\rho\ real\ = \left(\frac{m\ polyS}{V\ polyS}\right) = \left(\frac{m\ 2 - m\ 1}{V\ pyc - V4}\right) = \left(\frac{m\ 2 - m\ 1}{V\ pyc - m\ oil/\rho\ oil}\right) = \left(\frac{m\ 2 - m\ 1}{V\ pyc - \{(m\ 4 - m2)/[(m\ 3 - m\ 1)/V\ pyc]\}}\right)$$

Where m_{polyS} is the mass of PolyS-porous material added to the pycnometer, m_1 is the mass of the empty pycnometer, m_2 is the mass of the pycnometer with the added polymer, V_{polyS} is the actual volume of added polysulfide, V_{pyc} is the volume of the pycnometer, V_4 is the volume of mineral oil added to completely fill the pycnometer containing the polysulfide, m_{oil} is the mass of oil used to completely fill the empty pycnometer, ρ oil is the density of the mineral oil used, m_4 is the mass of the pycnometer with the polysulfide and oil, and m_3 is the mass of the pycnometer completely filled with only mineral oil.

Adapted 9K Culture Medium

The cultivation of *Acidithiobacillus thiooxidans* was performed with an adapted 9K culture medium containing: 3 g/L of $(NH_4)_2SO_4$, 0.5 g/L K_2HPO_4, 0.5 g/L $MgSO_4.7H_2O$, 0.1 g/L KCl, and 1% (m/v) of S^0.[115] The pH of the medium was corrected to 2.8 with diluted H_2SO_4. For the pre-culture, elemental sulfur powder was used as the S^0 source and 10% (v/v) of stock culture were added to the culture medium. After 10 days of incubation, 10% (v/v) of this pre-culture was added to a new culture medium for the sulfur oxidation test, using different S^0 sources. The materials and nutrient medium used to prepare the pre-culture and the oxidation test were previously sterilized in an autoclave at 120ºC for 20 minutes. Microorganism incubation was performed in a vertical laminar flow hood, using 250 mL erlenmeyer flasks equipped with cotton lids containing 50 mL of nutritive medium. Incubation of the pre-culture and of the oxidation test were conducted during 10 days in an orbital shaker incubator at 30 °C and 150 rpm.

Soil Characterization

TABLE A1: Chemical characterization of the studied soil. OM = organic matter; SB = sum of bases; CEC = cation-exchange capacity; V = soil base saturation.

pH	OM	P	H+Al	K	Ca	Mg	SB	CEC	V
$CaCl_2$	g/dm^3	mg/dm^3			$mmolc/dm^3$				%
5.5	15	8	19	0.3	11	11	22	40	54

SEM Images of NaCl, PolyS-salt, and PolyS-porous

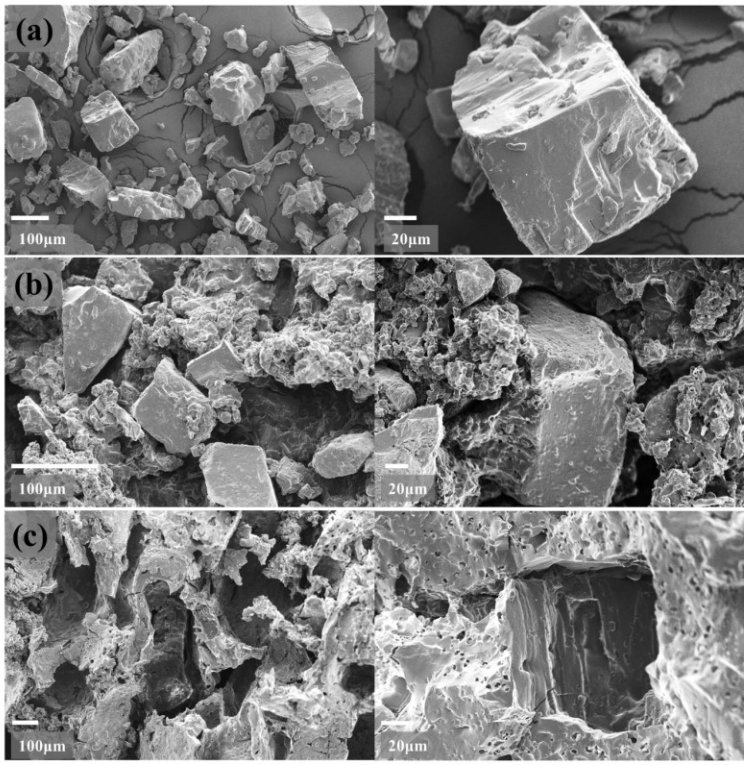

FIGURE A3: SEM images in different magnitude of (a) NaCl, (b) PolyS-salt, and (c) PolyS-porous.

Calibration Curve of Sulfur DSC Endotherms

The percentual of unreacted S_8 present in the porous polysulfide material was estimated using DSC thermograms.[48] First, a calibration curve was obtained (FIGURE A4),[65] based on the DSC melting peak area of pure elemental sulfur in varying masses. The same calibration curve was used in previous research from the group and can be seen on the supplementary materials from Valle et al., 2019 and 2021.[65,107] Residual sulfur in the PolyS-porous material (wt%) was then estimated based on the relation between the energy from the melting peaks in FIGURE 3.3c and the energy that a pure S_8 endotherm would present with the same mass (based on the calibration curve), as shown in TABLE A2.

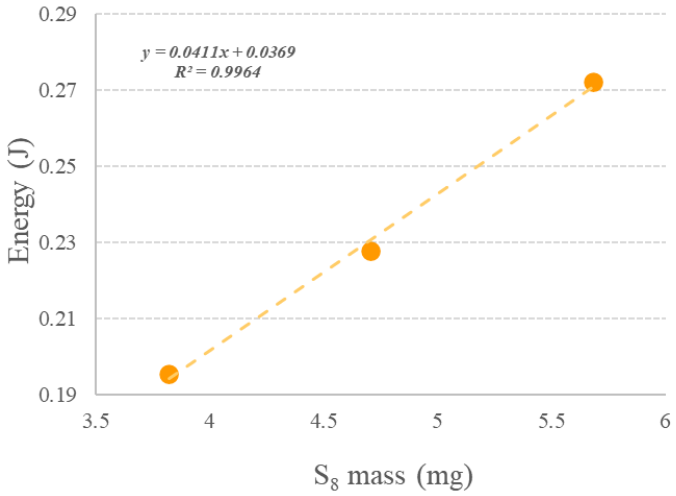

FIGURE A4: Calibration curve based on different pure S_8 masses and respective DSC melting endotherm areas.[65]

TABLE A2: Estimated residual sulfur in the PolyS-porous material (wt%), based on the relation between the analyzed mass, the melt endotherm energy, and the theoretical energy of pure S_8.

Mass (g)	ΔH (J/g)	Energy (J)	Energy of 100% S_8 (J)	$S_{8\ residual}$ (wt% of PolyS-porous)
0.005	12.99	0.065	0.243	27

SEM Images of S_8-pellet and PolyS-porous After Soil Incubation

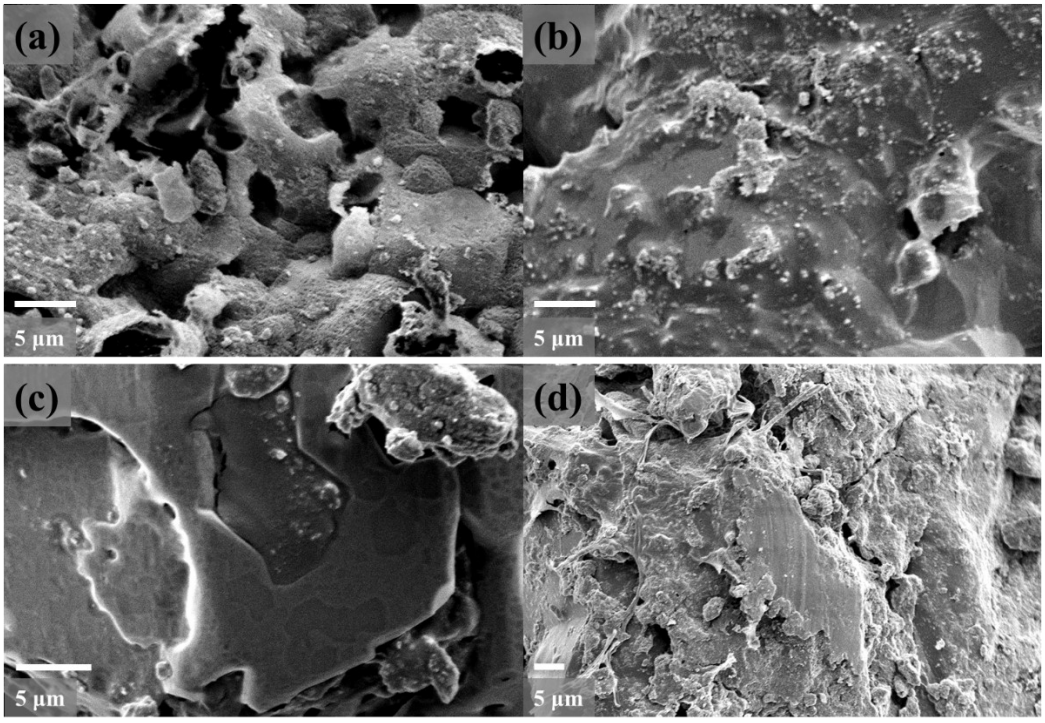

FIGURE A5: SEM images of (a) S_8-pellet, (b) S_8-pellet + *A. thiooxidans*, (c) PolyS-porous, and (d) PolyS-porous + *A. thiooxidans* after 60 days of incubation in soil.

Appendix B

Supporting Information from Section 4 - Chapter II.

TABLE B1: Chemical composition of struvite and Bayovar rock by X-ray fluorescence (XRF, PANalytical).

Oxide Species	Struvite	Bayóvar rock
	mass %	
P_2O_5	22.5	30.7
MgO	13.1	0.5
Al_2O_3	0.9	1.0
CaO	1.5	46.6
Fe_2O_3	0.1	0.9

Determination of the phosphorus content from the materials

The total phosphorus content of the materials was determined based on the official method from the Brazilian Ministry of Agriculture, Livestock and Farm Supplies (MAPA).[117] For the extraction of P, a fixed mass of the samples was added to a digestion tube with 30 mL of concentrated nitric acid (HNO_3) and 5 mL of concentrated hydrochloric acid (HCl). The system was kept under heating in a digestion block until complete release of brown vapors (NO_2), reaching a clear solution. After cooling to room temperature, the solution was filtered with a medium porosity filter paper and transferred to a 50 mL volumetric flask, completed with distilled water. The determination of P was performed according to the colorimetric method from Murphy and Riley, with absorbance measurements in an UV-spectrophotometer (FEMTO 700 Plus) at 880 nm wavelenght.[131]

TABLE B2: Chemical characterization of the studied soil. The Oxisol from brazilian cerrado was collected from the soil top layer (0-20 cm) of an agricultural region of São Carlos, in São Paulo State, Brazil. The soil was dried in an oven at 40 ºC for 24 hours and sieved (< 2.0 mm). Soil acidity was corrected before the experiment by application of limestone powder at proportion 3:1 wt [172].

pH $CaCl_2$	pH H_2O	OM g/dm^3	P mg/dm^3	H+Al	K	Ca	Mg	SB	CEC	V	S
						$mmolc/dm^3$				%	mg/dm^3
4.3	6.2	18	8	36	1.7	8	4	14	50	27	5

OM = organic Matter; SB = sum of bases; CEC = cation-exchange capacity; V = percentage of soil base saturation.

FIGURE B1. (a) From left to right: PolyS-Str25, PolyS-Str50, PolyS-Str75 and pure struvite; (b) From left to right: PolyS-Bay25, PolyS-Bay50, PolyS-Bay75 and pure Bayóvar rock.

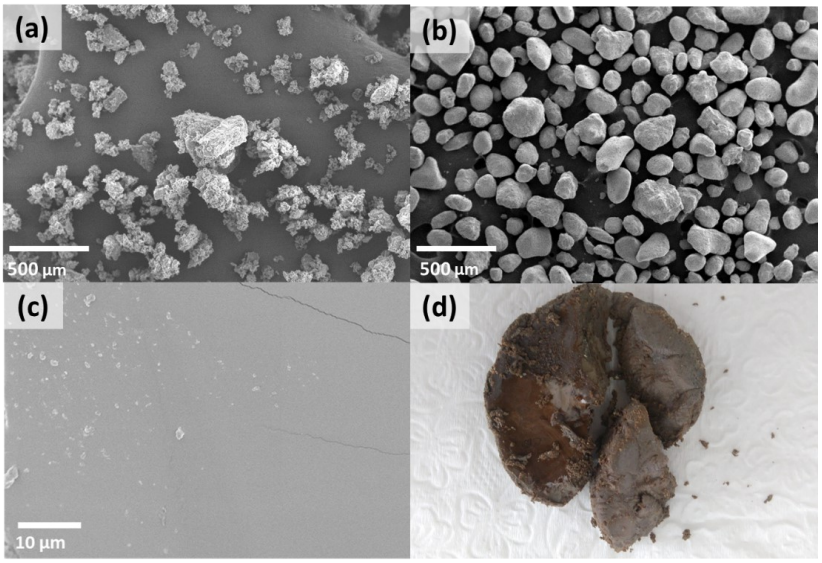

FIGURE B2: SEM images of (a) struvite, (b) Bayóvar rock and (c) pure polysulfide (50% S_8, 50% SO); (d) Picture of the pure soybean oil-based polysulfide.

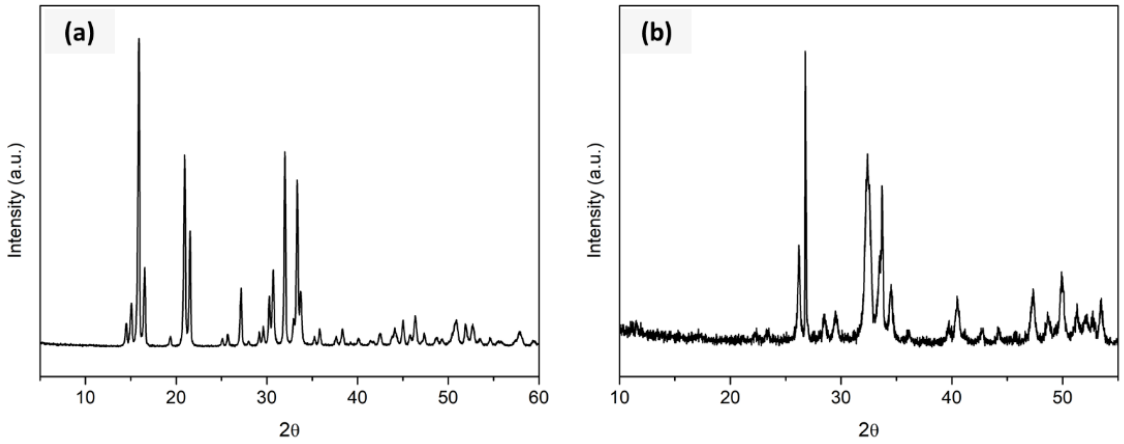

FIGURE B3: XRD spectra of (a) struvite and (b) Bayóvar rock.

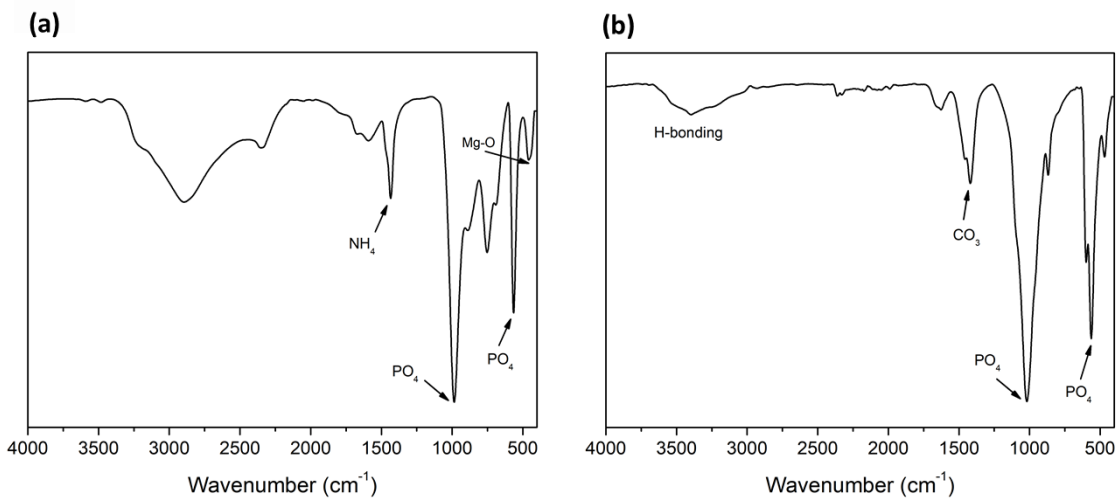

FIGURE B4: FTIR spectra of (a) struvite and (b) Bayóvar rock.

TABLE B3: List of FTIR main signals and band assignments from struvite (STR), soybean oil (SO) and the struvite composites (PolyS-Str25, PolyS-Str50 and PolyS-Str75)[136–140].

Wavenumber (cm-1)					Band Assignment
STR	**SO**	**PolyS-Str25**	**PolyS-Str50**	**PolyS-Str75**	
-	-	3419	3416	3419	H2O stretching (dittmarite)
3400-2143	-	-	-	-	H2O and NH4 stretching (struvite)
-	-	3200	3196	3194	NH4 stretching (dittmarite)
-	3010	-	-	-	H-C=C stretching (ester)
-	-	2734	2748	2748	NH4 stretching (dittmarite)
-	1744	1741	1741	1741	C=O stretching (ester)
-	1654	1659	1655	1655	C=C stretching (ester)/ H2O bending (dittmarite)
1434	-	1431	1431	1431	NH4 bending (struvite/ dittmarite)
-	-	1051	1047	1051	PO4 asymmetric stretching (dittmarite)
985	-	-	-	-	PO4 symmetric stretching (struvite)
-	-	970	968	970	PO4 symmetric stretching (dittmarite)
-	-	768	762	758	POP stretching
-	-	629	629	629	Mg-O stretching (dittmarite)
565	-	577	569	577	PO4 bending (struvite/dittmarite)
-	-	465	472	465	S-S stretching
459	-	-	-	-	Mg-O stretching (struvite)

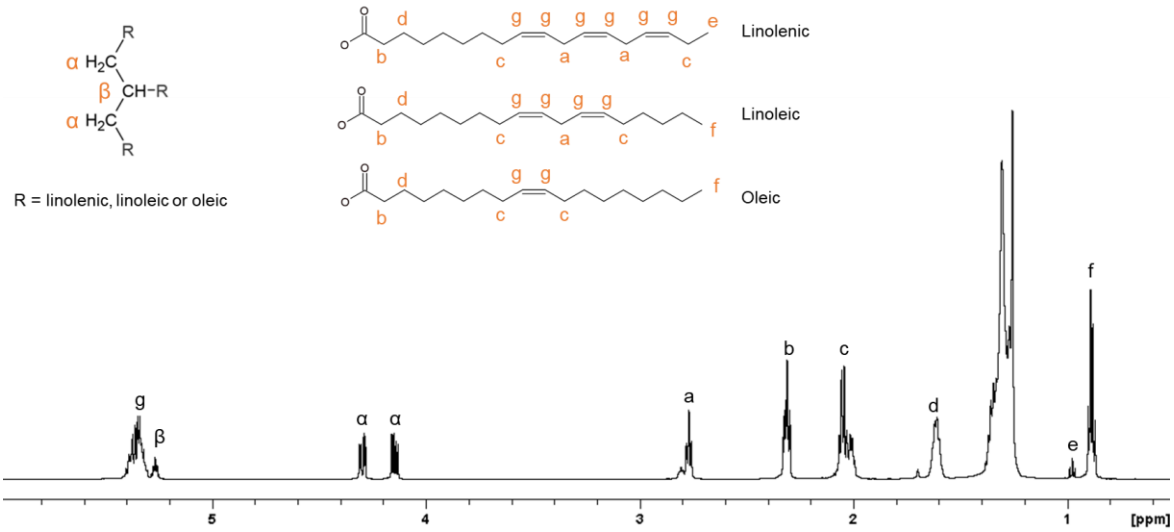

FIGURE B5: ^{1}H NMR spectrum of soybean oil. δ = 0.86-0.91 ppm (-CH_3, f), δ = 0.96-0.99 ppm (linolenic -CH_3, e), δ = 1.56-1.67 ppm (-(CH_2)n- CH_2- CH_2-COO, d), δ = 1.97-2.11 ppm (bis-allylic group - CH_2-CH=CH, c), δ = 2.26-2.37 ppm (-CH_2-COO, b), δ = 2.73-2.84 ppm (allylic group CH=CH-CH_2-CH=CH, a), δ = 4.11-4.19 and 4.26-4.35 ppm (glycerol CH_2, α), δ = 5.23-5.29 ppm (glycerol CH, β) and δ = 5.29-5.43 ppm (CH=CH, g). $CDCl_3$ (δ = 7.27 ppm) was used to dissolve the vegetable oil.

TABLE B4: Fatty acid composition of pristine soybean oil, determined by method of Barison and co-workers.[143]

Fatty Acid	Content (%)	Reference area of glycerol signal	Corresponding signal	Subtraction
Unsaturated	**83.3**	**16.7**	**C**	**-**
Linolenic	6.8	22.2	E	-
Linoleic	46.8	33.3	A	2 x [linolenic]
Oleic	29.8	16.7	C	[linolenic]+[linoleic]
Saturated	**16.7**	**33.3**	**B**	**[unsaturated]**

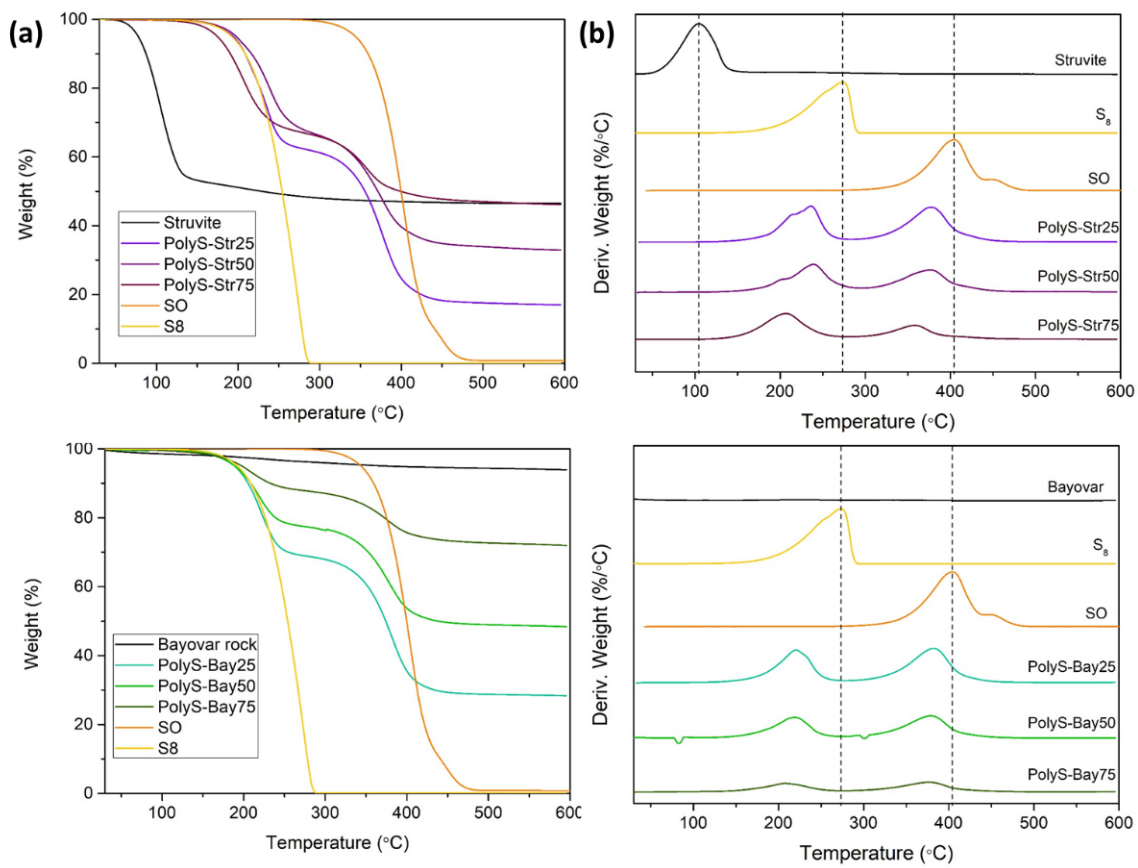

FIGURE B6: (a) TGA curves of starting materials and struvite and Bayovar composites (top and bottom, respectively); (b) DTG curves of starting materials and struvite and Bayovar composites (top and bottom, respectively).

TABLE B5: Peak temperatures from DTG, the percentual of weight loss from each event and final residue.

Sample	Ti (°C)	Tmax (°C)	Tf (°C)	Weight Loss (%)	Residue (%)
PolyS-Str25	113	236 (*216 s*)	278	37	17
	288	377	465	46	
PolyS-Str50	115	239 (*205 s*)	290	34	33
	301	376	475	33	
PolyS-Str75	95	207	273	33	46
	285	358	455	20	
PolyS-Bay25	115	221	268	31	28
	286	382	463	41	
PolyS-Bay50	124	219	270	22	48
	282	378	465	30	
PolyS-Bay75	129	207	273	12	72
	281	377	460	16	
Elemental Sulfur	154	273	292	100	0
Soybean Oil	262	404 (*448 s*)	495	100	0
Struvite	42	105	165	53	47
Bayovar	0	230	600	6	94

Calibration curve from DSC endotherms

DSC thermograms were used to estimate the percentage of residual S_8 present in the polysulfide composites.[48] For this, a calibration curve was used (FIGURE A7),[65] based on the correlation between different pure elemental sulfur masses and respective DSC melting peak areas.

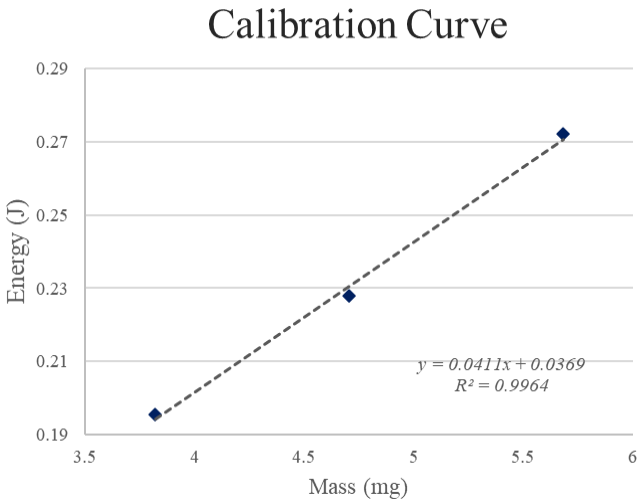

FIGURE B7: Calibration curve from pure S_8 masses and respective areas from DSC melting endotherms.[65]

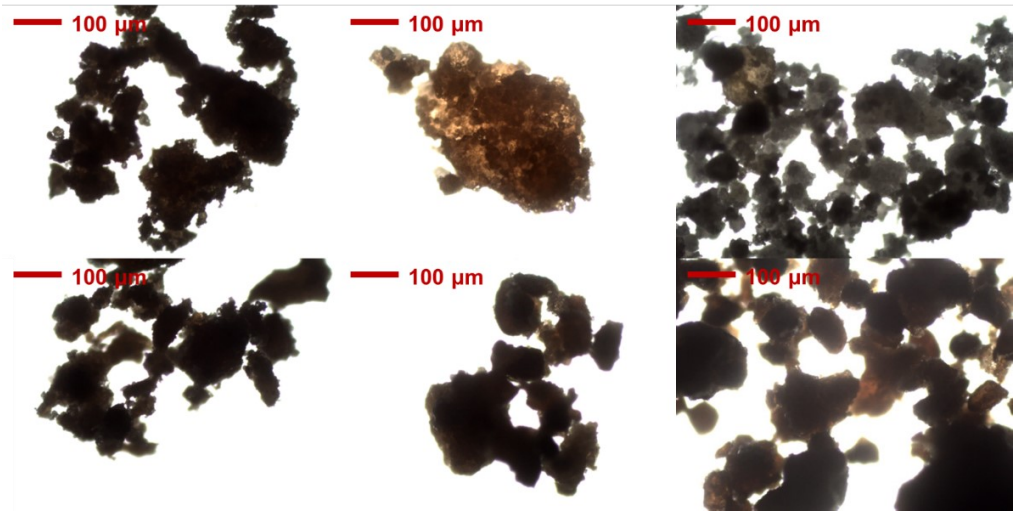

FIGURE B8: Optical microscopy images of PolyS-Str25 (top left), PolyS-Str50 (top middle), PolyS-Str75 (top right), PolyS-Bay25 (bottom left), PolyS-Bay50 (bottom middle) and PolyS-Bay75 (bottom right).

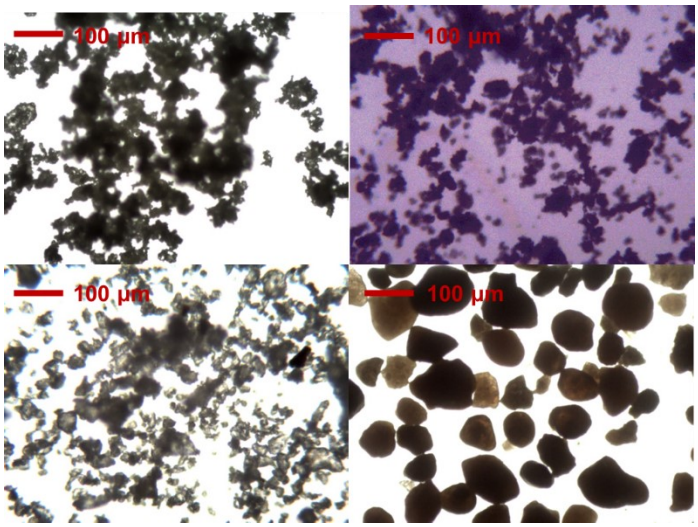

FIGURE B9: Optical microscopy images of elemental sulfur (top left), single superphosphate (top right), struvite (bottom left) and Bayóvar rock (bottom right).

TABLE B6: Nutrient concentration of the treatments with a fixed dose of phosphorous (100 mg of P per kg of soil).

Treatment	P (%)	S (%)	P added (mg/kg of soil)	S added (mg/kg of soil)
Control (-)	-	-	-	-
SSP	10	8	**100**	80
S8	-	98	-	80
Struvite	11	-	**100**	-
Bayovar	13	-	**100**	-
PolyS-Str25	3.4	40.8	**100**	1200
PolyS-Str50	7.8	29.8	**100**	382
PolyS-Str75	10.7	15.1	**100**	141
PolyS-Bay25	2.9	37.5	**100**	1293
PolyS-Bay50	6.8	25.3	**100**	372
PolyS-Bay75	9.2	14.2	**100**	154

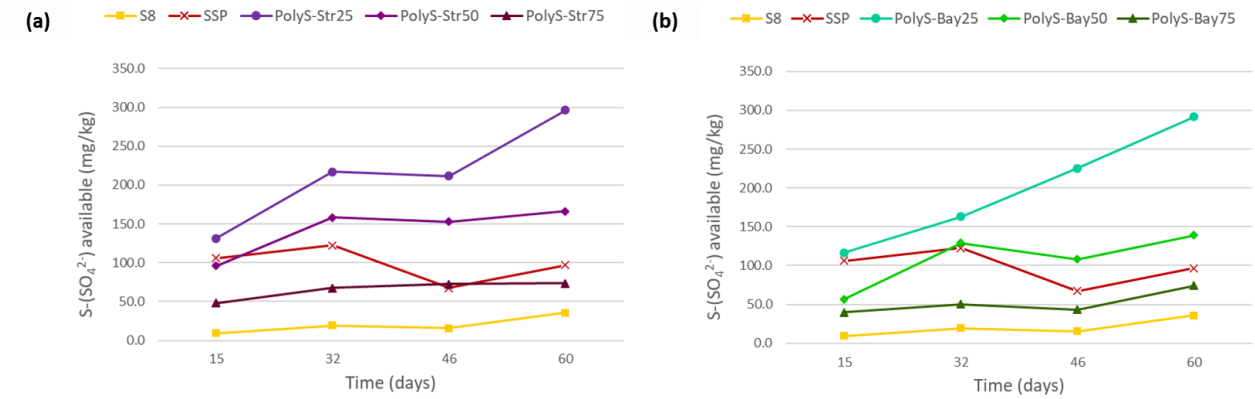

FIGURE B10: Sulfate (mg/kg of soil) produced after 15, 32, 46 and 60 days by (a) PolyS-Str composites and (b) PolyS-Bay composites, in relation to S_8 and SSP.

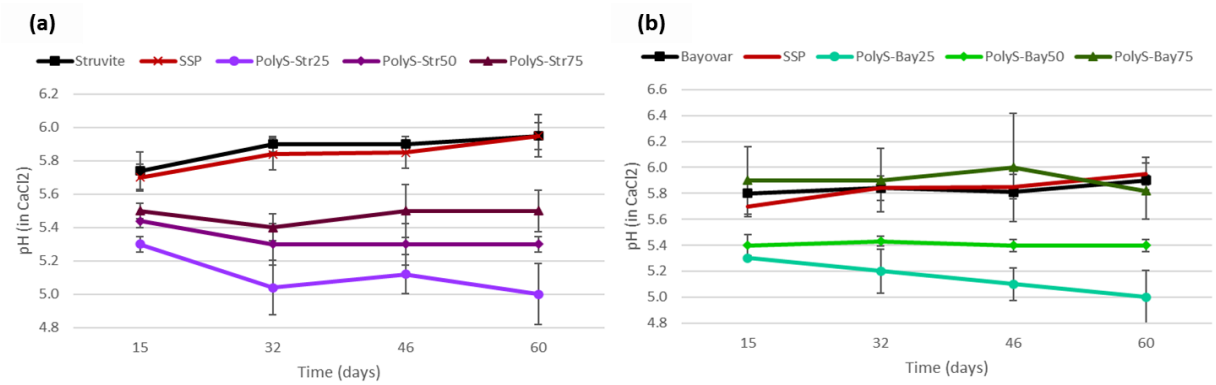

FIGURE B11: pH measurements of the incubated soil after 15, 32, 46 and 60 days for (a) Struvite, SSP and PolyS-Str composites and (b) Bayóvar rock, SSP and PolyS-Bay composites. The pure soil control had a 6.0 pH during the test.

Appendix C

Supporting Information from Section 5 - Chapter III.

TABLE C1: Treatments and respective fertilizers used to complete doses of 50 mg of S/kg, 200 mg of P/kg, and 300 mg of N/kg.

Treatment	Fertilizer	%S	%P	%N	fert mg/soil kg
Control	-	-	-	-	-
TSP/AS	TSP	-	18	-	1111.1
	Ammonium sulfate	24	-	21	208.3
	NH_4NO_3	-	-	33	776.5
St/S8	Elemental Sulfur (S_8)	98	-	-	51.0
	Struvite	-	11.1	6.3	1801.8
	NH_4NO_3	-	-	33	565.1
St 25/PS	25 wt% struvite/ 75 wt% polysulfide	40.8	3.4	1.7	122.5
	Struvite	-	11.1	6.3	1764.3
	NH_4NO_3	-	-	33	566.0
St 50/PS	50 wt% struvite/ 50 wt% polysulfide	29.8	7.8	3	167.8
	Struvite	-	11.1	6.3	1683.9
	NH_4NO_3	-	-	33	572.4
St 75/PS	75 wt% struvite/ 25 wt% polysulfide	15.1	10.7	5.4	331.1
	Struvite	-	11.1	6.3	1482.6
	NH_4NO_3	-	-	33	571.9

TABLE C2: Substrate characterization. Field capacity was estimated to be around 39.1%.

Substrate characterization		
Parameter	**Unit**	**Value**
dry substance	%	57.2
bulk density (wet)	g/dm^3	435.0
bulk density (dry)	g/dm^3	249.0
pH (in CaCl)		5.8
conductivity (in H_2O)	µS/cm	32.0
salt (as KCl in H_2O)	g/dm^3	< 0.1
salt (as KCl in $CaSO_4$)	g/dm^3	< 0.1
nitrogen (mineral)	mg/kg	36.0
ammonium-N	mg/kg	30.0
nitrate-N	mg/kg	6.0
phosphorus (P_2O_5)	mg/kg	44.0
potassium (K_2O)	mg/kg	44.0
magnesium	mg/kg	320.0
sulfur (in SO_4^{2-})	mg/kg	33.6
organic carbon	%	19.3

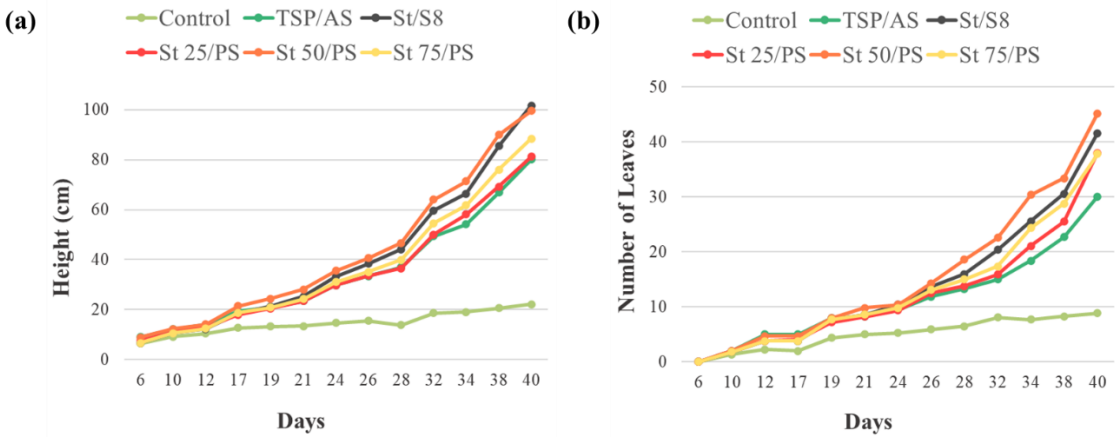

FIGURE C1: Dynamic growth trends of average (a) plant height and (b) number of leaves over time (n = 9 for Control and St 50/PS, n=8 for St/S8, St

25/PS, and St 75/PS, and n=7 for TSP/AS).

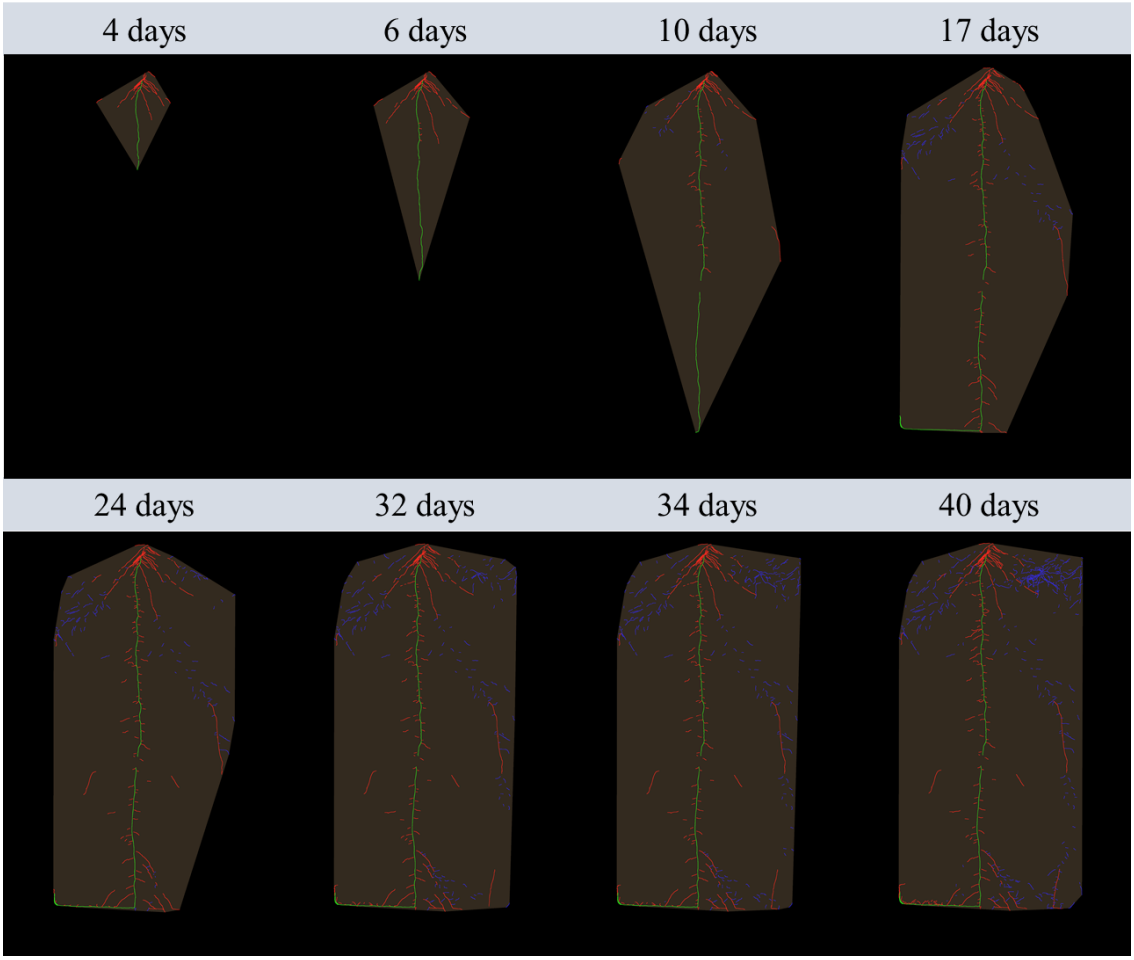

FIGURE C2: Color coded rhizotron images of the control with no fertilizer over time. Primary roots, first order lateral roots and second order lateral roots are represented by the colors green, red and blue, respectively.

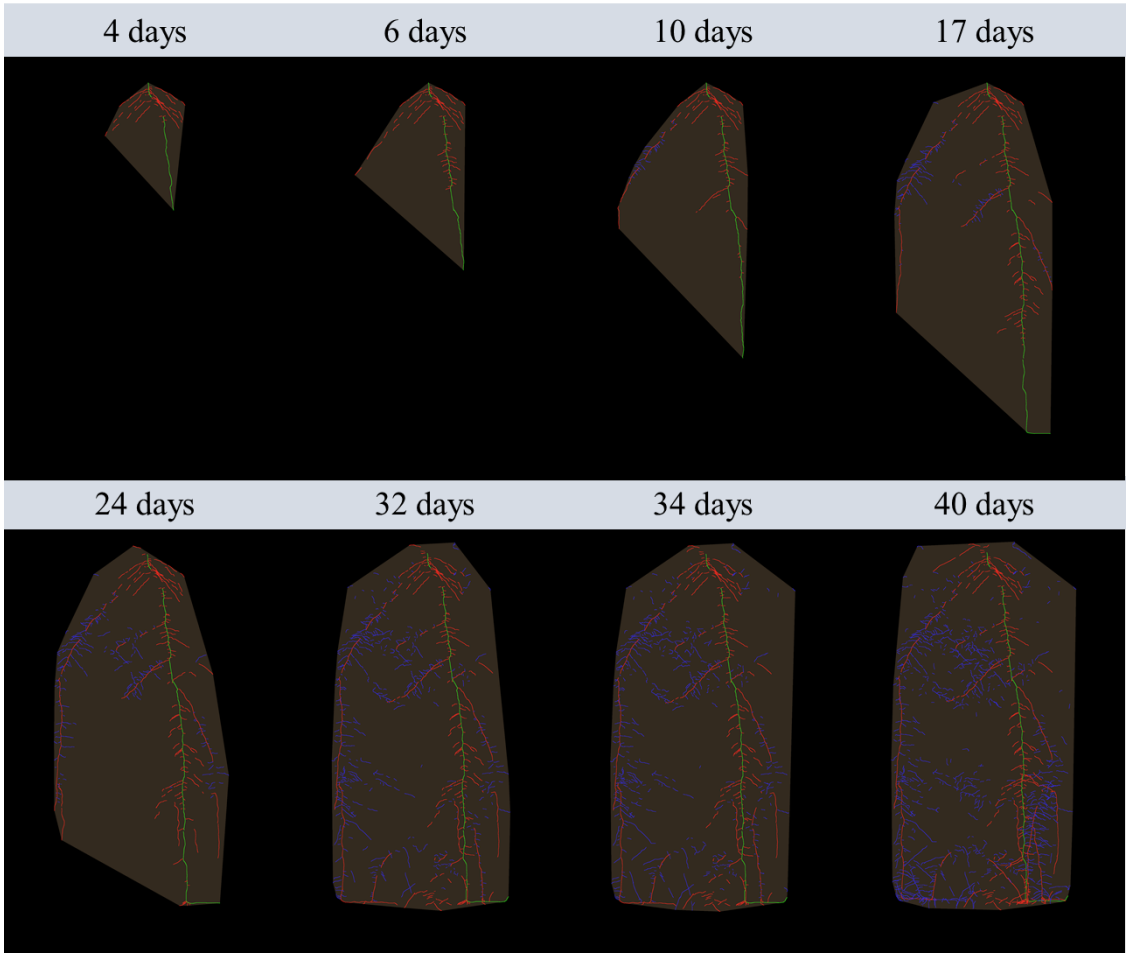

FIGURE C3: Color coded rhizotron images of the positive control (TSP/AS), with triple superphosphate and ammonium sulphate, over time. Primary roots, first order lateral roots and second order lateral roots are represented by the colors green, red and blue, respectively.

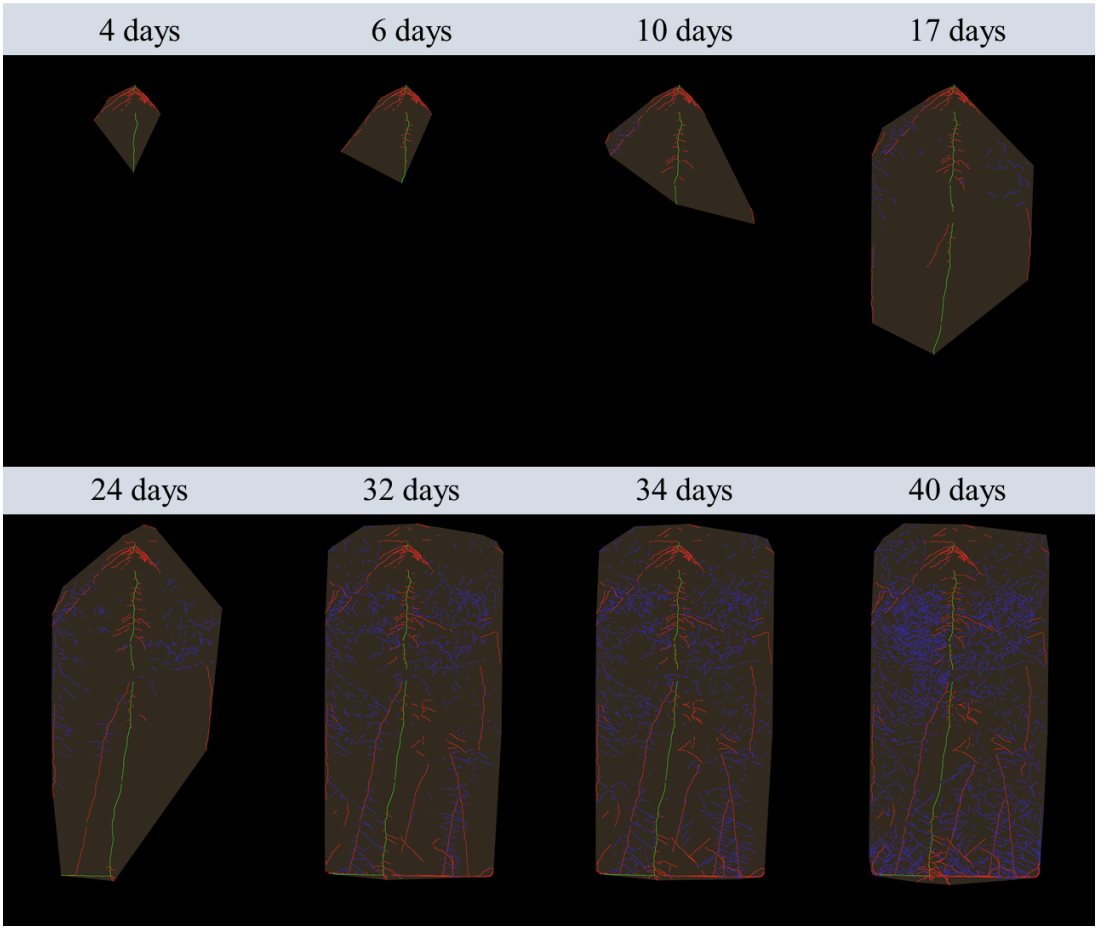

FIGURE C4: Color coded rhizotron images of the pure elemental sulfur and struvite mixture (St/S8) over time. Primary roots, first order lateral roots and second order lateral roots are represented by the colors green, red and blue, respectively.

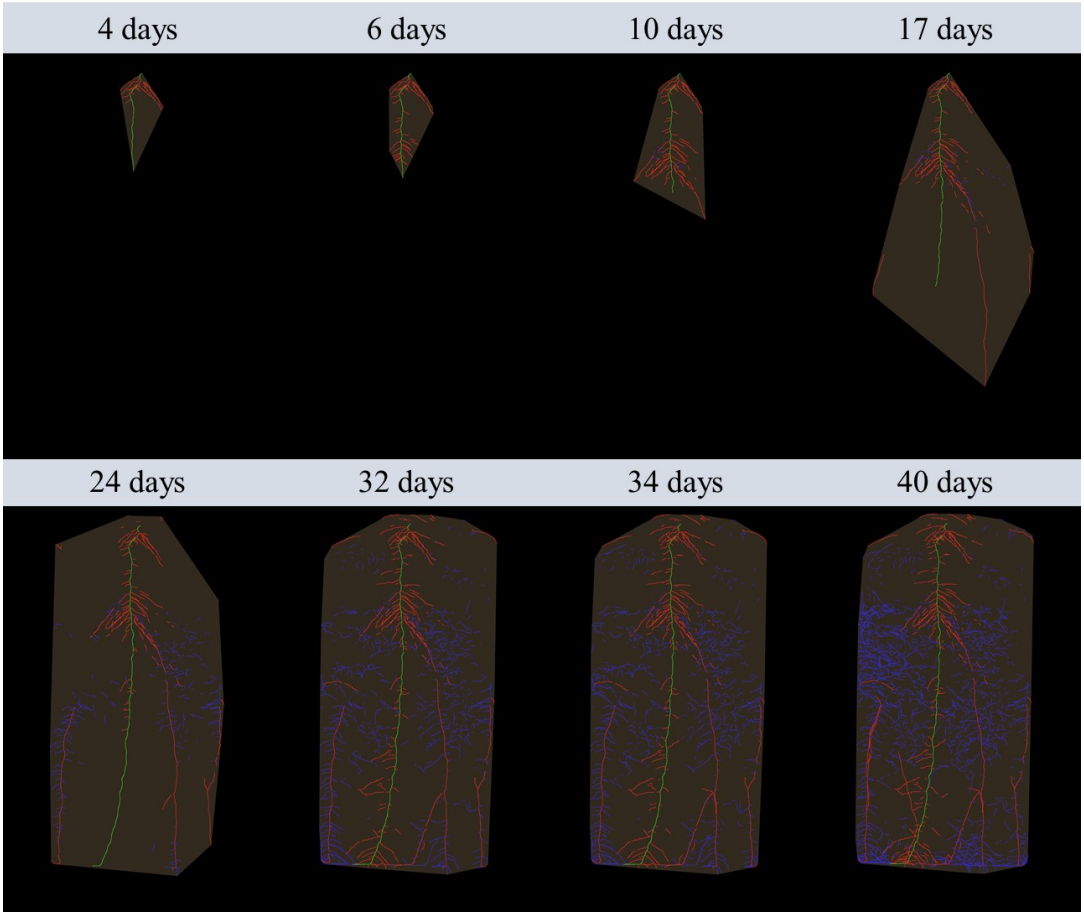

FIGURE C5: Color coded rhizotron images of the composite with 25 wt% struvite and 75 wt% polysulfide (St 25/PS) over time. Primary roots, first order lateral roots and second order lateral roots are represented by the colors green, red and blue, respectively.

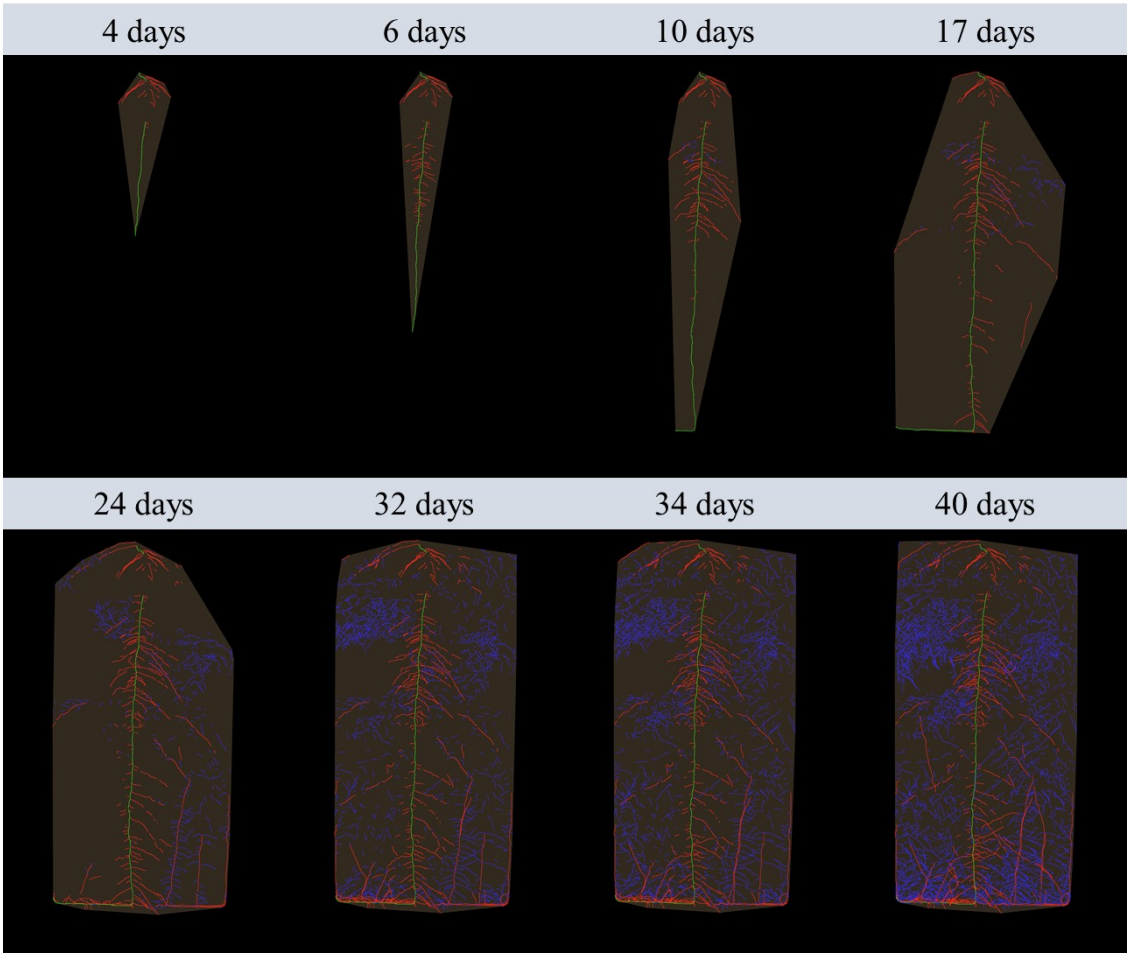

FIGURE C6: Color coded rhizotron images of the composite with 50 wt% struvite and 50 wt% polysulfide (St 50/PS) over time. Primary roots, first order lateral roots and second order lateral roots are represented by the colors green, red and blue, respectively.

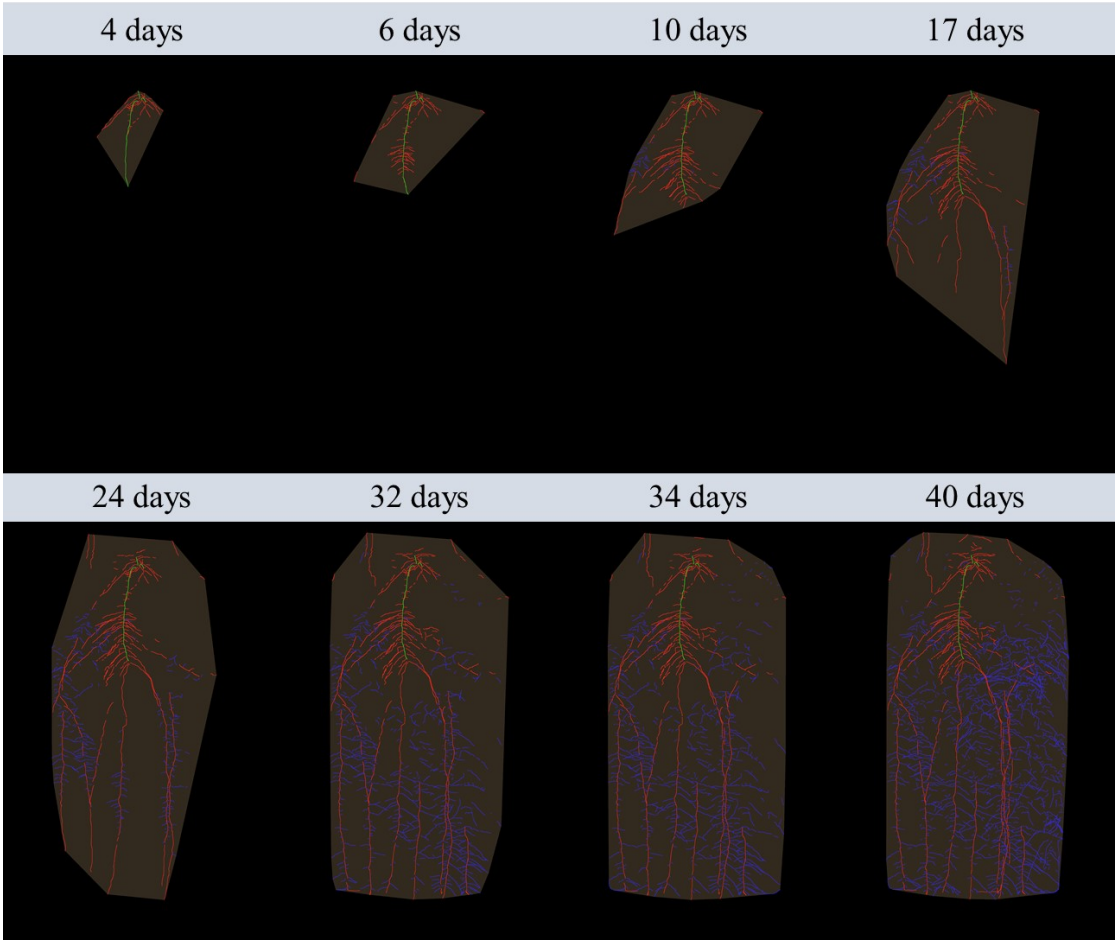

FIGURE C7: Color coded rhizotron images of the composite with 75 wt% struvite and 25 wt% polysulfide (St 75/PS) over time. Primary roots, first order lateral roots and second order lateral roots are represented by the colors green, red and blue, respectively.

TABLE C3: Average visible root lengths (primary roots, first and second order lateral roots, and the total), root system depth and convex hull area, at 40 days after sowing. Indexes a, b, and c represent statistical differences between treatments ($p < 0.05$).

Treatment	Primary Root Length (cm)	First Order Lateral Root Length (cm)	Second Order Lateral Root Length (cm)
Control	47.3 *a*	202.5 *c*	202.2 *c*
TSP/AS	42.7 *a*	368.2 *bc*	548.8 *bc*
St/S8	41.1 *a*	357.5 *bc*	1246.5 *a*
St 25/PS	55.5 *a*	377.4 *bc*	910.9 *ab*
St 50/PS	63.1 *a*	565.1 *a*	1400.2 *a*
St 75/PS	40.9 *a*	430.7 *ab*	1069.6 *ab*
Treatment	Total Root Length (cm)	Root System Depth (cm)	Convex Hull Area (cm^2)
Control	452.0 *c*	52.5 *a*	1116.8 *a*
TSP/AS	959.8 *bc*	50.4 *a*	1155.6 *a*
St/S8	1645.1 *ab*	53.5 *a*	1291.4 *a*
St 25/PS	1343.9 *ab*	53.4 *a*	1262.7 *a*
St 50/PS	2028.5 *a*	53.8 *a*	1355.2 *a*
St 75/PS	1541.2 *ab*	52.4 *a*	1270.0 *a*

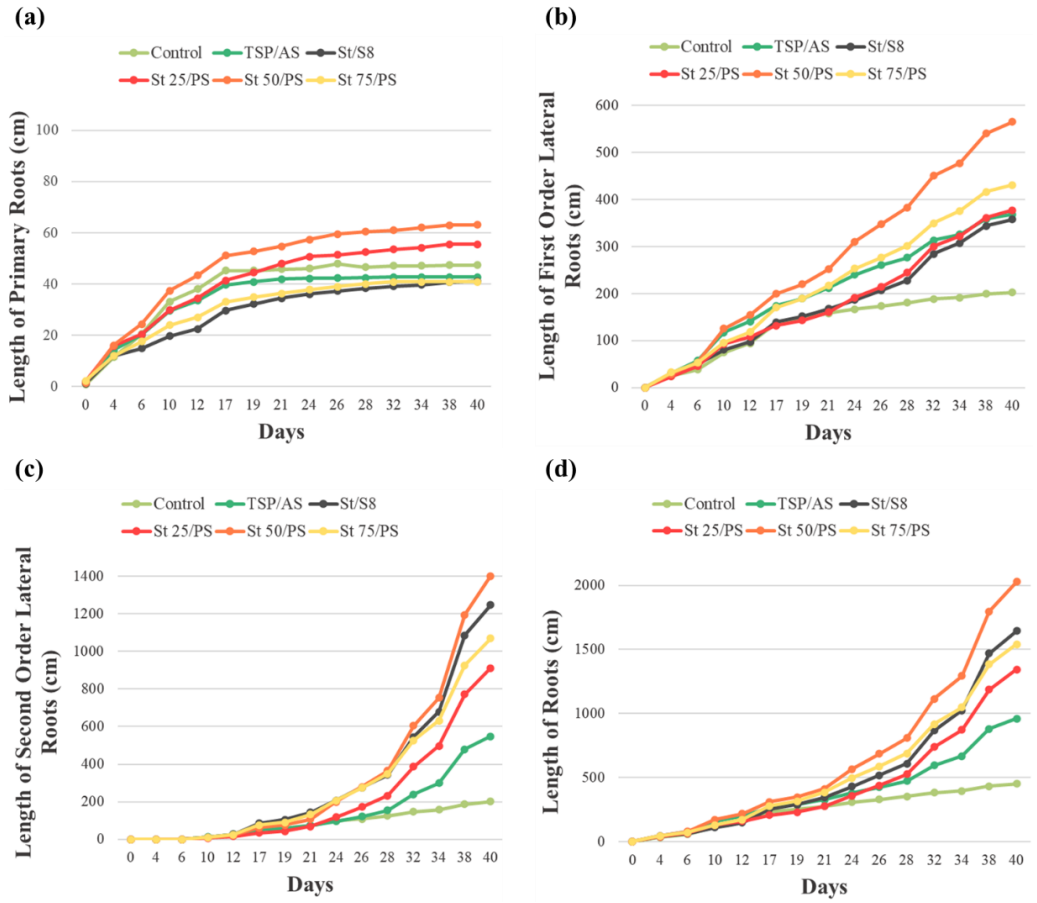

FIGURE C8: Dynamic growth trends of average total root length of (a) primary roots, (b) first order lateral roots, (c) second order lateral roots, and (d) their sum, over the time of plant cultivation (n = 10).

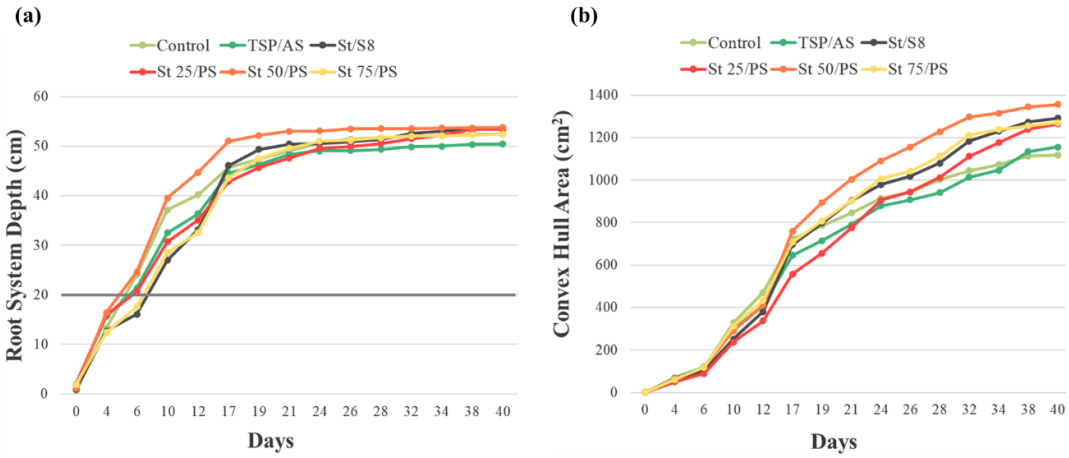

FIGURE C9: Dynamic growth trends of average (a) root system depth and (b)

convex hull area over the time of plant cultivation (n = 10). The fertilizer layer is marked (grey line) in (a) at 20 cm from the rhizotron top surface.

TABLE C4: Average total root length, root diameter, and root surface area of each rhizotron depth layer. A= top layer (10 cm), B = middle layer (20 cm), and C = bottom layer (~26 cm). Indexes a and b signal statistical differences between layers for each treatment individually ($p < 0.05$).

Root Measurements				
Treatment	**Layer**	Total Length (cm)	Diameter (mm)	Surface Area (cm^2)
Control	A	640.8 *a*	0.35 *a*	71.8 *a*
	B	372.6 *a*	0.33 *a*	37.1 *a*
	C	578.8 *a*	0.33 *a*	58.1 *a*
TSP/AS	A	217.1 *a*	0.58 *a*	38.6 *a*
	B	315.6 *a*	0.35 *b*	34.1 *a*
	C	449.5 *a*	0.34 *b*	45.5 *a*
St/S8	A	216.0 *a*	0.72 *a*	46.1 *a*
	B	496.7 *a*	0.42 *b*	66.7 *a*
	C	859.3 *a*	0.35 *b*	102.6 *a*
St 25/PS	A	254.3 *a*	0.68 *a*	53.8 *a*
	B	566.3 *a*	0.42 *b*	79.2 *a*
	C	1121.4 *a*	0.35 *b*	123.0 *a*
St 50/PS	A	526.5 *b*	0.61 *a*	101.9 *b*
	B	1348.5 *ab*	0.46 *b*	190.1 *ab*
	C	2415.6 *a*	0.38 *b*	300.5 *a*
St 75/PS	A	464.7 *b*	0.66 *a*	84.9 *a*
	B	1374.1 *ab*	0.42 *b*	180.1 *a*
	C	1836.0 *a*	0.37 *b*	216.4 *a*

TABLE C5: Average relative root length (%) partitioned in diameter classes. Root lengths from each section were divided by the total root length (of all sections). Indexes a and b signal statistical differences between treatments, in relation to the diameter section ($p < 0.05$).

Relative Root Length (%)						
	Diameter section (mm)					
Treatment	$0 < D \leq 0.1$	$0.1 < D \leq 0.2$	$0.2 < D \leq 0.3$	$0.3 < D \leq 0.4$	$0.4 < D \leq 0.5$	$D > 0.5$
Control	5.7 *a*	25.7 *a*	32.8 *a*	13.4 *a*	11.1 *a*	11.2 *b*
TSP/AS	5.3 *a*	20.1 *ab*	27.9 *a*	15.5 *a*	14.0 *a*	17.2 *ab*
St/S8	4.2 *a*	16.5 *b*	27.0 *a*	15.7 *a*	12.2 *a*	24.4 *a*
St 25/PS	4.5 *a*	17.8 *ab*	27.7 *a*	16.6 *a*	12.8 *a*	20.7 *a*
St 50/PS	3.5 *a*	14.7 *b*	27.9 *a*	17.0 *a*	13.0 *a*	23.8 *a*
St 75/PS	4.1 *a*	18.1 *b*	29.6 *a*	15.5 *a*	12.0 *a*	20.7 *a*

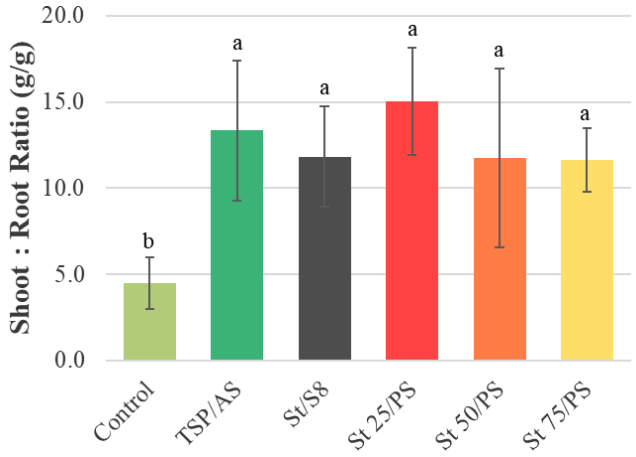

FIGURE C10: Effects on shoot:root ratio, related to plant dry biomass (n = 7 for Control, n=6 for St/S8, and n=5 for TSP/AS, St 25/PS, St 50/PS, and St 75/PS). Bars show mean values ± standard deviations. Indexes a and b identify significant statistical differences between treatments ($p < 0.05$).

TABLE C6: Average shoot (top) and root (bottom) elemental composition (wt%). Indexes a, b, and c indicate significant differences between the treatments, related to each element ($p < 0.05$).

Shoot Elemental Composition (wt %)					
Treatment	P	S	N	Mg	K
Control	0.28 *c*	0.34 *a*	0.74 *c*	0.28 *b*	1.22 *c*
TSP/AS	1.15 *a*	0.27 *b*	4.16 *ab*	0.36 *ab*	2.50 *a*
St/S8	0.78 *b*	0.23 *b*	3.70 *b*	0.35 *ab*	2.22 *ab*
St 25/PS	0.99 *ab*	0.26 *b*	4.01 *ab*	0.38 *a*	2.53 *ab*
St 50/PS	0.76 *b*	0.28 *b*	4.34 *ab*	0.44 *a*	2.02 *b*
St 75/PS	0.92 *ab*	0.28 *b*	4.52 *a*	0.44 *a*	2.35 *ab*

Root Elemental Composition (wt %)					
Treatment	P	S	N	Mg	K
Control	0.08 *b*	0.10 *a*	1.09 *b*	0.09 *a*	0.02 *a*
TSP/AS	0.17 *a*	0.09 *a*	1.96 *a*	0.08 *a*	0.05 *a*
St/S8	0.16 *a*	0.10 *a*	1.55 *ab*	0.09 *a*	0.06 *a*
St 25/PS	0.16 *a*	0.09 *a*	1.50 *ab*	0.08 *a*	0.06 *a*
St 50/PS	0.15 *ab*	0.10 *a*	1.58 *ab*	0.10 *a*	0.04 *a*
St 75/PS	0.15 *a*	0.11 *a*	1.82 *a*	0.09 *a*	0.04 *a*

TABLE C7: Average root elemental composition (wt %) from each depth layer. A= top layer (10 cm), B = middle layer (20 cm), and C = bottom layer (~26 cm). Indexes a, b, and c signal statistical differences between layers of each element, for each treatment individually ($p < 0.05$). Not enough material was available from Control-C and TPS/AS-B to perform the ICP-OES analysis to determine P, S, Mg, and K concentrations (indicated with a bar). Therefore, statistical analysis was not conducted to compare layers from the Control and TPS/AS regarding those elements.

Root Elemental Composition (wt %)							
Treatment	**Layer**	P	S	N	Mg	K	C
Control	A	0.08	0.10	0.8 *a*	0.08	0.02	43.93 *a*
	B	0.07	0.12	1.20 *a*	0.11	0.03	42.97 *a*
	C	-	-	1.20 *a*	-	-	43.23 *a*
TSP/AS	A	0.17	0.07	1.19 *b*	0.07	0.05	44.97 *a*
	B	-	-	2.36 *a*	-	-	43.86 *a*
	C	0.18	0.17	2.71 *a*	0.12	0.01	43.66 *a*
St/S8	A	0.14 *a*	0.06 *b*	0.86 *b*	0.07 *b*	0.09 *a*	44.69 *a*
	B	0.20 *a*	0.13 *a*	1.95 *a*	0.12 *a*	0.04 *a*	44.06 *a*
	C	0.13 *a*	0.12 *a*	2.18 *a*	0.09 *b*	0.02 *a*	43.93 *a*
St 25/PS	A	0.16 *a*	0.06 *b*	0.99 *b*	0.07 *a*	0.09 *a*	44.23 *a*
	B	0.16 *a*	0.12 *a*	1.85 *a*	0.09 *a*	0.04 *a*	44.24 *a*
	C	0.14 *a*	0.12 *a*	1.98 *a*	0.08 *a*	0.02 *a*	44.32 *a*
St 50/PS	A	0.13 *a*	0.06 *c*	0.92 *b*	0.09 *a*	0.05 *a*	45.75 *a*
	B	0.16 *a*	0.11 *b*	1.72 *a*	0.10 *a*	0.04 *ab*	44.92 *b*
	C	0.15 *a*	0.15 *a*	2.18 *a*	0.12 *a*	0.02 *b*	44.67 *b*
St 75/PS	A	0.14 *a*	0.07 *b*	1.06 *b*	0.07 *b*	0.05 *a*	44.72 *a*
	B	0.20 *a*	0.13 *a*	2.18 *ab*	0.10 *a*	0.03 *ab*	43.88 *b*
	C	0.15 *a*	0.16 *a*	2.44 *a*	0.12 *a*	0.02 *b*	43.65 *b*

TABLE C8: Substrate concentration of available P (mg/dm^3) and available S (mg/dm^3) after soybean harvest, from each depth layer. A= top layer (10 cm), B = middle layer (20 cm), and C = bottom layer (~26 cm). Indexes a, b, and c signal statistical differences between layers, for each treatment and nutrient individually ($p < 0.05$).

Treatment	Layer	P available (mg/dm^3)	S available (mg/dm^3)	N total (mg/dm3)
Control	A	15.8 *a*	8.0 *b*	3144.0 *a*
	B	17.7 *a*	9.7 *b*	3218.7 *a*
	C	16.0 *a*	20.2 *a*	2325.0 *a*
TSP/AS	A	16.8 *b*	7.8 *b*	2568.0 *b*
	B	164.0 *a*	56.0 *a*	4721.5 *a*
	C	28.8 *b*	68.8 *a*	3886.9 *ab*
St/S8	A	15.9 *b*	8.2 *b*	2640.0 *a*
	B	236.6 *a*	45.6 *a*	3763.0 *a*
	C	18.0 *b*	42.3 *a*	3946.5 *a*
St 25/PS	A	17.8 *b*	8.7 *c*	3456.0 *a*
	B	207.4 *a*	35.1 *b*	3266.0 *a*
	C	17.6 *b*	54.6 *a*	2897.3 *a*
St 50/PS	A	14.9 *b*	8.3 *b*	2220.0 *a*
	B	222.1 *a*	55.6 *a*	2698.0 *a*
	C	18.1 *b*	64.6 *a*	2646.9 *a*
St 75/PS	A	18.0 *b*	15.9 *b*	3120.0 *a*
	B	202.4 *a*	55.1 *a*	3550.0 *a*
	C	25.1 *b*	54.9 *a*	2801.9 *a*